AD-A065 935 IOWA UNIV IOWA CITY DIV OF MATERIALS ENGINEERING F/G 1/3
SUBSTRUCTURING METHODS FOR DESIGN SENSITIVITY ANALYSIS AND STRU--ETC(U)
AUG 77 A K GOVIL, J S ARORA, E J HAU DAAK11-77-C-0023
UNCLASSIFIED TR-34 NL

1 OF 3
AD A065935

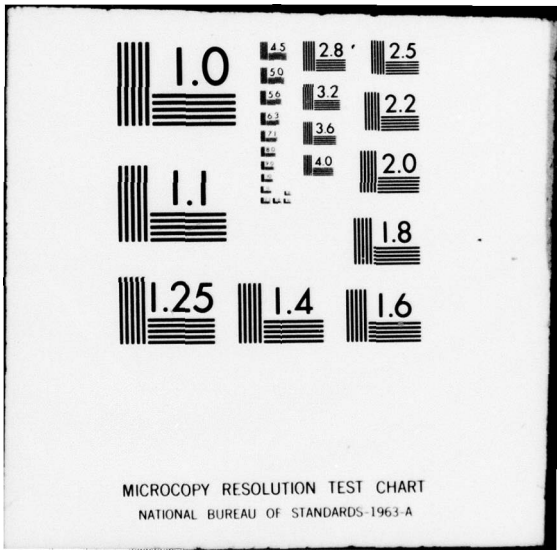
1.0
1.1
1.25
1.4
1.6
1.8
2.0
2.2
2.5
2.8
3.2
3.6
4.0
4.5
5.0
5.6
MICROCOPY RESOLUTION TEST CHART
NATIONAL BUREAU OF STANDARDS-1963-A

LEVEL II

Technical Report No. 34

SUBSTRUCTURING METHODS FOR DESIGN SENSITIVITY ANALYSIS AND STRUCTURAL OPTIMIZATION

An Interim Technical Report

by

A. K. Govil, J. S. Arora, and E. J. Haug

August 1977

For

U.S. Army Ballistic Research Laboratory
Aberdeen Proving Ground
Maryland 21005

STRUCTURAL VULNERABILITY REDUCTION AND SURVIVABILITY PROGRAM

Research Contract No. DAAK11-77-C-0023

Division of Materials Engineering
College of Engineering
The University of Iowa
Iowa City, Iowa 52242

LEVEL II

Technical Report No. 34

SUBSTRUCTURING METHODS FOR DESIGN SENSITIVITY ANALYSIS AND STRUCTURAL OPTIMIZATION

An Interim Technical Report

by

A.K. Govil, J.S. Arora, and E.J. Haug

August 1977

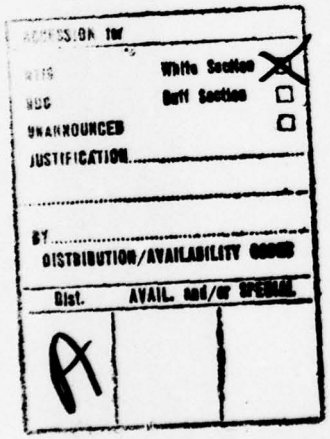

For

U.S. Army Ballistic Research Laboratory

Aberdeen Proving Ground

Maryland 21005

STRUCTURAL VULNERABILITY REDUCTION AND SURVIVABILITY PROGRAM

Research Contract No. DAAK11-77-C-0023

Division of Materials Engineering
College of Engineering
The University of Iowa
Iowa City, Iowa 52242

Unclassified

SECURITY CLASSIFICATION OF THIS PAGE (When Data Entered)

REPORT DOCUMENTATION PAGE	READ INSTRUCTIONS BEFORE COMPLETING FORM
1. REPORT NUMBER: TR-34	2. GOVT ACCESSION NO. / 3. RECIPIENT'S CATALOG NUMBER
4. TITLE (and Subtitle): Substructuring Methods for Design Sensitivity Analysis and Structural Optimization	5. TYPE OF REPORT & PERIOD COVERED: Interim Technical Report, May 1977 to August 1977
	6. PERFORMING ORG. REPORT NUMBER: 34
7. AUTHOR(s): A.K. Govil, J.S. Arora, E.J. Haug	8. CONTRACT OR GRANT NUMBER(s): DAAK11-77-C-0023; DAAA09-76-C-2013
9. PERFORMING ORGANIZATION NAME AND ADDRESS: Division of Materials Engineering, College of Engineering, University of Iowa, Iowa City, Ia 52242	10. PROGRAM ELEMENT, PROJECT, TASK AREA & WORK UNIT NUMBERS
11. CONTROLLING OFFICE NAME AND ADDRESS: U.S. Army Ballistic Research Laboratory, Attn: DRDAR-BLB, Aberdeen Proving Ground, Maryland 21005	12. REPORT DATE: August 1977; 13. NUMBER OF PAGES: 226
14. MONITORING AGENCY NAME & ADDRESS(if different from Controlling Office): 229p.	15. SECURITY CLASS. (of this report): Unclassified; 15a. DECLASSIFICATION/DOWNGRADING SCHEDULE

16. DISTRIBUTION STATEMENT (of this Report)

Approved for public release; distribution unlimited

17. DISTRIBUTION STATEMENT (of the abstract entered in Block 20, if different from Report)

Approved for public release; distribution unlimited

18. SUPPLEMENTARY NOTES

19. KEY WORDS (Continue on reverse side if necessary and identify by block number)

Optimal Design, Fail-Safe, Substructuring, Design Sensitivity, Trusses, Wing Structures, Framed Structures

20. ABSTRACT (Continue on reverse side if necessary and identify by block number)

This report presents an iterative method for optimal design of large scale structures that incorporates the concept of substructuring. Design sensitivity analysis for the method is developed in a state space setting, in which the symmetry of the structural stiffness matrix is utilized to define efficient adjoint calculations that yield explicit design derivatives. The entire procedure is then presented as a convenient computational algorithm. Applications of the method are given for optimal design of two and three dimensional truss, idealized wing, and framed structures. Computer programs based on the present algorithm

(continued on back side)

DD FORM 1 JAN 73 1473 EDITION OF 1 NOV 65 IS OBSOLETE S/N 0102-014-6601 | 409 250

Unclassified

SECURITY CLASSIFICATION OF THIS PAGE (When Data Entered)

are presented for three truss structures (10 member plane cantilever truss, 200 member plane truss, 63 member space truss), three idealized wing structures (18 element wing box beam, 39 element rectangular wing, 150 element swept wing), and three framed structures (one-bay two-story plane frame, two-bay six-story plane frame, 48 element space frame). Results obtained with the substructuring formulation are compared first with results obtained without substructuring and then with results obtained with other methods. It is concluded that the algorithm with substructuring is more efficient than the one without substructuring, with computational times reduced by up to 66%. Finally, results obtained with the present method are compared with other available results and a reduction in computing time per iteration by factors ranging from 2.4 to 19 is obtained. Based on these comparisons and the range of problems solved, it is shown that the method is "general" and computationally efficient. Finally, extensions of the method to fail-safe design of large-practical structures are discussed.

TABLE OF CONTENTS

LIST OF TABLES

LIST OF FIGURES

LIST OF SYMBOLS

A_1, A_2, A_3	scalars defined in Eqs. (3.3-9) to (3.3-11)
a_i	a positive constant $0 \leq a_i \leq 1.0$ (see Section 2.6)
B	a subscript used to indicate quantities associated with boundary coordinates
b	a vector of design parameters
b^L	lower bound on b
b^U	upper bound on b
C	a matrix defined in Eq. (2.5-7)
C_1	a matrix defined in Eq. (2.5-4)
C_2	a matrix defined in Eq. (2.5-5)
c_1, c_2	dimension of vectors ϕ^s and ϕ^d
D	total number of design parameters
$\bar{D}$	a vector defined by Eq. (3.6-13)
d	superscript for design variable constraint
e	superscript for eigenvalue constraint
F_B	a vector of effective boundary forces for the entire structure
f	natural frequency in cycles per sec.
F_1 to F_6	member forces at a point (x_1, x_2, x_3)
G	a matrix defined in Eq. (2.5-17)
$\bar{G}$, $\bar{G}_A$, $\bar{G}_B$	parameters associated with effective length factor (k)

H	a matrix defined in Eq. (2.6-13)
H_{11}, H_{12}, H_{21}, H_{22}	submatrices of H (see Eqs. (3.6-6) to (3.6-9))
I	a subscript used to indicate quantities associated with interior coordinate
I_i	moment of inertia of the ith member
J, $\bar{J}$	cost functions defined by Eqs. (2.4-1) and (2.2-1) respectively
k	effective length factor (see Eqs. (6.3-3) and (6.3-4))
K(b)	stiffness matrix for the entire structure; (N, N)
K_B	boundary stiffness matrix for the entire structure; (n, n)
K_{BB}, K_{BI}, K_{IB}, K_{II}	submatrices of K(b)
L	total number of substructures
ℓ_i	length of the ith member
$\bar{\ell}_i$	equivalent length of the ith member
M(b)	mass matrix for the entire structure; (N, N)
M_B	boundary mass matrix for the entire structure; (n, n)
M_{BB}, M_{BI}, M_{IB}, M_{II}	submatrices of M(b)
m	total number of interior degrees of freedom
m(r)	number of interior degrees of freedom for the rth substructure
N	total number of degrees of freedom
n	total number of boundary degrees of freedom

$n(r)$	number of boundary degrees of freedom for the rth substructure
$p^{(r)}$	a vector of member forces for the rth substructure
P_1 to P_6	member end forces in local coordinate system
Q	a matrix defined in Eq. (2.3-5)
$\bar{Q}$	a parameter associated with shear stress (see Eq. (6.3-16))
R	mean radius
R^L	lower bound on R
R^U	upper bound on R
$\bar{R}(y)$	Rayleigh Quotient defined in Eq. (2.3-15)
R_i^*	response ratio (see Eq. (3.4-4))
r	superscript for rth substructure
$\bar{r}$	reduction ratio (see Eq.(3.7-1))
$S(b)$	a vector of externally applied loads
S_B	a subvector of S associated with the boundary degrees of freedom
S_I	a subvector of S associated with the interior degrees of freedom
s	superscript for stress and displacement constraints
s1, s2	superscripts defined for constraints of Eqs. (2.4-3) and (2.4-4), respectively
t	thickness
t^L	lower bound on t
t^U	upper bound on t
U	matrix defined in Eq. (3.2-1)

w	distributed load per unit length
W	weighting matrix
W_i	coefficient of weighting matrix associated with ith design variable
$\bar{w}_i$	multiplier associated with W (see Eq.(5.3-1))
x_1, x_2, x_3	cartesian coordinates
y	eigenvector associated with Eq. (2.2-3)
y_B	eigenvector associated with Eq. (2.3-16)
y_I	eigenvector associated with interior degrees of freedom
z	a vector of nodal displacements for the entire structure
z^a	a vector of allowable nodal displacements for the entire structure
z_B	a vector of boundary displacements for the entire structure
z_I	a vector of interior displacements for the entire structure
δb	a vector of small changes in the design parameter b
δz_I	a vector of small changes in the vector z_I
δz_B	a vector of small changes in the vector z_B
$\delta b_1, \delta b_2$	defined in Eq. (2.6-10) and (2.6-11), respectively
α_i	step size defined in Eq. (3.3-8)
$\bar{\alpha}_i$	positive constant (see Eq. (4.2-4))
$\beta(r)$	a Boolean transformation matrix for the rth substructure

σ	normal stress due to axial force and/or bending moment at a point (x_1, x_2, x_3)
σ^c	calculated stress
σ^a, σ^{a-}, σ^{a+}	allowable stresses (see Section 4.2)
σ^b	critical buckling stress for axial compression alone (see Eq. (4.2-3))
τ	shear stress due to shear force and/or twisting moment at a point (x_1, x_2, x_3)
σ_{cr}, τ_{cr}	critical stresses (see Appendix 3)
γ, γ_1, γ_2	dimension of the function ψ, ϕ^{s1}, and ϕ^{s2}, respectively
$\bar{\gamma}(r)$	number of components of $\tilde{\phi}^{s1}$ that depend upon $z_I^{(r)}$
θ	angle defined in Fig. 6.1
$\bar{\theta}_i$	constant defined for critical buckling of ith member
ρ_i	material density of members of the ith group
μ	Lagrange multiplier vector
μ^1, μ^2	components of μ
η	step size defined in Eq. (3.8-1)
ζ, ζ_B	eigenvalues associated with Eqs. (2.2-3) and (2.3-16), respectively
$\bar{\phi}^s$, ϕ^s, ϕ^{s1}, ϕ^{s2}, ϕ^d	vector constraint functions defined by Eqs. (2.2-4), (2.4-2) to (2.4-4), and (2.2-5), respectively
ϕ^e	scalar constraint function defined by Eq. (2.2-6)
ψ	a general vector function (see Section 2.5.1)
λ_I, λ_B	adjoint matrices obtained from Eqs. (2.5-8) and (2.5-12), respectively

λ_I^J, λ_B^J, λ_I^{s1}, λ_B^{s1}, λ_B^{s2}	adjoint matrices obtained from Eqs. (2.5-30) to (2.5-34), respectively
Λ^J, Λ^{s1}, Λ^{s2}, Λ^d, Λ^e, Λ^{eJ}	matrices whose columns represent sensitivity vectors, defined in Eqs. (2.5-24) to (2.5-29), and (2.6-7), respectively

ABBREVIATIONS

CST	constant strain triangular elements
NG(r)	number of groups in the rth substructure
NLC	number of loading conditions
NM(j)	number of members in the jth group
ODPS	optimal design problem with substructuring
SSP	symmetric shear panel
SPSP	symmetric pure shear panel
TP(r)	type of element in the rth substructure
WCTS	wing-carry-through structure

PREFACE

This report represents the Ph.D. research of Dr. A.K. Govil, done under the supervision of Professors J.S. Arora and E.J. Haug. The research was initiated and chapters one through four completed under U.S. Army Research Contract No. DAAA09-76-C-2013, from the Rock Island Arsenal. The applications of Chapter five and six were completed under Research Contract No. DAAK11-77-C-0023, from the Ballistics Research Laboratory at Aberdeen Proving Ground, Maryland. The complete results are presented in this report, for convenience and ease of use.

CHAPTER 1

INTRODUCTION

1.1 Purpose and Scope of the Study

The purpose of this report is to present an optimal structural design method that integrates the concept of substructuring into its formulation in an effective way, and to suggest extensions of the method to fail-safe design of structures. While substructuring is commonly used in the analysis of large structures, no general method of optimization of such structures that incorporates substructuring has appeared in the literature. Therefore, an efficient method for design sensitivity analysis with substructuring is developed using a state space formulation in which design and state variables are treated separately and explicitly. The displacement method of structural analysis, an efficient design sensitivity analysis, and the Kuhn-Tucker necessary conditions of nonlinear programming are employed to develop an iterative optimal design algorithm. Further, the overall efficiency of the algorithm is enhanced through carefully coordinated use of design variable linking, the ϵ-active constraint concept, and a finite element analysis method that is organized with the design optimization task in mind.

Incorporation of the substructuring concept in analysis essentially means partitioning of the structure into substructures. Using this concept, the nodal coordinates are partitioned into two subsets: 1) coordinates common to various substructures, defined as boundary coordinates, and 2) coordinates that occur only at interior nodes of substructures, defined as interior coordinates. The equilibrium

equations for the structures are partitioned accordingly. The present algorithm exploits these partitioned equations, both in structural analysis and in the design sensitivity analysis, in an efficient way.

To illustrate applicability of the method and to study its efficiency, several structures of given configuration are optimized. These include both two and three dimensional truss, idealized wing, and frame structures. Many of these structures have been used in the literature to compare optimization techniques [1-8]. Constraints on stresses and displacements under multiple loading conditions, on natural frequency, and on design variables are imposed. First, results obtained with the present algorithm for truss examples are compared with results obtained without substructuring [1]. It is shown that the algorithm with substructuring, especially for moderate to large scale structures, is more efficient than an algorithm without substructuring. It is shown that the present method of state space design sensitivity analysis and optimization is considerably faster than results presented in the literature [2-8].

In fail-safe design of structures, one includes projected damage conditions in the design procedure. These damage conditions may include damage to a set of members of structures or to some joints. The substructuring concepts are highly significant in fail-safe design, because they would allow one to treat a large number of damage conditions very efficiently. The reason for this high efficiency is that structural analysis and design sensitivity analysis for damaged structures will be very efficient when substructuring concepts are employed. This efficiency results because if damage to the structure

occurs only in a substructure, then structural matrices for only that substructure are modified and need to be recomputed.

1.2 Review of Literature

As pointed out earlier, a general procedure for optimal structural design with substructuring has not been developed in the literature. A paper by Kirsch, Reiss, and Shamir [9] is the only exception in which the problem of optimum design of a structure by partitioning it into a number of substructures is considered. Their procedure is to sequentially optimize each substructure, with respect to its own design variables, while keeping other design variables constant. This iterative procedure is inefficient and can lead to non-optimal solutions, as pointed out by the authors.

A procedure for calculating derivatives of nodal displacements by formal differentiation of various substructure equations is developed by Noor and Lowder [10]. This procedure will be required when the optimal design problem is defined in design space alone. However, when the problem is defined in a state space setting, advantages of self-adjointness of the structural problem can be fully brought to bear to develop efficient design sensitivity analysis procedures.

Applications of optimization theory in structures have been a subject of great interest during the past two decades. It has been recognized that in order for an algorithm to be applicable to large structures, such as aircraft, multi-story buildings, and transmission towers, it must be computationally efficient and compact. It must be

executed on existing computer hardware, without exceeding available memory capacity, and be computationally fast, i.e., the time spent in each redesign cycle is kept to a minimum. A very detailed review of literature on optimal design has appeared in papers by Wasiutynski and Brandt [11], Sheu and Prager [12], and Arora and Haug [1]. For extensive bibliographies covering various aspects of optimal design and an evaluation of the state-of-the-art until 1976, the reader is referred to these articles. Also recent books by Schmit [13], Pope and Schmit [14], and Gallagher and Zienkiewicz [15] summarize the state-of-the-art quite nicely.

Two philosophically different approaches to optimization have been advocated: 1) Optimality Criteria Methods, and 2) Search Methods based on gradient calculations. Methods based on optimality criteria are clled indirect and employ repeated application of some optimality criteria, or necessary condition for optimality. Many researchers [3-7,16] have recently presented algorithms and results based on such methods.

Many gradient based methods are also available in the literature. Among these are the Sequential Unconstrained Minimization Techniques (SUMT) [17] used by many researchers [2,18-21], the Steepest Descent methods of nonlinear programming [22-25], and the State Space Gradient Projection Method developed initially by Bryson and co-workers [26] for optimal control and later adapted for a wide range of structural and mechanical design problems [1,27-33]. These approaches are collectively referred to as mathematical programming methods. They all rely on gradient calculations, each employing this gradient information in its own iterative algorithm.

Most recently, Schmit and Miura [2,18], Dobbs and Nelson [5], Rizzi [3,4] and Berke and Khot [6] have stated the structural optimization problem in design space. On the other hand, Haug, Arora, and co-workers [27-33] have pursued a different approach in defining the problem. In their approach, the problem is defined in a state space setting, i.e., the state and design variables are treated separately and explicitly in the problem. With the latter approach the design sensitivity analysis is performed very efficiently.

CHAPTER 2

PROBLEM DEFINITION AND DERIVATION OF THE METHOD

2.1 Introduction

In this chapter, a method for optimal structural design using substructuring is developed. Constraints are imposed on member stresses, nodal displacements, natural frequency, and design variables. In the following development first a general optimal design problem is defined. Since substructuring is anticipated in the present work, the general problem is then reformulated by introducing the concept of boundary and interior coordinates. Hereafter, this problem is called the "Optimal Design Problem with Substructuring - ODPS". Design sensitivity analysis for the ODPS is developed and then an algorithm is presented in a convenient step-by-step format.

2.2 State Space Definition of an Optimal Design Problem

A general optimal design problem for structures in the state space setting may be defined as follows: find a design variable vector b that minimizes a cost function

$$\bar{J} = \bar{J}(b,z,\zeta) \tag{2.2-1}$$

satifying the equilibrium equations (state equations)

$$K(b)z = S(b) \tag{2.2-2}$$

$$K(b)y = \zeta M(b)y \tag{2.2-3}$$

and subject to the constraints

$$\bar{\phi}^s(b,z) \leq 0 \tag{2.2-4}$$

$$\phi^d(b) \leq 0 \tag{2.2-5}$$

and

$$\phi^e(\zeta) \leq 0 \tag{2.2-6}$$

where

b = vector of D design parameters, such as cross-sectional areas, moment of inertia, thickness, etc.,

z = state variable vector of N nodal displacements,

N = number of degrees of freedom of the structure,

K(b) = (N,N) structural stiffness matrix,

M(b) = (N,N) structural mass matrix,

S(b) = vector of N nodal loads on the structure,

y = an eigenvector of nodal displacements, corresponding to the lowest eigenvalues ζ,

ζ = the lowest eigenvalue of Eq. (2.2-3).

Further note that $\phi^e(\zeta) \in R^1$, $\bar{\phi}^s(b,z) \in R^{c_1}$, and $\phi^d(b) \in R^{c_2}$. Therefore, the total number of constraints is $c = 1 + c_1 + c_2$, and the inequality applies to each component of the vector functions defined in Eqs. (2.2-4) and (2.2-5).

The cost function of Eq. (2.2-1) is quite general and may depend upon weight of the structure, displacements of critical points, certain critical member forces, or perhaps natural frequency of the structure. The cost function depends only on the design variables if it represents weight of the structure. The inequality (2.2-4) represents constraints that depend upon state and design variables. These are the member stress and the nodal displacement constraints. The inequality (2.2-5) represents constraints that depend only on design variables. These may represent either explicit bounds on the design variables or any relationship between them. The inequality (2.2-6) represents a constraint on the lowest eigenvalue of Eq. (2.2-3) ($\zeta \geq \zeta_o$; ζ_o = allowable lowest eigenvalue) which is related to the fundamental frequency of the structure (frequency $f = \sqrt{\zeta}/2\pi$ Hertz). In the present work, constraints on only the lowest eigenvalue are considered, but constraints on higher eigenvalues, if desired, can also be included [32].

It should also be noted here that the lowest eigenvalue of Eq. (2.2-3) may also be related to the buckling load for the structure. In that case, the matrix M will be a geometric stiffness matrix for the structure [34] and Eq. (2.2-6) will represent a constraint on the buckling load for the structure. This type of a constraint can be treated in the algorithm developed herein.

It may be pointed out here that Schmit and Miura [2], Rizzi [3], Dobbs and Nelson [5], and others [6-8,16,18] have stated the optimal design problem in purely design space. Generally, the cost function of Eq. (2.2-1) and constraints of Eq. (2.2-4) are also explicit

functions of the state variables (nodal displacements) z, which renders them as implicit functions of the design variable vector b. This requires that the matrix $\frac{\partial z}{\partial b}$ be explicitly calculated during sensitivity analysis. For structural problems this approach is highly inefficient and is not used in the present work.

In order to incorporate the substructuring concept, the optimal design problem must be reformulated in terms of the boundary and interior coordinates. The next section presents structural analysis by substructuring, before the problem is redefined in terms of new state variables.

2.3 Structural Analysis by Substructuring

2.3.1 Static Analysis

In structural analysis using the substructuring concept, the stiffness matrix K, and the vectors z and S are partitioned and Eq. (2.2-2) is written as follows:

$$\begin{bmatrix} K_{BB} & K_{BI} \\ K_{IB} & K_{II} \end{bmatrix} \begin{bmatrix} z_B \\ z_I \end{bmatrix} = \begin{bmatrix} S_B \\ S_I \end{bmatrix} \qquad (2.3\text{-}1)$$

where the subscripts B and I refer to boundary and interior quantities for all substructures, z_B and $S_B \in R^n$, z_I and $S_I \in R^m$, n is the number of boundary degrees of freedom, and $m = N - n$ is the number of interior degrees of freedom. Submatrices such as K_{BB}, K_{BI}, S_B, etc., have

compatible dimensions and will be understood to be functions of the design variable b.

Now, the interior displacements z_I are eliminated from Eq. (2.3-1) and the following reduced equation is obtained:

$$K_B z_B = F_B \tag{2.3-2}$$

where

$$\underset{(n,n)}{K_B} = K_{BB} + K_{BI}Q \tag{2.3-3}$$

$$\underset{(n,1)}{F_B} = S_B + Q^T S_I \tag{2.3-4}$$

and

$$\underset{(m,n)}{Q} = -K_{II}^{-1} K_{IB} \tag{2.3-5}$$

Here, K_B is a boundary stiffness matrix for the entire structure, and $F_B \in R^n$ is the vector of effective boundary forces. It should be noted that efficient decomposition procedures are used to decompose K_{II} and then solve for Q in Eq. (2.3-5). For more computational details Chapter 3 should be consulted. The boundary stiffness matrix K_B and the effective boundary force vector F_B are synthesized by considering contributions from all substructures. For this purpose, the equilibrium equations for a substructure, which is considered as an isolated free-body, are also expressed in the following partitioned form:

$$\begin{bmatrix} K_{BB}^{(r)} & K_{BI}^{(r)} \\ K_{IB}^{(r)} & K_{II}^{(r)} \end{bmatrix} \begin{bmatrix} z_B^{(r)} \\ z_I^{(r)} \end{bmatrix} = \begin{bmatrix} S_B^{(r)} \\ S_I^{(r)} \end{bmatrix} \tag{2.3-6}$$

where the superscript r refers to the rth substructure and subscripts B and I refer to boundary and interior quantities, respectively. Let n(r) and m(r) represent the number of boundary and interior coordinates of the rth substructure, respectively. It may be noted that $m = \sum_{r=1}^{L} m(r)$, where L is the total number of substructures. Then, $K_{BB}^{(r)} = [n(r), n(r)]$, $K_{IB}^{(r)} = [m(r), n(r)]$, $K_{BI}^{(r)} = [n(r), m(r)]$, $K_{II}^{(r)} = [m(r), m(r)]$, $z_B^{(r)}$ and $S_B^{(r)} \in R^{n(r)}$, and $z_I^{(r)}$ and $S_I^{(r)} \in R^{m(r)}$. From the second line of Eq. (2.3-6),

$$z_I^{(r)} = \left[K_{II}^{(r)}\right]^{-1} \left[S_I^{(r)} - K_{IB}^{(r)} \; z_B^{(r)}\right] \tag{2.3-7}$$

Now, substituting Eq. (2.3-7) into the first line of Eq. (2.3-6), one obtains

$$K_B^{(r)} \; z_B^{(r)} = F_B^{(r)} \tag{2.3-8}$$

where

$$\underset{[n(r),n(r)]}{K_B^{(r)}} = K_{BB}^{(r)} + K_{BI}^{(r)} \; Q^{(r)} \tag{2.3-9}$$

$$F_{B\,[n(r),1]}^{(r)} = S_B^{(r)} + Q^{(r)^T} S_I^{(r)} \tag{2.3-10}$$

and

$$Q_{[m(r),n(r)]}^{(r)} = - \left[K_{II}^{(r)}\right]^{-1} K_{IB}^{(r)} \tag{2.3-11}$$

The boundary stiffness matrix $K_B^{(r)}$ and the effective boundary force vector $F_B^{(r)}$ for each substructure are computed from Eqs. (2.3-9) and (2.3-10), respectively. Finally, K_B and F_B are assembled according to the following equations:

$$K_B = \sum_{r=1}^{L} \beta^{(r)^T} K_B^{(r)} \beta^{(r)} \quad , \tag{2.3-12}$$

and

$$F_B = S_B + \sum_{r=1}^{L} \beta^{(r)^T} Q^{(r)^T} S_I^{(r)} \tag{2.3-13}$$

where $\beta^{(r)}$ is a Boolean transformation matrix of dimension $[n(r),n]$.

Using the reduced equilibrium equation (2.3-2), the boundary displacements z_B are computed by a suitable numerical procedure. The interior displacements are then computed for each substructure, using Eq. (2.3-7). Lastly, element forces for the rth substructure are computed from

$$p^{(r)} = K^{(r)} z^{(r)} \tag{2.3-14}$$

where $p^{(r)}$ is a vector of all element forces, $K^{(r)}$ is a stiffness matrix, and $z^{(r)}$ is a vector of nodal displacements. This completes static analysis of a structure, using the substructuring formulation.

2.3.2 Frequency Analysis

The natural frequency of a structure is computed from Eq. (2.2-3). A number of techniques, such as Subspace Iteration [35], Jacobi Iteration [35], Householder's Method [36], and a method based on Sturn Sequence properties described by Gupta [37], Wilkinson [38] and others [39,40,41] are available in the literature for solution of the general eigenvalue problem defined by Eq. (2.2-3). However, these techniques require computation of stiffness and mass matrices for the entire structure and decomposition of the stiffness matrix. For a large structure, this is not desirable, since it defeats the purpose of substructuring. The technique of frequency analysis used should either take full advantage of substructuring or it should not require calculation and storage of matrices K and M for the entire structure. There are many component mode substitution techniques available in the literature that may be used. For a complete survey of such techniques, the reader is referred to Arora's paper [42]. These techniques take full advantage of substructuring. However, they are not suitable for integration into an optimal design algorithm, because they introduce design variable dependent transformations that complicate the design sensitivity analysis.

There is one technique, however, that has all the features needed to solve the present problem. It is based on minimization of the Rayleigh Quotient

$$\bar{R}(y) = \frac{y^T K y}{y^T M y} \tag{2.3-15}$$

subject to appropriate constraints on orthogonality of eigenvectors. This approach of finding the eigenvalues and the corresponding eigenvectors has been discussed and used successfully by many researchers, such as Fox and Kapoor [19], Wilkinson [38], and Bradbury and Fletcher [43]. Further it has been concluded by these researchers that the method of conjugate gradients is quite suitable for the minimization of the function of Eq. (2.3-15), because it is efficient and requires minimum additional computer storage. Also, the method does not require generation and storage of the matrices K and M for the entire structure, because all calculations can proceed elementwise. For more details the reader is referred to Refs. 19 and 43.

There is, however, one difficulty with this procedure of computing eigenvalues. Convergence to an eigenvalue and the corresponding eigenvector can be quite slow if a good initial guess of eigenvector is not known. Some methods of selecting initial eigenvectors have been suggested [19,43,44], but no general procedure exists to alleviate this problem. Therefore, in the present work, an approximate eigenvalue problem is solved to obtain a good starting point for the conjugate gradient method. The approximate eigenvalue problem is defined, using the procedure of Refs. 34, 44, 45, and 46, as follows:

$$K_B y_B = \zeta_B M_B y_B \tag{2.3-16}$$

where M_B is a (n,n) condensed mass matrix, ζ_B is an eigenvalue, and $y_B \in R^n$ is a vector of generalized coordinates associated with the boundary degrees of freedom. The procedure for defining the approximate eigenvalue problem is summarized in Appendix I, for easy reference.

The approximate eigenvalue problem of Eq. (2.3-16) may be solved by any of the previously mentioned methods, because K_B and its decomposition are available from static analysis of the structure. In the present work, the method of Subspace Iteration [35], which has been used quite successfully [1,30,47], is employed. Once y_B is known, the approximate eigenvector for the entire structure is computed from the following equation (Appendix I):

$$y = \begin{bmatrix} I \\ \\ Q \end{bmatrix} y_B \qquad (2.3\text{-}17)$$

Thus, in the proposed method of frequency analysis, the approximate problem of Eq. (2.3-16) is solved by Subspace Iteration [35] only in the first iteration. In all subsequent iterations, the method of conjugate gradients is used to minimize the Rayleigh Quotient to obtain the lowest eigenvalue and the corresponding eigenvector.

2.4 Statement of the Optimal Design Problem with Substructuring (ODPS)

In this section, the optimal design problem of Section 2.2 is redefined in terms of new state variables z_B and z_I, as follows: find a design variable vector b that minimizes the cost function

$$J = J(b, z_B, z_I, \zeta) \tag{2.4-1}$$

satisfies the equilibrium equations (state equations)

$$K_B z_B = F_B \tag{2.3-2R}$$

$$K_{II}^{(r)} z_I^{(r)} = S_I^{(r)} - K_{IB}^{(r)} z_B^{(r)} \quad ; \quad r = 1 \text{ to } L \tag{2.3-7R}$$

$$Ky = \zeta My \tag{2.2-3R}$$

and satisfies the constraints

$$\phi^s(b, z_B, z_I) \leq 0 \tag{2.4-2}$$

$$\phi^d(b) \leq 0 \tag{2.2-5R}$$

$$\phi^e(\zeta) \leq 0 \tag{2.2-6R}$$

where $\phi^s(b, z_B, z_I) \in R^{c_1}$, $\phi^d(b) \in R^{c_2}$ and $\phi^e(\zeta) \in R^1$. For computational convenience and efficiency, it is desirable to divide the member forces and nodal displacements, for which design sensitivity information is required, into two subsets: 1) a subset consisting of member forces and nodal displacements that explicitly depend upon the design parameters b, boundary displacements z_B, and interior displacements z_I; and 2) a subset consisting of member forces and nodal displacements that depend on design parameters b and the boundary displacements z_B only. Thus, the constraints of Eq. (2.4-2) are rewritten as:

$$\phi^{s1}(b, z_B, z_I) \leq 0 \tag{2.4-3}$$

$$\phi^{s2}(b, z_B) \leq 0 \tag{2.4-4}$$

where $\phi^{s1}(b, z_B, z_I) \in R^{\gamma_1}$ and $\phi^{s2}(b, z_B) \in R^{\gamma_2}$, such that $c_1 = \gamma_1 + \gamma_2$.

Terms which are used frequently in subsequent chapters are now defined.

Def: The set of points $b \in R^D$ that satisfies constraints of Eqs. (2.2-5), (2.2-6), (2.4-3), and (2.4-4) is called the constraint set for ODPS.

Def: A constraint $\phi_i \leq 0$ is said to be active if $\phi_i \geq 0$.

Def: A constraint $\phi_i \leq 0$ is said to be ε-active if $\phi_i + \varepsilon \geq 0$, where ε is a small positive number.

It should be noted here that assumptions on continuous differentiability of cost and constraint functions, linear independence of constraint gradients, and closedness and boundedness of the constraint set are made in the present work.

2.5 Design Sensitivity Analysis with Substructuring

The philosophy of an iterative technique is to start with the best engineering estimate of the design variable vector b and to improve it until an optimum is reached. One must determine the effect of a design change on the cost and constraint functions before a

design improvement δb can be calculated. This is known as design sensitivity analysis. In this section, design sensitivity matrices for cost and constraint functions are derived. In the derivation first order Taylor's expansion and certain adjoint relationships are employed. First, the design sensitivity analysis of a general function is considered. Then the analysis is specialized to the ODPS, defined in Section 2.4.

2.5.1 General Approach

Let $\psi(b, z_B, z_I, \zeta) \in R^{\gamma}$ represents a general vector function. The function ψ will be scalar if it represents the cost function. When the design is changed by a small amount δb, the displacements z_B and z_I, and the eigenvalue ζ will also change by small amounts δz_B, δz_I, and $\delta\zeta$; due to the well posed nature of the structural analysis problem. Let $\delta\psi$ represent a first order change in the function ψ. Then, taking b, z_B, z_I, and ζ as independent variables, $\delta\psi$ is given as

$$\delta\psi = \frac{\partial\psi}{\partial b}\,\delta b + \frac{\partial\psi}{\partial z_B}\,\delta z_B + \frac{\partial\psi}{\partial z_I}\,\delta z_I + \frac{\partial\psi}{\partial\zeta}\,\delta\zeta \qquad (2.5\text{-}1)$$

where the derivatives $\frac{\partial\psi}{\partial b}$, $\frac{\partial\psi}{\partial z_B}$, $\frac{\partial\psi}{\partial z_I}$, and $\frac{\partial\psi}{\partial\zeta}$ are computed at the previously known values of b, z_B, z_I, and ζ. The problem is now to express $\frac{\partial\psi}{\partial z_B}\,\delta z_B$, $\frac{\partial\psi}{\partial z_I}\,\delta z_I$, and $\frac{\partial\psi}{\partial\zeta}\,\delta\zeta$ in terms of δb, so that $\delta\psi$ in Eq. (2.5-1) is expressed as $\frac{d\psi}{db}\,\delta b$. Let us first consider the terms $\frac{\partial\psi}{\partial z_B}\,\delta z_B$ and $\frac{\partial\psi}{\partial z_I}\,\delta z_I$. In order to obtain these expressions in terms of δb, first order expansions of the partitioned state Eq. (2.3-1), are written as:

$$K_{BB}\ \delta z_B + K_{BI}\ \delta z_I = C_1\ \delta b \tag{2.5-2}$$

$$K_{IB}\ \delta z_B + K_{II}\ \delta z_I = C_2\ \delta b \tag{2.5-3}$$

where

$$\underset{(n,D)}{C_1} = \frac{\partial S_B}{\partial b} - \frac{\partial}{\partial b}\ (K_{BB}\ z_B) - \frac{\partial}{\partial b}\ (K_{BI}\ z_I) \tag{2.5-4}$$

and

$$\underset{(m,D)}{C_2} = \frac{\partial S_I}{\partial b} - \frac{\partial}{\partial b}\ (K_{IB}\ z_B) - \frac{\partial}{\partial b}\ (K_{II}\ z_I) \tag{2.5-5}$$

These derivatives are evaluated at the known values of b, z_B, and z_I. Using Eq. (2.5-3), one eliminates δz_I from Eq. (2.5-2) to obtain

$$K_B\ \delta z_B = C\delta b \tag{2.5-6}$$

where

$$\underset{(n,D)}{C} = C_1 + Q^T C_2 \tag{2.5-7}$$

Equation (2.5-6) is simply a first order expansion of Eq. (2.3-2). Now, define an adjoint matrix $\lambda_I(m,\gamma)$ to be a solution of

$$K_{II}\ \lambda_I = \frac{\partial \psi^T}{\partial z_I} \tag{2.5-8}$$

Taking the transpose of Eq. (2.5-8), postmultiplying by δz_I, and substituting from Eq. (2.5-3), one obtains

$$\lambda_I^T[C_2\ \delta b - K_{IB}\ \delta z_B] = \frac{\partial \psi}{\partial z_I}\ \delta z_I \tag{2.5.9}$$

The right hand side of Eq. (2.5-9) is exactly the term needed in Eq. (2.5-1), so making a substitution, one obtains

$$\delta\psi = \left[\frac{\partial \psi}{\partial b} + \lambda_I^T\ C_2\right]\ \delta b + \left[\frac{\partial \psi}{\partial z_B} - \lambda_I^T\ K_{IB}\right]\delta z_B + \frac{\partial \psi}{\partial \zeta}\ \delta\zeta \tag{2.5-10}$$

Another adjoint matrix $\lambda_B(n,\gamma)$ is defined to be a solution of

$$K_B\lambda_B = \frac{\partial \psi^T}{\partial z_B} - K_{BI}\ \lambda_I \tag{2.5-11}$$

Substituting for λ_I from Eq. (2.5-8) and making use of Eq. (2.3-5), one reduces Eq. (2.5-11) to

$$K_B\lambda_B = \frac{\partial \psi^T}{\partial z_B} + Q^T\ \frac{\partial \psi^T}{\partial z_I} \tag{2.5-12}$$

Thus, λ_B is a solution of Eq. (2.5-12). Taking the transpose of Eq. (2.5-11), postmultiplying by δz_B, and using Eq. (2.5-6), one obtains

$$\lambda_B^T\ C\delta b = \left[\frac{\partial \psi}{\partial z_B} - \lambda_I^T\ K_{IB}\right]\ \delta z_B \tag{2.5-13}$$

The right hand side of Eq. (2.5-13) is exactly the term needed in Eq. (2.5-10), so making a substitution, one obtains

$$\delta\psi = \left[\frac{\partial\psi}{\partial b} + \lambda_I^T C_2 + \lambda_B^T C\right] \delta b + \frac{\partial\psi}{\partial\zeta}\delta\zeta \qquad (2.5\text{-}14)$$

Now one must treat the expression $\frac{\partial\psi}{\partial\zeta}\delta\zeta$. The design sensitivity analysis of the eigenvalue ζ has been considered by many researchers [19,27,30]. Therefore, this development is only summarized here. From the first order expansion of Eq. (2.2-3) and, using the fact that K(b) and M(b) are symmetric, one obtains the following expression for $\delta\zeta$:

$$\delta\zeta = \left[y^T\left\{\frac{\partial}{\partial b}[K(b)y] - \zeta\frac{\partial}{\partial b}[M(b)y]\right\}\right] \delta b / y^T M(b) y \qquad (2.5\text{-}15)$$

Substituting this expression for $\delta\zeta$ in Eq. (2.5-14), one obtains

$$\delta\psi = G^T \delta b \qquad (2.5\text{-}16)$$

where

$$\underset{(D,\gamma)}{G} = \frac{\partial\psi^T}{\partial b} + C_2^T \lambda_I + C^T \lambda_B + \lambda^e \qquad (2.5\text{-}17)$$

and

$$\lambda^e = \left[\frac{\partial}{\partial b}\left\{K(b)y\right\} - \zeta\frac{\partial}{\partial b}\left\{M(b)y\right\}\right]^T y \frac{\partial\psi^T}{\partial\zeta} \Big/ y^T M(b) y \qquad (2.5\text{-}18)$$

Equation (2.5-16) is the desired relationship between the design change and the changes in member forces, nodal displacements, cost function, and eigenvalue. Columns of the matrix G are the required design sensitivity vectors.

In Refs. 2, 3, 5, and 16, the optimal design problem is formulated in design space only. Thus, a design sensitivity matrix G corresponding to Eq. (2.5-17) must be expressed as

$$G = \left[\frac{\partial \psi}{\partial b} + \frac{\partial \psi}{\partial z_B} \frac{\partial z_B}{\partial b} + \frac{\partial \psi}{\partial z_I} \frac{\partial z_I}{\partial b} + \frac{\partial \psi}{\partial \zeta} \frac{\partial \zeta}{\partial b} \right]^T \qquad (2.5\text{-}17a)$$

This method of computing the matrix G requires explicit calculations of matrices $\frac{\partial z_B}{\partial b}$, $\frac{\partial z_I}{\partial b}$, and $\frac{\partial \zeta}{\partial b}$. Computation of $\frac{\partial \zeta}{\partial b}$ may be calculated as in Eq. (2.5-18). Calculation of $\frac{\partial z_B}{\partial b}$ and $\frac{\partial z_I}{\partial b}$, however, is accomplished by formally differentiating the state equations (2.3-2) and (2.3-7), respectively.

It is shown in Ref. 10 that the equation for calculation of the matrix $\frac{\partial z_B}{\partial b}$ is similar to Eq. (2.5-12), but with a different right hand side. The equation for calculation of $\frac{\partial z_I}{\partial b}$ can be derived using $\frac{\partial z_B}{\partial b}$, and is similar to Eq. (2.5-8), but with a different right hand side. Some of the calculations of this approach are similar to the state space approach, but the major difference is in the number of vectors in the right hand side of Eqs. (2.5-8) and (2.5-12) and in the number of calculations required to generate the right hand side. In the state space formulation, the right hand sides of these equations are generated quite readily. Also, the number of vectors in the right hand side of Eq. (2.5-8) is equal to the number of active constraints that depend upon any component of the vector z_I. Similarly, the number of vectors in the right hand side of Eq. (2.5-12) is equal to the total number of active constraints. In the purely design space formulation, the

number of vectors in the right hand side of Eqs. (2.5-8) and (2.5-12) is equal to the interior and boundary degrees of freedom for the entire structure. This number is generally much larger than the number of active constraints. Thus, the state space formulation should be more efficient.

2.5.2 Reduction of Design Sensitivity Matrices for the ODPS

In the following development, let a ~ over a constraint function represent inclusion of only the active constraints. Linear expansions of the cost function of Eq. (2.4-1) and the constraints of Eqs. (2.4-3), (2.4-4), (2.2-5), and (2.2-6), with the procedure outlined above, yield the following expressions:

$$\delta J = \Lambda^{J^T} \delta b \tag{2.5-19}$$

$$\delta \tilde{\phi}^{s1} = \Lambda^{s1^T} \delta b \tag{2.5-20}$$

$$\delta \tilde{\phi}^{s2} = \Lambda^{s2^T} \delta b \tag{2.5-21}$$

$$\delta \tilde{\phi}^{d} = \Lambda^{d^T} \delta b \tag{2.5-22}$$

and

$$\delta \tilde{\phi}^{e} = \Lambda^{e^T} \delta b \tag{2.5-23}$$

where the vector Λ^J and other Λ matrices are obtained from Eqs. (2.5-15), (2.5-17), and (2.5-18), as follows:

$$\Lambda^J = \frac{\partial J^T}{\partial b} + C_2^T \lambda_I^J + C^T \lambda_B^J + \Lambda^{eJ} \tag{2.5-24}$$

$$\Lambda^{s1} = \frac{\partial \tilde{\phi}^{s1^T}}{\partial b} + C_2^T \lambda_I^{s1} + C^T \lambda_B^{s1} \tag{2.5-25}$$

$$\Lambda^{s2} = \frac{\partial \tilde{\phi}^{s2^T}}{\partial b} + C^T \lambda_B^{s2} \tag{2.5-26}$$

$$\Lambda^d = \frac{\partial \tilde{\phi}^{d^T}}{\partial b} \tag{2.5-27}$$

$$\Lambda^e = \frac{\partial \tilde{\phi}^e}{\partial \zeta} \left[\frac{\partial}{\partial b} \left\{ K(b)y \right\} - \zeta \frac{\partial}{\partial b} \left\{ M(b)y \right\} \right]^T y / y^T M(b) y \tag{2.5-28}$$

and

$$\Lambda^{eJ} = \frac{\partial J}{\partial \zeta} \left[\frac{\partial}{\partial b} \left\{ K(b)y \right\} - \zeta \frac{\partial}{\partial b} \left\{ M(b)y \right\} \right]^T y / y^T M(b) y \tag{2.5-29}$$

The vectors λ_I^J and λ_B^J, and the matrices λ_I^{s1}, λ_B^{s1}, and λ_B^{s2} are solutions of the following equations:

$$K_{II} \lambda_I^J = \frac{\partial J^T}{\partial z_I} \tag{2.5-30}$$

$$K_B \lambda_B^J = \frac{\partial J^T}{\partial z_B} + Q^T \frac{\partial J^T}{\partial z_I} \tag{2.5-31}$$

$$K_{II}\ \lambda_I^{s1} = \frac{\partial \tilde{\phi}^{s1^T}}{\partial z_I} \tag{2.5-32}$$

$$K_B\ \lambda_B^{s1} = \frac{\partial \tilde{\phi}^{s1^T}}{\partial z_B} + Q^T \frac{\partial \tilde{\phi}^{s1^T}}{\partial z_I} \tag{2.5-33}$$

and

$$K_B\ \lambda_B^{s2} = \frac{\partial \tilde{\phi}^{s2^T}}{\partial z_B} \tag{2.5-34}$$

2.6 Optimal Design Algorithm

Now, certain restrictions are placed on the linearized constraint functions. It is required that the design change δb be computed in such a manner that it corrects, or at least improves, all the violated constraints. These requirements on Eqs. (2.5-20) to (2.5-23), can be stated in the form of the following inequalities:

$$\Lambda^{s1^T}\ \delta b \leq \Delta\tilde{\phi}^{s1} \tag{2.6-1}$$

$$\Lambda^{s2^T}\ \delta b \leq \Delta\tilde{\phi}^{s2} \tag{2.6-2}$$

$$\Lambda^{d^T}\ \delta b \leq \Delta\tilde{\phi}^{d} \tag{2.6-3}$$

$$\Lambda^{e^T}\ \delta b \leq \Delta\tilde{\phi}^{e} \tag{2.6-4}$$

where $\Delta\tilde{\phi}^{s1}$, $\Delta\tilde{\phi}^{s2}$, $\Delta\tilde{\phi}^{d}$, and $\Delta\tilde{\phi}^{e}$ are desired corrections in constraint violations. If a constraint $\phi_i \leq 0$ is active, then $\Delta\tilde{\phi}_i = -a_i\phi_i$ with $a_i \geq 0$. The positive multiplier $a_i (0 \leq a_i \leq 1.0)$ is chosen by the designer and is simply a scale factor for the amount of violation to be corrected. In many instances, it may be desirable to call for only a partial correction of the constraint violation. In such a case $a_i < 1$. If full correction of the constraint violation is required then $a_i = 1$.

The constraints of Eqs. (2.6-1) to (2.6-4) have similar forms, so they can be written in a compact form as

$$A^T \delta b \leq \Delta\tilde{\phi} \tag{2.6-5}$$

where

$$A = \left[A^{s1} \; A^{s2} \; A^{d} \; A^{e}\right] \tag{2.6-6}$$

and

$$\Delta\tilde{\phi} = \left[\Delta\tilde{\phi}^{s1^T} \; \Delta\tilde{\phi}^{s2^T} \; \Delta\tilde{\phi}^{d^T} \; \Delta\tilde{\phi}^{e^T}\right]^T \tag{2.6-7}$$

The reduced problem of computing an optimum design change δb can now be stated as follows: find δb to minimize the cost function of Eq. (2.5-19), subject to the constraint of Eq. (2.6-5) and the step size constraint

$$\delta b^T W \delta b \leq \varepsilon^2 \tag{2.6-8}$$

where W is a positive definite weighting matrix and ξ is a small number. The matrix W, usually diagonal, is used to assign weights to the various components of δb and is often necessary when components of b represent different physical quantities of different orders of magnitude. The reduced ODPS defined above is exactly the problem defined in Refs. 1 and 27. An application of the Kuhn-Tucker conditions of nonlinear programming gives the following solution [1,27]:

$$\delta b = \eta \delta b^1 + \delta b^2 \tag{2.6-9}$$

$$\delta b^1 = -W^{-1} [\Lambda^J + \Lambda \mu^1] \tag{2.6-10}$$

$$\delta b^2 = -W^{-1} \Lambda \mu^2 \tag{2.6-11}$$

$$H[\mu^1 \vdots \mu^2] = [(-\Lambda^T W^{-1} \Lambda^J) \vdots -\Delta\tilde{\phi}] \tag{2.6-12}$$

$$H = \Lambda^T W^{-1} \Lambda \tag{2.6-13}$$

$$\mu = \mu^1 + (1/\eta)\, \mu^2 \tag{2.6-14}$$

where $\eta > 0$ is a step size to be chosen by the designer and $\mu \geq 0$ is a Lagrange multiplier vector. The method of step size selection is the same as used in Refs. 27, 33, and 41.

The method can now be described by the following step-by-step algorithm:

Step 1. At the jth design point $b^{(j)}$, generate the matrices $K_{II}^{(r)}$ and $K_{IB}^{(r)}$ for each substructure. Decompose each $K_{II}^{(r)}$ and

calculate the matrix $Q^{(r)}$ from Eq. (2.3-11). Store the decomposed part of the matrix $K_{II}^{(r)}$ and the matrix $Q^{(r)}$ for later calculations. Calculate the boundary stiffness matrix K_B and the effective boundary load vector F_B from Eqs. (2.3-12) and (2.3-13), respectively. Decompose the matrix K_B and store it for later use.

Step 2. Calculate the boundary displacements z_B from Eq. (2.3-2) and the interior displacements $z_I^{(r)}$ for each substructure from Eq. (2.3-7).

Step 3. Calculate the lowest eigenvalue and corresponding eigenvector from Eq. (2.3-15). If j=1, then an approximate eigenvector for the Rayleigh Quotient is obtained from Eqs. (2.3-16) and (2.3-17).

Step 4. Compute the vectors λ_I^J and λ_B^J from Eqs. (2.5-30) and (2.5-31), respectively. Assemble the matrix Λ^J of Eq. (2.5-24).

Step 5. Check the frequency constraint of Eq. (2.2-6). If it is violated, then compute Λ^e of Eq. (2.5-28), and put $\Delta\tilde{\phi}^e = -a_i\tilde{\phi}_i^e$.

Step 6. Check the constraints of Eq. (2.4-2) and form the vectors $\tilde{\phi}^{s1}$ and $\tilde{\phi}^{s2}$ of Eqs. (2.4-3) and (2.4-4), respectively. Calculate the sensitivity information $\frac{\partial\tilde{\phi}^{s1}}{\partial b}$, $\frac{\partial\tilde{\phi}^{s1}}{\partial z_B}$, and $\frac{\partial\tilde{\phi}^{s1}}{\partial z_I}$. Calculate $\frac{\partial\tilde{\phi}^{s2}}{\partial b}$, and $\frac{\partial\tilde{\phi}^{s2}}{\partial z_B}$ simultaneously. Also calculate $\Delta\tilde{\phi}^{s1}$ and $\Delta\tilde{\phi}^{s2}$.

Step 7. Calculate $\lambda_I^{s1(r)}$ for each substructure from Eq. (2.5-32). Also, calculate the matrices λ_B^{s1} and λ_B^{s2} from Eqs. (2.5-33) and (2.5-34), respectively. The latter calculations are performed simultaneously.

Step 8. Calculate the matrices C_1 and C_2 from Eqs. (2.5-4) and (2.5-5), respectively. Also, calculate the matrix C from Eq. (2.5-7).

Step 9. Assemble the matrices Λ^{s1} and Λ^{s2} of Eqs. (2.5-25) and (2.5-26), respectively.

Step 10. Check the constraints of Eq. (2.2-5) and form a vector $\tilde{\phi}^d$. Compute the matrix Λ^d of Eq. (2.5-27). Also, compute $\Delta\tilde{\phi}^d$.

Step 11. Finally, assemble the matrix Λ and $\Delta\tilde{\phi}$ of Eqs. (2.6-6) and (2.6-7), respectively.

Step 12. Compute μ^1 and μ^2 from Eq. (2.6-12). Choose a step size η and compute the Lagrange multiplier from Eq. (2.6-14).

Step 13. Check the sign of each component of μ. If any component of μ is negative, remove the corresponding row from Λ^T and $\Delta\tilde{\phi}$ and return to Step 12.

Step 14. Compute δb^1, δb^2, and δb from Eqs. (2.6-10), (2.6-11), and (2.6-9), respectively. Put $b^{(j+1)} = b^{(j)} + \delta b$ and $y^{(j+1)} = y^{(j)}$.

Step 15. If all constraints are satisfied and $||\delta b^1||_2 = [\delta b^{1^T} W \delta b^1]^{1/2}$ is sufficiently small [27], terminate the process. Otherwise, return to Step 1 with $b^{(j+1)}$ as the best available design.

CHAPTER 3

DISCUSSION OF THE METHOD AND COMPUTATIONAL CONSIDERATIONS

3.1 Introduction

The method for ODPS of Chapter 2 is quite general and can be applied to any type of structure, because no assumption is made regarding the type of structural elements. However, details of application of the method to various types of structures, such as trusses, frames, plates, aircraft wing structures, and shells, will be quite different. This is due to the fact that the structural analysis and the design sensitivity analysis are quite different for different types of structures. The types of design variables for different structures are also of a different nature. Therefore, in this chapter, only those computational aspects of the method which are common to all types of structures are discussed.

3.2 Design Variable Linking

Due to many practical design considerations, such as symmetry in the structure, fabrication, and joint connections, it is desirable to constrain some elements of a structure to the same design variable values. This is also known as grouping of elements [30] or linking of design variables. Elements of the structure are divided into a number of groups and one design variable is assigned to each group of elements. Recently, Pickett, Rubinstein, and Nelson [48] have tried to generalize

the idea of reducing the number of design variables by using the well known reduced basis concept. A reduced set of design variables is introduced by the transformation

$$\tilde{b} = Ub \tag{3.2-1}$$

where

$\tilde{b}$ = a vector of $\tilde{D}$ original design variables,

b = a vector of D reduced original variables,

U = a matrix $(\tilde{D},D)$ whose columns are the base vectors,

and $\tilde{D} >> D$. A number of techniques have been suggested [48] for selecting the base vectors, including

(i) design variable linking,

(ii) optimality criteria solutions, and

(iii) upper and lower bound solutions.

Techniques for selection of base vectors for a reduced design basis, however, need further work [1,48,49] and are, therefore, not employed with the present algorithm. When design variable linking is used, the form of the matrix U is quite simple. The ith row of U contains only a unit positive element at the jth location, indicating that the ith element is linked to the jth design variable. In the case where design variable linking is not required, U is simply the identity matrix. Design variable linking can be readily incorporated in the algorithm of Chapter 2.

3.3 Computational Considerations in Structural Analysis

Structural analysis is an important part of the optimal design algorithm. Therefore, extra effort should be devoted to make this portion of the algorithm as efficient as possible. In this section, structural analysis computations relative to ODPS are briefly described.

In static analysis of structures, the response variables to be determined are the boundary displacements z_B, the interior displacements for each substructure $z_I^{(r)}$, the lowest eigenvalue ζ, and the element stresses. Before these response quantities can be computed, the boundary stiffness matrix K_B and the interior stiffness matrices for each substructure $K_{II}^{(r)}$ must be computed. The former matrix is computed by summing contributions from each substructure (Eq. (2.3-12)). The nodes of a substructure are numbered in a manner such that they give smallest bandwidth for $K_{II}^{(r)}$. The interior stiffness matrices are decomposed and saved for later use. The matrix $Q^{(r)}$ is also computed for each substructure and saved. Contribution to the effective boundary load matrix from the interior load matrix for each substructure is also computed here. The boundary nodes for the entire structure are numbered in a way such that K_B has the smallest bandwidth. The matrix K_B is also decomposed and saved for later use. The boundary displacements z_B for the entire structure, under all loading conditions, are computed from Eq. (2.3-2). Then, each substructure is considered separately and the interior displacements $z_I^{(r)}$ are computed from Eq. (2.3-7). Finally element forces $p^{(r)}$ for each substructure are

computed from Eq. (2.3-14). It may be noted here that the element forces are computed elementwise, without assembling the matrix $K^{(r)}$.

In frequency analysis, the fundamental frequency of the structure is computed by minimizing the Rayleigh Quotient of Eq. (2.3-15). Thus, the problem is to find an eigenvector y such that the Rayleigh Quotient of Eq. (2.3-15) is minimized, subject to one of the following normalization constraints:

(i) The Euclidean norm constraint, i.e., $y^T y = 1$

(ii) The M-norm constraint, i.e., $y^T My = 1$

(iii) The sum (L_1) norm constraint, i.e., $\sum_i |y_i| = 1$, and

(iv) The maximum (L_∞) norm constraint, i.e., $\max_i |y_i| = 1$.

These constraints make the minimization problem for Eq. (2.3-15) constrained. The last constraint being the simplest, is employed by many researchers [19,43]. In this approach, $\max_i |y_i|$ is determined at the first iteration of the minimization procedure and the vector is scaled so that this component is unity. The corresponding component of gradient of the Rayleigh Quotient is set to zero. The minimization problem is then treated as an unconstrained problem.

The first three approaches can also be used, in which case a component of the eigenvector is found from the equality constraint and eliminated from Eq. (2.3-15). The reduced minimization problem is then unconstrained. The later approaches, however, introduce complications in the structural problem, because matrices K and M will have to be computed and stored. Therefore, in the present approach, constraint

(iv) is selected, since it can easily be programmed as an integral part of the finite element formulation of the ODPS.

The Rayleigh Quotient and its gradient

$$\nabla\bar{R}(y) = 2(Ky - \bar{R}(y)My)/(y^T My) \tag{3.3-1}$$

are computed by considering an element of the structure at a time. Thus, all calculations for frequency analysis proceed elementwise. As pointed out in Chapter 2, the conjugate gradient method is used for the minimization of Rayleigh Quotient. In this method, one starts with an initial estimate y_o of the eigenvector. The conjugate gradient algorithm is described by the following iterative equation:

$$y_{i+1} = y_i + \alpha_i s_i \quad ; \quad i = 0,1,2,... \tag{3.3-2}$$

where

$$s_{i+1} = - g_{i+1} + \beta_i s_i \tag{3.3-3}$$

$$g_{i+1} = \nabla\bar{R}(y_{i+1}) \tag{3.3-4}$$

$$\beta_i = \frac{|g_{i+1}|^2}{|g_i|^2} \tag{3.3-5}$$

$$s_o = - g_o \tag{3.3-6}$$

$$g_o = \nabla\bar{R}(y_o) \tag{3.3-7}$$

and α_i is a step size for the ith iteration. In determining the step size, a quadratic interpolation formula is used. The necessary condition, i.e., $\frac{d}{d\alpha_i}[\bar{R}(y_i + \alpha_i s_i)] = 0$, yields the following quadratic expression for determining α_i [43]:

$$A_1\alpha_i^2 + A_2\alpha_i + A_3 = 0 \tag{3.3-8}$$

where

$$A_1 = (s_i^T K s_i)(y_i^T M s_i) - (y_i^T K s_i)(s_i^T M s_i) \tag{3.3-9}$$

$$A_2 = (s_i^T K s_i)(y_i^T M y_i) - (y_i^T K y_i)(s_i^T M s_i) \tag{3.3-10}$$

$$A_3 = (y_i^T K s_i)(y_i^T M y_i) - (y_i^T K y_i)(y_i^T M s_i) \tag{3.3-11}$$

Two roots of Eq. (3.3-8) correspond to the maximum and minimum values of Rayleigh Quotient in the direction s_i. Further the positive and negative roots of Eq. (3.3-8) correspond to the minimum and maximum function values [43]. This forms a convenient criterion for selecting the value of α_i. It may be pointed out here that most computations in the Rayleigh Quotient, its gradient, and the step size can proceed simultaneously.

As pointed out earlier, a good estimate of the eigenvector must be available for fast convergence of the conjugate gradient method. Therefore, the approximate eigenvalue problem of Eq. (2.3-16) is solved to obtain a good starting eigenvector. The Subspace Iteration method

[35], used for solving the approximate eigenvalue problem, requires computation of the boundary mass matrix M_B. This matrix is assembled in the same way as the matrix K_B. After the first design cycle, the approximate problem of Eq. (2.3-16) is not solved, since the previous solution provides a good initial estimate of the eigenvector for the subsequent design cycle. Thus, substructuring is not required for frequency analysis after first design cycle. Finally, convergence criteria, based on the function value, norm of the eigenvector, and the gradient of Rayleigh Quotient, are used [19, 38]. These are expressed as

$$\left| \frac{\bar{R}(y_{i+1}) - \bar{R}(y_i)}{\bar{R}(y_i)} \right| \leq \varepsilon_1 \tag{3.3-12}$$

$$||y_{i+1} - y_i||_2 \leq \varepsilon_2 \tag{3.3-13}$$

and

$$||\nabla \bar{R}(y_i)||_2 \leq \varepsilon_3 \tag{3.3-14}$$

where $\varepsilon_i > 0$, i = 1 to 3, are specified small numbers.

3.4 Multiple Loading Conditions and Constraint Checks

Most structures are designed to withstand multiple loading conditions. This situation is handled in formulation of the ODPS by expanding the state variable vectors z_B and z_I to include all states.

The element force vector is expanded accordingly, and the stress and displacement constraints are checked under each loading condition.

The number of constraints in ODPS is quite large. So, an effort should be made to logically delete constraints which will not be critical at the optimum. In the present research, the idea of "worst violated constraint" is used, in order to eliminate redundant constraints. In the case of stress constraints, worst violation under all loading conditions and for all elements of a group is imposed, instead of for each element under each loading condition. Thus, the ith stress constraint is

$$\phi_i \leq 0 \tag{3.4-1}$$

where

$$\phi_i = \max_{j,k} \{\phi^s_{ijk}\ (b, z_B, z_I)\},$$

$$j = 1 \text{ to NMG; and } k = 1 \text{ to NLC} \tag{3.4-2}$$

where NMG is the number of elements in the ith group and NLC is the number of loading conditions. Similarly, a displacement constraint for the ith degree of freedom is imposed on the worst violation, under all loading conditions

$$\phi_i = \max_{j} \{\phi^s_{ij}\ (b, z_B, z_I)\},\ \ j = 1 \text{ to NLC} \tag{3.4-3}$$

In this procedure, the number of violated constraints is reduced considerably. Also, design sensitivity calculations of redundant constraints are not performed, which improves efficiency of the algorithm.

A number of other computational aspects are also considered in the present algorithm. For example, all constraints of the problem are normalized with respect to their limit values. Thus each constraint is expressed as

$$\phi_i \equiv R_i^* - 1.0 \leq 0 \tag{3.4-4}$$

where R_i^* is a response ratio. The correction to any violated constraint is then given by

$$\Delta\tilde{\phi}_i = a_i (1.0 - R_i^*) \tag{3.4-5}$$

This procedure facilitates comparison of amount of the violation in various constraints.

Further, the ε-active constraint concept [1,47,50] is implemented quite readily in the algorithm. If a constraint is nearly tight, then it is included in the violated constraint set. This procedure increases the number of constraint violations but eventually helps in avoiding oscillations in constraint violations.

3.5 Computational Considerations in Design Sensitivity Analysis

Computation of the sensitivity vectors $\frac{\partial J}{\partial b}$, $\frac{\partial J}{\partial z_I}$, $\frac{\partial J}{\partial z_B}$, and $\frac{\partial J}{\partial \zeta}$ and sensitivity matrices $\frac{\partial \tilde{\phi}^{s1}}{\partial b}$, $\frac{\partial \tilde{\phi}^{s1}}{\partial z_B}$, $\frac{\partial \tilde{\phi}^{s1}}{\partial z_I}$, $\frac{\partial \tilde{\phi}^{s2}}{\partial z_B}$, $\frac{\partial \tilde{\phi}^{d}}{\partial b}$, and $\frac{\partial \tilde{\phi}^{e}}{\partial \zeta}$ are

quite easy, once the form of the cost function and the constraint function have been determined.

Now consider computation of the matrix Λ of Eq. (2.6-6). This requires generation of matrices Λ^{s1}, Λ^{s2}, Λ^{d}, and Λ^{e}, which further require the calculation of matrices λ_I^{s1}, λ_B^{s1}, λ_B^{s2}, C_2,C, etc. The computation of matrix λ_I^{s1} from Eq. (2.5-32) can proceed substrucure-wise, since K_{II} for each substructure is completely uncoupled and is available from static analysis in the decomposed form. Let $\bar{\gamma}(r)$ be the number of components of $\tilde{\phi}^{s1}$ that depend upon $z_I^{(r)}$. Then $\gamma_1 = \sum_{r=1}^{L} \bar{\gamma}(r)$. The matrix $\frac{\partial \tilde{\phi}^{s1}}{\partial z_I}$ is partitioned as

$$\frac{\partial \tilde{\phi}^{s1}}{\partial z_I} = \begin{bmatrix} \frac{\partial \tilde{\phi}^{s1}}{\partial z_I^{(1)}} & & 0 \\ & \frac{\partial \tilde{\phi}^{s1}}{\partial z_I^{(2)}} & \\ & & \ddots \\ 0 & & \frac{\partial \tilde{\phi}^{s1}}{\partial z_I^{(L)}} \end{bmatrix} \tag{3.5-1}$$

where $\frac{\partial \tilde{\phi}^{s1}}{\partial z_I^{(r)}}$ is a $[\bar{\gamma}(r), m(r)]$ matrix. The matrix λ_I^{s1} is partitioned accordingly as

$$\lambda_I^{s1} = \begin{bmatrix} \lambda_I^{s1(1)} & & 0 \\ & \lambda_I^{s1(2)} & \\ & & \ddots \\ 0 & & \lambda_I^{s1(L)} \end{bmatrix} \tag{3.5-2}$$

where each $\lambda_I^{sl(r)}$ is a [m(r), $\bar{\gamma}$(r)] matrix. Now, the matrix $\lambda_I^{sl(r)}$ is computed from the equation

$$K_{II}^{(r)} \lambda_I^{sl(r)} = \left[\frac{\partial \tilde{\phi}^{sl}}{\partial z_I^{(r)}} \right]^T \tag{3.5-3}$$

In case design variable linking of elements across substructure boundaries does not occur and S_I is taken independent of b, the matrix C_2 of Eq. (2.5-5) is also partitioned as

$$C_2 = \begin{bmatrix} C_2^{(1)} & & 0 \\ & C_2^{(2)} & \\ & & \ddots \\ 0 & & C_2^{(L)} \end{bmatrix} \tag{3.5-4}$$

where each $C_2^{(r)}$ is a [m(r), D(r)] matrix and is given for the rth substructure by an expression similar to Eq. (2.5-5). Here, D(r) is the number of design variables for the rth substructure and $D = \sum_{r=1}^{L} D(r)$. Now, the matrix $C_2^T \lambda_I^{sl}$ of Eq. (2.5-25) is

$$C_2^T \lambda_I^{sl} = \begin{bmatrix} C_2^{(1)^T} \lambda_I^{sl(1)} & & 0 \\ & \ddots & \\ 0 & & C_2^{(L)^T} \lambda_I^{sl(L)} \end{bmatrix} \tag{3.5-5}$$

where each $C_2^{(r)^T} \lambda_I^{sl(r)}$ is a [D(r), $\bar{\gamma}$(r)] matrix.

In computing the matrix λ_B^{sl} from Eq. (2.5-33), a matrix $\frac{\partial \tilde{\phi}^{sl}}{\partial z_I} Q$ is required. This matrix is also computed quite readily, since the matrix Q in partitioned form is available from static analysis. Therefore, $Q^T \frac{\partial \tilde{\phi}^{sl}{}^T}{\partial z_I}$ is given as

$$Q^T \frac{\partial \tilde{\phi}^{sl}{}^T}{\partial z_I} = \begin{bmatrix} Q^{(1)T} \frac{\partial \tilde{\phi}^{sl}{}^T}{\partial z_I^{(1)}} & & 0 \\ & \ddots & \\ 0 & & Q^{(L)T} \frac{\partial \tilde{\phi}^{sl}{}^T}{\partial z_I^{(L)}} \end{bmatrix} \tag{3.5-6}$$

where each matrix $Q^{(r)T} \frac{\partial \tilde{\phi}^{sl}{}^T}{\partial z_I^{(r)}}$ is an $[n(r), \bar{\gamma}(r)]$ matrix.

Computation of the matrix $Q^T C_2$ in Eq. (2.5-7) is also carried out by considering one substructure at a time. From Eqs. (3.5-4) and (2.3-11) one obtains

$$Q^T C_2 = \begin{bmatrix} Q^{(1)T} C_2^{(1)} & & 0 \\ & \ddots & \\ 0 & & Q^{(L)T} C_2^{(L)} \end{bmatrix} \tag{3.5-7}$$

In calculation of matrices C_1 and C_2 of Eqs. (2.5-4) and (2.5-5), respectively, the terms $\frac{\partial S_B}{\partial b}$ and $\frac{\partial S_I}{\partial b}$ are quite simple, once the dependence of externally applied loads on the design variable is known. Usually, S_B and S_I are taken to be independent of the design variables.

Therefore, the terms $\frac{\partial S_B}{\partial b}$ and $\frac{\partial S_I}{\partial b}$ drop out of these equations. Other matrices, such as $\frac{\partial}{\partial b}(K_{BB}\ z_B)$, $\frac{\partial}{\partial b}(K_{BI}\ z_I)$, $\frac{\partial}{\partial b}(K_{IB}\ z_B)$, and $\frac{\partial}{\partial b}(K_{II}\ z_I)$, are assembled quite conveniently, elementwise. In this case, there are a few nonzero elements and only these are considered in calculations. Thus, knowing the matrices C_1 and C_2, matrix C of Eq. (2.5-7) is easily computed. Also, it is noted that computations for λ_B^{s1} and λ_B^{s2} proceed simultaneously. Further, computation of matrices $\frac{\partial}{\partial b}(Ky)$ and $\frac{\partial}{\partial b}(My)$ of Eqs. (2.5-28) and (2.5-29) are performed elementwise.

In case design variable linking of elements across substructure boundaries does occur, the matrix C_2 of Eq. (2.5-5) is not uncoupled, as given by Eq. (3.5-4). In this case, one needs to define a global numbering system for the design variables. It is easily seen that all computations still proceed substructurewise.

Calculation of the matrix Λ^J is similar to that of the matrix Λ.

3.6 Lagrange Multiplier Calculations

The Lagrange multiplier vector μ that is required for computation of the optimum design change δb is computed using Eq. (2.6-14). In order to enhance computational efficiency, special properties of the matrix Λ of Eq. (2.6-6) can be exploited. It may be noted that matrices Λ^{s1}, Λ^{s2}, and Λ^e do not possess any special properties, whereas Λ^d does when only fixed bounds on design variables are considered. Thus, the matrix Λ of Eq. (2.6-6) can be rewritten in partitioned form as

$$\Lambda = [\Lambda^{*} \quad \Lambda^{d}] \tag{3.6-1}$$

where

$$\Lambda^{*} = [\Lambda^{s1} \quad \Lambda^{s2} \quad \Lambda^{e}] \tag{3.6-2}$$

Similarly, $\Delta\tilde{\phi}$ of Eq. (2.6-7) and the coefficient matrix H of Eq. (2.6-13) can be partitioned as

$$\Delta\tilde{\phi} = \left[\Delta\tilde{\phi}^{*T} \quad \Delta\tilde{\phi}^{dT}\right]^{T} \tag{3.6-3}$$

and

$$H = \begin{bmatrix} H_{11} & H_{12} \\ H_{21} & H_{22} \end{bmatrix} \tag{3.6-4}$$

where

$$\Delta\tilde{\phi}^{*T} = \left[\Delta\tilde{\phi}^{s1T} \; \Delta\tilde{\phi}^{s2T} \; \Delta\tilde{\phi}^{eT}\right] \tag{3.6-5}$$

$$H_{11} = \Lambda^{*T} W^{-1} \Lambda^{*} \tag{3.6-6}$$

$$H_{12} = \Lambda^{*T} W^{-1} \Lambda^{d} \tag{3.6-7}$$

$$H_{21} = \Lambda^{dT} W^{-1} \Lambda^{*} \tag{3.6-8}$$

$$H_{22} = \Lambda^{dT} W^{-1} \Lambda^{d} \tag{3.6-9}$$

Further, when only bounds on design variables are considered, the matrix H_{22} is diagonal. This property of the matrix H is effectively utilized in computation of Lagrange multipliers. By expanding Eq. (2.6-12) and writing it for μ^1 in partitioned form, one obtains

$$\begin{bmatrix} H_{11} & H_{12} \\ H_{21} & H_{22} \end{bmatrix} \begin{bmatrix} \mu_1^1 \\ \mu_2^1 \end{bmatrix} = \begin{bmatrix} \bar{D}_1 \\ \bar{D}_2 \end{bmatrix} \tag{3.6-10}$$

where

$$\mu^1 = \begin{bmatrix} \mu_1^1 \\ \mu_2^1 \end{bmatrix} \tag{3.6-11}$$

$$\bar{D} = \begin{bmatrix} \bar{D}_1 \\ \bar{D}_2 \end{bmatrix} \tag{3.6-12}$$

and

$$\bar{D} = -\Lambda^T W^{-1} \Lambda^J \tag{3.6-13}$$

From Eq. (3.6-10), one obtains

$$H^* \mu_1^1 = D^* \tag{3.6-14}$$

and

$$\mu_2^1 = \left[H_{22}^{-1}\right] \left[\bar{D}_2 - H_{21}\, \mu_1^1\right] \tag{3.6-15}$$

where

$$H^* = H_{11} + A\, H_{21} \tag{3.6-16}$$

$$D^* = \bar{D}_1 + A\, \bar{D}_2 \tag{3.6-17}$$

and

$$A = - H_{12}\, H_{22}^{-1} \tag{3.6-18}$$

Thus μ_1^1 and μ_2^1 are determined from Eqs. (3.6-14) and (3.6-15), respectively. The vector μ^2 is computed using a similar approach. In the present work, a Gaussian elimination procedure with "total pivoting" is used for solving Eq. (3.6-14). Further, this method is adapted to handle dependent set of equations in Eq. (2.6-6). Other techniques, such as the Gram-Schmidt orthogonalization method, can also be used for removing dependent equations but they are usually computationally inefficient.

Lastly, it should be pointed out that in multi-dimensional structural problems, the number of violated design variable constraints can be quite large. Hence, the above approach provides considerable savings in computing time, as well as in computer core storage requirements.

3.7 Step Size Determination

Determination of a proper step size η is quite critical for rapid convergence of the optimization algorithm. There are many techniques presented in the literature [31] for determining a step to be taken in the constrained steepest descent direction. A simple technique presented in Ref. 31 and used successfully by many researchers [27,33,41] is also used here. Briefly, it consists of choosing η to yield a few percent reduction in cost function, when $\Delta\tilde{\phi} = 0$. This implies that for a desired reduction ratio $\bar{r}$ in the cost function, the step size η can be expressed as

$$\eta = \frac{\bar{r} \times J}{\Lambda J^T \delta b^1} \qquad (3.7\text{-}1)$$

It may be pointed out here that choosing η is still an art. In the present work, step size is specified based on the amount of constraint violations. It is chosen to be quite large if the design point lies in the interior of the constraint set, whereas a moderate step size is selected if there are violations. Further, a provision can be made to change the step size, if necessary, during computations.

3.8 Convergence Criterion and Computational Checks

In order to check the calculations for δb, computational checks of Theorem 4-16 [31], are implemented at each iteration of the algorithm. For easy reference, these checks are:

$$\delta b^{2^T} W \delta b^1 = 0 \tag{3.8-1}$$

$$\Lambda^T \delta b^1 = 0 \tag{3.8-2}$$

$$\Lambda^T \delta b^2 = \Delta\tilde{\phi} \tag{3.8-3}$$

and

$$-\Lambda^{J^T} \delta b^1 \leq 0 \tag{3.8-4}$$

Finally, since the cost function of Eq. (2.4-1), state equations (2.2-3) and (2.3-1), and constraints of Eqs. (2.2-5), (2.2-6), and (2.4-2) meet the hypotheses of Theorem 4-17 [31], the $||\delta b^1||_2$ is monitored as a convergence check for the ODPS. It is shown in Ref. [31] that as the algorithm approaches the optimum, $||\delta b^1||_2 \to 0$.

CHAPTER 4

OPTIMAL DESIGN OF TRUSS STRUCTURES

4.1 Introduction

In this chapter, the method developed for general ODPS is applied to plane and space trusses. These types of structures are encountered quite frequently in practical situations. Most common among these are industrial buildings, transmission towers, and spacecraft structures such as dispenser trusses and antennas. In all these cases, it is desirable that the structure should simultaneously meet strength, deflection, and natural frequency requirements and be of minimum weight.

The class of trusses considered herein is assumed to have a specified geometry and the loads are applied only at the joints. The objective function is taken as the total weight of the structure and the design variable for each member is taken as its cross-sectional area. Finally, it is assumed that the trusses are loaded so as to deform only elastically. The displacement method of structural analysis is used, considering nodal displacements of the truss as the basic state variables. Equations developed for structural analysis in Chapter 2 are used here. The stiffness and mass matrices used herein for a truss element are well documented in the literature [34]. For a complete derivation, the reader is referred to Ref. 34.

4.2 Reduction of the Method to Trusses

The ODPS for trusses can be defined as follows: find the cross-sectional area of each member of the truss, such that its weight is minimized and state equations, and constrains on stress, buckling, displacement, frequency and member size remain satisfied.

The cost function of Eq. (2.4-1) is a linear function of design variables and it is given as

$$J(b) = \sum_{r=1}^{L} \sum_{i=1}^{NG(r)} \sum_{j=1}^{NM(i)} \rho_i \ell_j b_i \qquad (4.2\text{-}1)$$

where

ρ_i = material density of members of the ith group

b_i = cross-sectional area of members of the ith group

ℓ_j = length of the jth member of the ith group

NG(r) = number of groups in the rth substructure

NM(i) = number of members in ith group.

Since the cost function depends only on the design variables, some of the calculations of Chapter 3 are eliminated and the vector Λ^J of Eq. (2.5-24) is simply $\frac{\partial J^T}{\partial b}$, which is quite easy to calculate.

Next, the stress or buckling constraint of either Eq. (2.4-3) or (2.4-4), for a typical member is written as:

$$\phi^s \equiv \left|\frac{\sigma^c}{\sigma^a}\right| - 1.0 \leq 0 \qquad (4.2\text{-}2)$$

where σ^c and σ^a are the calculated and the allowable stresses for the member, respectively. In order to simultaneously implement stress and buckling constraints, the allowable stress σ^a is chosen as follows:

(i) for members in tension, $\sigma^a = \sigma^{a+}$, where σ^{a+} is the allowable tensile stress for the member, and

(ii) for members in compression, $\sigma^a = \min(\sigma^{a-}, \sigma^b)$, where $\sigma^{a-} > 0$ and $\sigma^b > 0$ are allowable compressive and critical buckling stresses for the member, respectively.

The stresses σ^{a+} and σ^{a-} are specified by the designer, whereas σ^b depends on the Euler buckling load and is given as

$$\sigma^b = \frac{\pi^2 E I}{\bar{\ell}^2 \bar{b}} \tag{4.2-3}$$

where E, $\bar{\ell}$, $\bar{b}$ and I are modulus of elasticity, equivalent length (for truss members $\bar{\ell} = \ell$), design variable, and moment of inertia of the typical member, respectively. In this research, it is assumed that the members in a design group have the same cross-sectional geometry and material properties. Thus, the moment of inertia can be expressed as

$$I = \bar{\alpha} \bar{b}^2 \tag{4.2-4}$$

where $\bar{\alpha}$ is a positive constant that depends only on the cross-sectional geometry of the member. This constant is specified by the designer quite readily [31,41]. Thus, Eq. (4.2-3) is rewritten as

$$\sigma^b = \bar{\theta} \bar{b} \tag{4.2-5}$$

where

$$\bar{\theta} = \frac{\pi^2 \, E \, \bar{\alpha}}{\bar{\ell}^2} \tag{4.2-6}$$

If the constraint of Eq. (4.2-2) is violated, then

$$\Delta\tilde{\phi}^s = -a\left[\left|\frac{\sigma^c}{\sigma^a}\right| - 1.0\right] \tag{4.2-7}$$

In the example problems considered herein, the value of the constant 'a' is taken to be unity.

The displacement constraint, of either Eq. (2.4-3) or (2.4-4), for a typical degree of freedom is expressed as:

$$\phi^s \equiv \left|\frac{z}{z^a}\right| - 1.0 \leq 0 \tag{4.2-8}$$

where z and z^a are the calculated and the allowable displacements, respectively. If this constraint for the typical displacement component is violated, then

$$\Delta\tilde{\phi}^s = -\left[\left|\frac{z}{z^a}\right| - 1.0\right] \tag{4.2-9}$$

It may be pointed out here that static analysis and constraint checks on stress, buckling, and displacement proceed substructurewise. The sensitivity analysis proceeds as explained in Chapter 3 and matrices Λ^{s1} and Λ^{s2} are assembled at this stage.

The constraint of Eq. (2.2-6) is imposed only on the lowest eigenvalue of the truss ($\zeta = (2\pi f)^2$). Using the method stated in Section 2.3.2, the lowest eigenvalue ζ and the associated eigenvector y are obtained. Thus, the eigenvalue constraint is written as

$$\phi^e(\zeta) \equiv 1.0 - \frac{\zeta}{\zeta_o} \leq 0 \tag{4.2-10}$$

where ζ_o is related to a resonant frequency of the structure. If this constraint is violated, then

$$\Delta\tilde{\phi}^e = -(1.0 - \frac{\zeta}{\zeta_o}) \quad , \quad \text{and} \quad \frac{\partial\tilde{\phi}^e}{\partial\zeta} = -\frac{1}{\zeta_o} \tag{4.2-11}$$

Finally, the design variable constraint $\phi^d(b)$ of Eq. (2.2-5) is considered. For a typical design variable it is expressed as

$$b_i^L \leq b_i \leq b_i^U \tag{4.2-12}$$

where b_i^L and b_i^U are the lower and upper bounds on the ith design variable, respectively. The inequality of Eq. (4.2-12) may be split into two parts as follows:

(i) Lower bound design variable constraint

$$\phi^d(b) \equiv 1.0 - \frac{b_i}{b_i^L} \leq 0 \tag{4.2-13}$$

and

(ii) Upper bound design variable constraint

$$\phi^d(b) \equiv \frac{b_i}{b_i^U} - 1.0 \leq 0 \tag{4.2-14}$$

If a constraint of Eq. (4.2-13) is violated, then

$$\Delta\tilde{\phi}^d = -\left(1.0 - \frac{b_i}{b_i^L}\right) \tag{4.2-15}$$

and

$$\frac{\partial\tilde{\phi}^d}{\partial b} = \left[0,\ldots,\ 0,\ -\frac{1}{b_i^L}\ ,\ 0,\ldots\ ,\ 0\right] \tag{4.2-16}$$

The upper bound design variable constraint is treated in a similar way.

4.3 Computer Program

In order to test the efficiency of the formulation of ODPS, a computer program that implements the algorithm of Chapter 2 is developed for plane and space trusses. A general flow diagram for the program is given in Fig. 4.1.

All the computational aspects of Chapter 3, i.e. multiple loading conditions, design variable linking, worst constraint violation concept, ε-active constraint concept, normalization of constraints, and computational checks have been incorporated in this program. Further, the element stiffness and mass matrices for truss elements are generated in each design cycle. In frequency analysis, provision is made in the

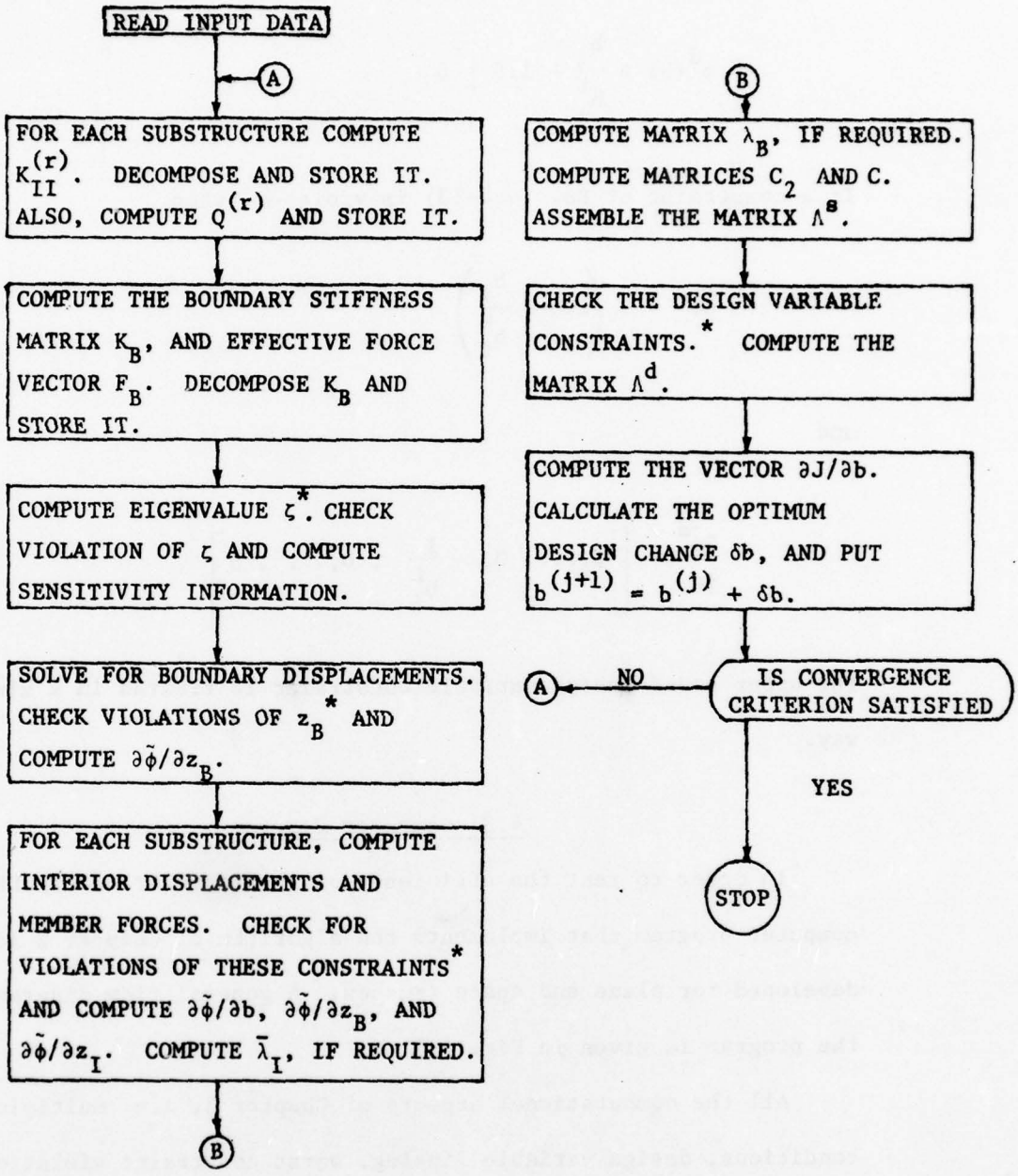

*If any constraint is not imposed, then skip the corresponding portion of the program.

Figure 4.1. Flow Diagram for the Computer Program

program for a restart of the method for minimization of Rayleigh's Quotient after a certain number of iterations. This approach speeds up convergence of the conjugate gradient method.

In order to improve the efficiency of the method, provision for stress-ratio design is made in the computer code. In this concept, design variables (member areas in the present case) are computed from the condition that stress in each member be at its limiting value. It may be pointed out here that this does not yield an optimum design under even the stress constraints for indeterminate structures, but gives a good starting point for the optimal design algorithm. A parameter is defined in the computer program for controlling the number of stress-ratio design cycles.

Also, provision is made in the computer program for assigning a predetermined value to any design variable at the start of the program. Thus, the number of design variables can be less than the number of groups for the truss. This is a valuable feature in the program, since it allows a designer to fix some member areas of the truss.

The δb^1 and δb^2 components corresponding to some design variables attain zero values after a few design iterations. This indicates that these design variables are at their optimum value at the current design iteration. It is assumed that they will remain at these values in subsequent iterations and are, therefore, kept fixed. However, at the final solution all design variables are released and the convergence criterion is checked. If the criterion is violated, then the problem is resolved. Also, stress constraints on all members of the structure

are imposed, irrespective of whether the design variable associated with the member is fixed or free.

4.4 Example Problems

The following three truss examples are solved using the computer program developed for trusses with substructuring formulation:

(i) Example 4.1: 10 Member Cantilever Truss

(ii) Example 4.2: 200 Member Plane Truss

(iii) Example 4.3: 63 Member Wing-Carry-Through Structure (WCTS)

These examples have been studied by several researchers [1-8] and thus serve as standard problems for testing a new algorithm. In subsequent subsections each problem is discussed separately. The results obtained are first compared with a similar formulation developed without using the substructuring concept [1], and then with completely different methods [2-8]. The computational times (in double precision) reported herein are for an IBM 360/65(H) computer.

In each example, the constant $\bar{\alpha}$ used to compute the moment of inertia of each member, for imposing buckling constraints, is taken as unity (see Eq. (4.2-4)) and the value of ε is taken as 0.1%, for imposing ε-active constraints. Further, the weighting matrix W (see Eq. (2.6-8)) is taken as an identity matrix.

4.4.1 Example 4.1: 10 Member Cantilever Truss

Figure 4.2 shows geometry and dimensions of the 10 member cantilever truss. In the present formulation, the truss is divided into two substructures, by partitioning it at joints 3 and 4. Thus, the

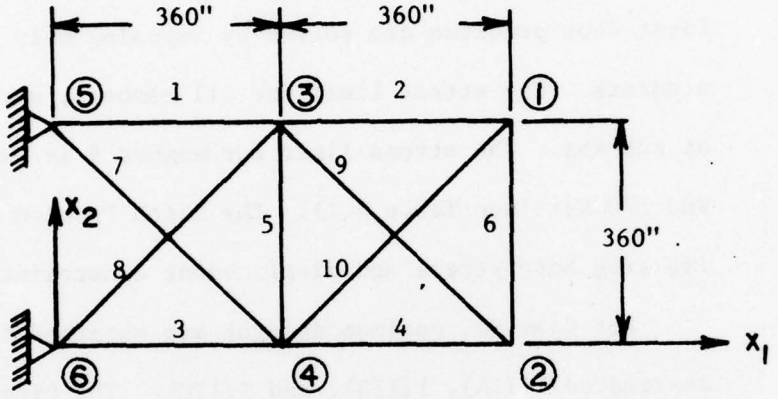

Figure 4.2. 10 Member Cantilever Truss

first substructure consists of members 2, 4, 6, 9, and 10, with four boundary and four interior degrees of freedom. The second substructure consists of members 1, 3, 5, 7, and 8, with four boundary and no interior degrees of freedom. The truss is designed for the two loading cases given in Table 4.1.

For Case I, the optimum design is obtained for five separate problems, designated 1(IA1), 1(IA2), 1(IA3), 1(IA4), and 1(IB). The first four problems are solved by imposing only the direct stress constraints. The stress limit for all members, except member 9, is kept at ±25 ksi. The stress limit for member 9 is varied as ±25, ±30, ±50, and ±70 ksi (see Table 4.1). The fifth Problem 1(IB) is solved by imposing both stress and displacement constraints.

For Case II, optimum designs are obtained for three problems, designated 1(IIA), 1(IIB), and 1(IIC). The first two problems are similar to Problems 1(IA1) and 1(IB), respectively, whereas the last Problem 1(IIC) considers all constraints, i.e., stress, buckling, displacement, and frequency constraints. Bounds on design variables are imposed in all the problems. Design data for all the problems of this example are given in Table 4.1. No design variable linking is used in this example.

Table 4.2 gives the final design, number of active constraints, maximum constraint violation, and $||\delta b^1||_2$ at the optimum design for each problem. It also gives the maximum value of $||\delta b^1||_2$, and a comparison of CPU times per design iteration for the present fomulation and a similar forumulation without substructuring [1]. A reduction of

TABLE 4.1. DESIGN DATA FOR 10 MEMBER CANTILEVER TRUSS

Modulus of elasticity = 10^4 ksi

Material density = 0.10 lb/in.^{3}

Initial value of A = 1.0 in.^{2}, where A is cross-sectional area

Lower limit on A = 0.10 in.^{2}

Upper limit on A = None

Displacement limit = ±2.0 in.

Resonant frequency = 22.0 Hz.

Stress limit = ±25 ksi

Number of loading conditions = 1

Load data:

Loading Case Number	Loading Condition	No. of Loaded Joints	Joint No.	Load Component (kips) in direction		
				x_1	x_2	x_3
I	1	2	2	0.0	-100.0	0.0
			4	0.0	-100.0	0.0
II	1	4	1	0.0	50.0	0.0
			2	0.0	-150.0	0.0
			3	0.0	50.0	0.0
			4	0.0	-150.0	0.0

Starting reduction ratio, $\bar{r}$:

Problem No.	1(IA1)	1(IA2)	1(IA3)	1(IA4)	1(IB)	1(IIA)	1(IIB)	1(IIC)
$\bar{r}$	0.018	0.091	0.090	0.090	0.081	0.001	0.081	0.040

For Problems 1(IA2), 1(IA3), and 1(IA4) the stress limit for member number 9 is ±30, ±50, and ±70 ksi, respectively, instead of ±25 ksi.

TABLE 4.2. RESULTS FOR 10 MEMBER CANTILEVER TRUSS

		Optimum Cross-sectional Area in $in.^2$						
Member Number		Case I				Case II		
		1(IA1)	1(IA2)	1(IA3) & 1(IA4)	1(IB)	1(IIA)	1(IIB)	1(IIC)
1		7.9379	7.9296	7.9000	30.6070	5.9478	23.5640	24.6840
2		0.1000	0.1000	0.1000	0.1000	0.1000	0.1000	1.0841
3		8.0621	8.0704	8.1000	29.9710	10.0520	25.2770	24.4380
4		3.9379	3.9296	3.9000	14.7510	3.9478	14.3430	12.8720
5		0.1000	0.1000	0.1000	0.1000	0.1000	0.1000	0.1000
6		0.1000	0.1000	0.1000	0.1000	2.0522	1.9698	1.9642
7		5.7447	5.7564	5.7983	8.5421	8.5592	12.4010	13.6920
8		5.5690	5.5573	5.5154	20.9750	2.7545	12.8500	16.4730
9		5.5690	4.6311	3.6769	20.8610	5.5830	20.2850	17.8020
10		0.1000	0.1000	0.1414	0.1000	0.1000	0.1000	0.1000
At Optimum	Wt. in lbs	1593.18	1545.13	1497.60	5076.56	1664.53	4676.13	4792.32
	No. of Active Constraints	10	10	9	2	10	4	6
	Max. Constraint Violation	0.62×10^{-3}	0.10×10^{-3}	0.69×10^{-4}	0.27×10^{-4}	0.59×10^{-5}	0.17×10^{-3}	0.24×10^{-7}
	$\|\|\delta b^1\|\|_2$	0.69×10^{-13}	0.78×10^{-13}	17.40	0.34	0.67×10^{-13}	0.34	23.54
Max. $\|\|\delta b^1\|\|_2$		56.08	51.17	100.30	49.48	--	71.81	130.30
Av. CPU Time/DI* in sec.								
Present		0.2273	0.2895	0.2991	0.2353	0.2170	0.2532	0.3932
Arora-Haug [1]		0.2900	--	--	0.2600	0.2800	0.2600	0.4000

*Design iteration.

approximately 1.5 to 23% in CPU times per design iteration is achieved with the present formulation.

For Problem 1(IA1), the set of active constraints at the optimum includes stress constraints in members 1, 3, 4, and 7 to 9, as well as minimum size constraints on members 2, 5, 6, and 10. The total number of active constraints is equal to the number of independent design variables. For Problem 1(IA2), the set of active stress constraints is the same as for Problem 1(IA1). For Problems 1(IA3) and 1(IA4), the optimal solutions are identical. This is due to the fact that for these two problems, the stress constraint for member 9 at optimum is not critical (stress in member 9 = -37.50 ksi). Thus increasing the stress limit in this member from ±50 ksi to ±70 ksi does not change the optimum solution. The set of active constraints, for the final design given in Table 4.2, includes stress constraints for members 1 to 4, 6 to 8, and 10, as well as the minimum size constraint on member 5. For Problem 1(IIA), the set of active constraints at optimum includes stress constraints for members 1, 3, 4 and 6 to 9, along with minimum size constraints on members 2, 5, and 10. The set of active constraints at the optimum for Problem 1(IB) includes only the downward vertical deflection constraint at nodes 1 and 2. For Problem 1(IIB), active constraints are the downward deflection at node 2, stress in members 5 and 6, and minimum size in member 2.

The last Problem 1(IIC) includes all the constraints. As shown in Table 4.2, six constraints are active: frequency bound, stress in members 2, 5, and 6, vertical downward deflection at node 2, and

minimum size in member 10. It may be pointed out here that the CPU time for each design iteration for this problem depends upon the number of conjugate gradient iterations performed. For this problem, an average of six conjugate gradient iterations are performed for the frequency analysis.

Tables 4.3 and 4.4 give the details of the computational times and the cost function history for all the problems, respectively. It is noted here that components of δb^1 and δb^2 associated with design variables for member 5 of Problem 1(IA1); members 3, 5, 6, and 10, of Problems 1(IB); and members 5 and 10 of Problem 1(IIB)are equal to zero after the 1st iteration. Hence in the subsequent iterations, these design variables are kept fixed. In the last iteration, these design variables are released in order to check the final convergence (see Section 4.3). Also, in each problem the step size parameter was monitored and adjusted at appropriate iterations, to obtain the final solution. The rate of convergence to the optimal solution (number of design cycles) is dependent on the step size. A very small step size can slow the rate of convergence, whereas a very large step may cause oscillations in the algorithm. For the Problem 1(IA4), an additional computer run was made by keeping the step size constant ($\bar{\tau} = 0.09$). The initial design was 1.0 $in.^2$ for all members and the stress-ratio design was performed only once. The final solution was obtained in 23 iterations, with the cost function history being 1582.03, 1631.02, 1656.86, 1636.97, 1612.25, 1591.74, 1570.42, 1517.97, 1533.06, 1518.48, 1446.24, 1458.16, 1516.78, 1505.48, 1517.48, 1515.83, 1513.56, 1511.27,

TABLE 4.3. COMPUTATIONAL TIMES IN SECONDS FOR 10 MEMBER CANTILEVER TRUSS

Problem	Total CPU Time For			Total CPU Time (2)+(3)+(4)
	Problem Setup	Stress-Ratio Design	Optimal Design*	
1	2	3	4	5
1(IA1)	0.547	0.593 (10)†	2.046 (9)‡	3.186
1(IA2)	0.525	0.833 (14)†	1.447 (5)‡	2.805
1(IA3)	0.570	0.067 (1)†	4.486 (15)‡	5.123
1(IB)	0.600	0.832 (14)†	3.529 (15)‡	4.961
1(IIA)	0.570	0.667 (10)†	---	1.237
1(IIB)	0.570	0.665 (10)†	4.052 (16)‡	5.287

*Includes CPU time required for analysis, sensitivity analysis, and optimization.

†Number of stress-ratio design iterations performed.

‡Number of design iterations performed.

TABLE 4.4. COST FUNCTION HISTORY FOR
10 MEMBER CANTILEVER TRUSS

DI† Number	Weight in lbs.					
	1(IA1)	1(IA2)	1(IA3)	1(IB)	1(IIA)	1(IIB)
1	1594.52	1593.17	1606.66	1592.26	1664.53‡	1664.53
2	1599.83	1572.26	1650.65	2486.86		2189.59
3	1605.87*	1551.30*	1651.29	3735.76		3236.84
4	1587.77	1542.07	1629.26	4734.86		4262.16
5	1597.11	1545.13‡	1603.79	5133.65*		4711.79
6	1595.97		1583.33	5123.27		4773.03
7	1594.61		1561.59	5115.11		4751.52
8	1593.99		1508.96	5106.08		4725.45*
9	1593.46		1526.74	5099.30*		4716.38
10	1593.18‡		1515.62	5091.32		4725.86
11			1524.06*	5086.62*		4722.60*
12			1509.12*	5080.94		4715.80*
13			1502.82*	5078.92*		4705.48*
14			1499.68*	5076.84		4692.04*
15			1498.11*	5076.76*		4679.51*
16			1497.60‡	5076.56‡		4674.74*
						4676.13‡

‡Underlined iteration is not counted as it is used for checking solution only.

*Means change in step size.

†Optimal design iteration.

1508.99, 1506.76, 1504.44, 1502.16, 1499.88, and 1497.60. The final solution is the same as in Problem 1(IA3), but the number of iterations in the latter case is greater. This shows the importance of a proper step size for faster convergence of the algorithm.

Finally Table 4.5 gives a comparison of final weights, number of analyses, average CPU times per design iteration and total times with other available results. For all the problems, the cost function is the same as obtained in Refs. 2 and 3, but there is some reduction in comparison with Ref. 5. Further, there is a significant reduction in computational times. With the present formulation, the CPU time per design iteration is reduced by factors of up to 5.6 and 2.4, in comparison to CPU times reported in Refs. 2 and 4, respectively. Note that the solutions are obtained using different computers. In order to convert the times from CDC 7600 to IBM 360/91 one needs to multiply the computing times with CDC 7600 by 5 [3]. Also in a private communication with IBM, it was found that the IBM 360/91 is about 8 times faster than IBM 360/65. Hence, in order to compare the times with the present work, one needs to multiply the times of Ref. 2 (IBM 360/91) and Refs. 3, and 4 (CDC 7600) by factors of 8 and 40, respectively.

4.4.2 Example 4.2: 200 Member Plane Truss

The second structure (Fig. 4.3) optimized by the present technique is a moderate size plane truss with 200 members and 150 degrees of freedom. For the purpose of obtaining computational times with different numbers of substructures, the following three cases are considered for this example:

TABLE 4.5. COMPARISON OF RESULTS FOR 10 MEMBER CANTILEVER TRUSS

		Problem					
		1(IA1)	1(IA2)	1(IA3)	1(IB)	1(IIA)	1(IIB)
Weight in lbs	Present	1593.18	1545.13	1497.60	5076.56	1665.53	4676.13
	Schmit-Miura [2]	1593.23	1545.17	1497.65	5076.85	1664.55	4676.93
	Rizzi [3]	1593.18	1545.13	1497.60	5076.66	1664.53	4676.92
	Dobbs-Nelson [5]	1622.00	1582.00	1509.00	5080.00	--	5059.70
No. of DI†	Present	9	5	15	15	0	16
	Schmit-Miura [2]	15	15	15	12	10	10
	Rizzi [3]	15	15	15	11	12	12
	Dobbs-Nelson [5]	10	14	114	14	--	11
Av. CPU Time/DI† in sec	Present‡	0.2273	0.2895	0.2991	0.2353	0.0	0.2532
	Schmit-Miura*[2]	0.1714	0.1767	0.1811	0.1697	0.1982	0.1755
	Rizzi**[4]	0.0166	0.0161	0.0187	0.0141	0.0169	0.0142
	Dobbs-Nelson [5]	--	--	--	--	--	--
Total CPU Time in sec	Present‡	3.1860	2.8050	5.1239	4.9613	1.2370	5.2868
	Schmit-Miura* [2]	2.8604	2.9296	3.0028	2.3537	2.2783	2.0383
	Rizzi**[4]	0.3160	0.3080	0.3490	0.2220	0.2710	0.2410
	Dobbs-Nelson [5]	--	--	--	--	--	--

† Design iteration.

‡ IBM 360/65(H).

* IBM 360/91. For comparison, time should be multiplied by 8.

** CDC 7600. For comparison, time should be multiplied by 40.

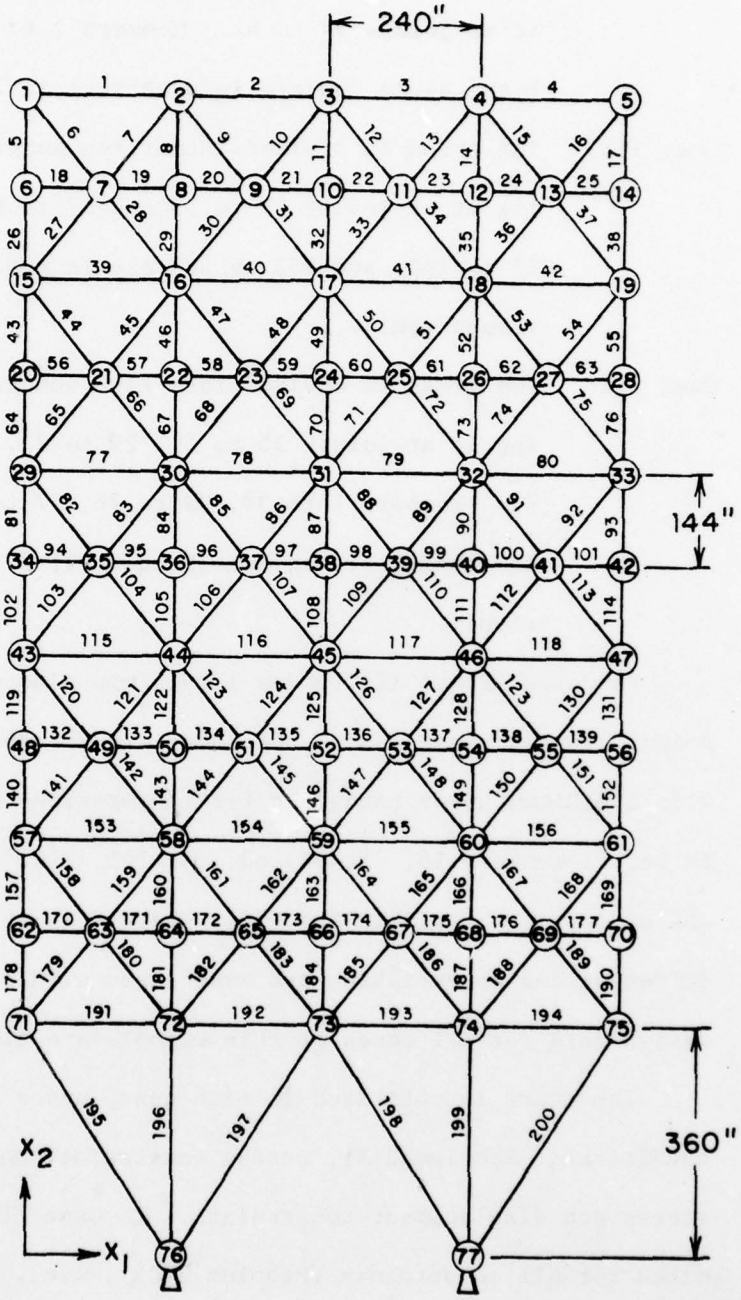

Figure 4.3. 200 Member Plane Truss

Case I: The truss is divided into two substructures by partitioning it at joints 34 to 42. Members 1 to 93 are in substructure 1 and 94 to 200 are in substructure 2.

Case II: The truss is divided into three substructures by partitioning it at joints 29 to 33 and 57 to 61. Members 1 to 76, 77 to 152, and 153 to 200 are in substructures 1, 2, and 3, respectively.

Case III: The truss is divided into five substructures by partitioning it at joints 15 to 19, 29 to 33, 43 to 47, and 57 to 61. Members 1 to 38, 39 to 76, 77 to 114, 115 to 152, and 153 to 200 are in substructure 1, 2, 3, 4, and 5, respectively.

In Cases II and III, nodes 1 to 5 are also considered as boundary nodes. In all these cases, the nodes are renumbered in order to provide a minimum upper bandwidth for the matrices K_B, $K_{BB}^{(r)}$, and $K_{II}^{(r)}$. In Ref. 1 members 18, 25, 56, 63, 94, 101, 132, and 139 are linked to the same design variable (no. 10), whereas in the present formulation different design variables are associated with these members. The design data for all cases of this example are given in Table 4.6.

The truss is optimized in each case, under two separate constraint conditions: Problem 2(A), stress constraints only, and Problem 2(B), stress and displacement constraints. In Case III, the truss is optimized for all constraints (Problem 2(C)), i.e., stress, displacement, buckling, and frequency constraints. Table 4.7 gives the final solution, number of active constraints, maximum constraint violation, and

TABLE 4.6. DESIGN DATA FOR 200 MEMBER PLANE TRUSS

Modulus of elasticity	= 30,000 ksi
Material density	= 0.283 lb/in.^{3}
Lower limit on cross-sectional areas	= 0.10 in.^{2}
Upper limit on cross-sectional areas	= None
Initial value of cross-sectional areas	= 1.0 in.^{2}
Stress limits	= ±30 ksi
Displacement limits	= ±0.5 in.
Resonant frequency	= 5.0 Hz.
Number of loading conditions	= 3
Load data:	

Loading Condition 1. One kip acting in positive x_1 direction at node points 1, 6, 15, 20, 29, 34, 43, 48, 57, 62, 71.

Loading Condition 2. 10 kips acting in negative x_2 direction at node points 1, 2, 3, 4, 5, 6, 8, 10, 12, 14, 15, 16, 17, 18, 19, 20, 22, 24, ..., 71, 72, 73, 74, 75.

Loading Condition 3. Loading Conditions 1 and 3 acting together.

Starting reduction ratio, $\bar{r}$ = $\begin{cases} 0.006 \text{ for Problem 2(A)} \\ 0.030 \text{ for Problem 2(B)} \\ 0.040 \text{ for Problem 2(C)} \end{cases}$

TABLE 4.7. RESULTS FOR 200 MEMBER PLANE TRUSS

Group No.	Member Numbers	Optimum Cross-Sectional Area in $in.^2$		
		Problem 2(A)	Problem 2(B)	Problem 2(C)
1	1,4	0.1000	0.1878	2.4571
2	2,3	0.1000	0.1000	2.6271
3	5,17	0.2469	4.7832	4.6970
4	6,16	0.1185	0.1703	1.1171
5	7,15	0.1000	0.1000	0.3270
6	8,14	0.3675	2.3462	1.9650
7	9,13	0.1000	0.1876	0.2549
8	10,12	0.1000	0.1000	0.9190
9	11	0.2454	2.8809	1.7910
10	18,25	0.1000	0.1000	0.2210
11	19,20,23,24	0.1000	0.1000	0.1000
12	21,22	0.1000	0.1000	0.1000
13	26,38	0.5815	6.7767	6.7390
14	27,37	0.1000	0.1000	0.1170
15	28,36	0.1736	0.2361	1.1600
16	29,35	0.7008	3.3133	2.8450
17	30,34	0.1000	0.1732	0.9100
18	31,33	0.1000	0.2227	0.2447
19	32	0.5792	4.1473	2.9270
20	39,42	0.1035	0.1000	0.4541
21	40,41	0.1000	0.1000	0.3257
22	43,55	0.6760	8.1292	7.4171
23	44,54	0.2489	0.2476	0.8670
24	45,53	0.1000	0.1000	0.1572
25	46,52	1.2622	4.4206	5.6820
26	47,51	0.1000	0.2802	0.6880
27	48,50	0.1000	0.2673	0.5190
28	49	0.8402	4.7929	3.7401
29	57,58,61,62	0.1000	0.1000	0.1408
30	59,60	0.1000	0.1002	0.1190
31	64,76	1.0080	9.3889	8.4891
32	65,75	0.1000	0.1000	0.2398
33	66,74	0.3103	0.3362	0.9540
34	67,73	1.5955	5.0733	6.4100
35	68,72	0.1000	0.3008	0.5181
36	69,71	0.1000	0.3096	0.7290
37	70	1.1731	5.5744	4.4271
38	77,80	0.1892	0.4967	0.9281
39	78,79	0.1000	0.3865	0.2628
40	81,93	1.0402	9.5196	8.3681
41	82,92	0.4108	0.9366	1.7621
42	83,91	0.1000	0.1000	0.1490
43	84,90	2.2576	6.2617	7.8100

TABLE 4.7. (cont'd.)

Group No.	Member Numbers	Optimum Cross-Sectional Area in $in.^2$		
		Problem 2(A)	Problem 2(B)	Problem 2(C)
44	85,89	0.1000	0.3508	0.8980
45	86,88	0.1000	0.4835	0.5779
46	87	1.4567	5.8679	5.0921
47	95,96,99,100	0.1000	0.1000	0.1012
48	97,98	0.1000	0.1000	0.1241
49	102,114	1.3481	10.4800	9.1651
50	103,113	0.1111	0.1108	0.2005
51	104,112	0.4795	1.0313	1.8621
52	105,111	2.5909	6.8203	8.3780
53	106,110	0.1007	0.5012	0.5439
54	107,109	0.1000	0.3754	0.8989
55	108	1.7922	6.4768	5.6151
56	115,118	0.2932	1.9807	1.4791
57	116,117	0.1000	1.4784	0.2829
58	119,131	1.2625	9.1546	8.3571
59	120,130	0.6050	3.1979	2.5540
60	121,129	0.1000	0.1000	0.1477
61	122,128	3.3587	9.0271	10.0360
62	123,127	0.1000	0.2074	0.8499
63	124,126	0.1069	0.9717	0.6821
64	125	2.0771	6.5338	6.1791
65	133,134,137,138	0.1000	0.1000	0.1000
66	135,136	0.1002	0.1219	0.1210
67	140,152	1.5748	9.9624	9.0011
68	141,151	0.1325	0.1341	0.1983
69	142,150	0.6817	3.3000	2.6930
70	143,149	3.6920	9.5771	10.5110
71	144,148	0.1092	0.9814	0.6610
72	145,147	0.1000	0.2269	0.8559
73	146	2.4116	7.0561	6.6231
74	153,156	0.4250	2.5500	2.2599
75	154,155	0.1000	0.6074	0.2332
76	157,169	1.3251	7.5376	7.1521
77	158,168	0.8462	4.1216	3.8200
78	159,167	0.1000	0.1000	0.1020
79	160,166	4.5880	13.3290	12.5160
80	161,165	0.1000	1.8691	1.8370
81	162,164	0.1276	0.3045	0.8090
82	163	2.6772	7.4246	7.1681
83	171,172,175,176	0.1000	0.1000	0.6620
84	173,174	0.1002	0.1000	0.6611
85	178,190	1.6597	8.2183	7.1961

TABLE 4.7. (cont'd.)

Group No.	Member Numbers	Optimum Cross-Sectional Area in $in.^2$		
		Problem 2(A)	Problem 2(B)	Problem 2(C)
86	179,189	0.1156	0.1000	0.3654
87	180,188	0.9181	4.1916	4.9040
88	181,187	4.9213	13.8330	12.5350
89	182,186	0.1339	0.3354	1.1069
90	183,185	0.1002	1.9082	2.1110
91	184	3.0100	7.8840	7.1751
92	191,194	1.2392	5.8649	5.3130
93	192,193	0.8521	3.4248	3.1651
94	195,200	2.3257	10.6560	9.9201
95	196,199	5.9232	17.7770	18.8650
96	197,198	2.5718	7.7140	8.9630
97	56,63	0.1000	0.1000	0.2210
98	94,101	0.1000	0.1000	0.2210
99	132,139	0.1000	0.1000	0.2210
100	170,177	0.1000	0.1000	0.1000
At Optimum	Wt. in lbs.	7,488	28,963	29,707
	No. of Active Constraints	90	28	25
	Max. Constraint Violation	0.71×10^{-4}	0.97×10^{-3}	0.14×10^{-2}
	$\|\|\delta b^1\|\|_2$	54.95	53.01	264.30
Max. $\|\|\delta b^1\|\|_2$		273.60	979.90	728.90

$||\delta b^1||_2$ at the optimum design for each problem, and the maximum value of $||\delta b^1||_2$. Also, final solutions could be obtained in about 12-15 iterations by monitoring the step size. Table 4.8 gives active constraints for the optimum solution reported in Table 4.7.

Table 4.9 shows a comparison of computational times between the present formulation and a similar formulation without substructuring [1]. The CPU time per design iteration depends upon many factors, such as the total number of constraint violations, the number of loading conditions, the number of substructures under which violations occur, etc. The CPU times per design iteration given in Table 4.9 are for the number of active constraints reported in Table 4.7. For the Problem 2(A), violations occurred in all substructures, in all loading conditions, and for all three cases. For the stress and displacement constraint case i.e., Problem 2(B), violations occurred in all substructures and in all loading conditions in some initial iterations. Near the optimum point, however, only displacement violations occurred under loading conditions 2 and 3, and in substructure 1 for all cases.

A comparison of CPU times for structural analysis indicates that as the number of substructures is increased from 2 to 5, the CPU time for analysis is reduced by a factor of more than 2. This reduction in CPU time for analysis is due to the reduced bandwidth of the matrix $K_{II}^{(r)}$. In comparison, the CPU time for structural analysis is 50% greater, with two substructures, and is 33% lower with five substructures. The CPU time per design iteration is reduced in all cases, with the greatest reduction occurring in Case III. This indicates that

TABLE 4.8. ACTIVE CONSTRAINTS AT THE OPTIMUM DESIGN FOR 200 MEMBER PLANE TRUSS

Problem 2(A): Case III

(i) Active Stress Constraints (50)*

Members 11, 17, 26, 32, 39, 43, 49, 64, 70, 77, 87, 108, 115, 125, 146, 163, and 184 under loading condition 2;

Members 14, 16, 28, 35, 44, 52, 66, 73, 82, 90, 104, 110, 111, 120, 126, 128, 142, 148, 149, 153, 158, 164, 166, 169, 179, 180, 187, 190, 193, 194, 198, 199, and 200 under loading condition 3.

(ii) Active Minimum Size Constraints (40)*

Design Variables 1, 2, 5, 7, 8, 10 to 12, 14, 17, 18, 21, 24, 26, 27, 29, 30, 32, 35, 36, 39, 42, 44, 45, 47, 48, 54, 57, 60, 62, 65, 72, 75, 78, 80, 83, and 97 to 100.

Problem 2(B): Case I

(i) Active Displacement Constraints (5)*

At nodes 1 and 6 in positive x_1 direction under loading condition 1; and at nodes 3 to 5 in negative x_2 direction under loading condition 3.

(ii) Active Minimum Size Constraints (23)*

Design Variables 2, 5, 8, 10 to 12, 14, 20, 21, 24, 29, 32, 42, 47, 48, 60, 65, 78, 83, 84, 86, 97, and 98.

Problem 2(C): Case III

(i) Active Stress Constraints (18)*

Members 37, 40, 53, 79, 91, and 167 under loading condition 1;
Member 179 under loading condition 2;
Members 7, 9, 18, 50, 56, 72, 88, 94, 110, 129, and 132 under loading condition 3.

TABLE 4.8. (cont'd.)

(ii)	Active Displacement Constraints (3)*
	At node 3 under loading condition 2, and at nodes 4 and 5 under loading condition 3 in negative x_2 direction.
(iii)	Active Minimum size constraints (4)*
	Design Variables 11, 12, 65, and 100.

* Number of active constraints

TABLE 4.9. COMPARISON OF COMPUTATIONAL TIMES FOR 200 MEMBER PLANE TRUSS
(All times in seconds)

		Present			Arora-Haug [1]
		Case I	Case II	Case III	
Problem 2(A)	CPU Time/SAI†	4.54	3.06	2.14	3.11
	CPU Time/DI‡	20.57	16.88	15.19	22.00
	Reduction in CPU Time/DI‡ with Ref. [1] in %	6.5	23.3	31.0	--
Problem 2(B)	CPU Time/DI‡	7.06	5.20	4.43	13.00
	Reduction in CPU Time/DI‡ with Ref. [1] in %	45.7	60.0	65.9	--
Problem 2(C)	CPU Time/DI‡	--	--	11.45	19.00
	Reduction in CPU Time/DI‡ with Ref. [1] in %	--	--	39.7	--

†Static analysis iteration

‡Design iteration

there is an optimum number of substructures, for a minimum computing time. When the number of substructures is below or above this optimum number, efficiency of the substructuring technique is reduced.

It may be observed from Table 4.7 that many design variables are at their lower bounds at the optimum design. A side computation was made by keeping these variables constant for Case I, with only stress constraints, in order to determine the reduction in computing time. For this run, computing time per design iteration was 12.4 seconds, as compared with 20.57 seconds, a reduction of approximately 40%. In many practical situations, it is known a priori that certain members of the structure must have assigned minimum areas or maximum areas. The above result indicates that the designer should take full advantage of such knowledge to achieve maximum efficiency.

For Problem 2(C), the number of conjugate gradient iterations for minimizing the Rayleigh Quotient is restricted to five. In the initial few iterations, the design changes significantly. Therefore, it is not advantageous to obtain a precise solution of the eigenvalue problem. The eigenvector obtained from the previous design cycle serves as a good approximation for the current design cycle. It may also be noted that, near the optimum, the conjugate gradient method takes only one iteration for convergence. For this problem a reduction of about 40% in computing time is achieved, as compared to results in Ref. 1.

The results of this example are not compared with Refs. 51 and 52, since the comparison was already made in Ref. 1.

4.4.3 Example 4.3: 63 Member Wing-Carry-Through Structure (WCTS)

Figure 4.4 shows the truss idealization of the 63 member wing-carry-through structure (WCTS). This problem was originally optimized by Berke and Khot [6] and later by Schmit and Miura [2], and Dobbs and Nelson [5]. For details regarding idealization of this structure, the reader is referred to Ref. 6.

In the present formulation, the structure is divided into two substructures by partitioning it at nodes 7 through 10. The first substructure consists of 31 members: 1 to 8, 17 to 20, 23 to 27, 30 to 33, 42 to 49, 58 and 59. The remaining 32 members are in the second substructure. Tables 4.10 and 4.11 define the nodal coordinates and member locations, respectively. Design data for the structure is given in Table 4.12. The loading conditions given in Table 4.12 are, according to Ref. 6, "derived from a 2g condition of a half million pound aircraft and from two assumed wing positions". The structure is designed for two cases:

(i) with stress constraints only (Problem 3(A))

(ii) with stress and torsional stiffness constraints (Problem 3(B)).

The torsional stiffness constraint of Ref. 6 is imposed by limiting the relative displacement of nodes 1 and 2 in the x_1 direction. This constraint is incorporated by a minor modification in the present computer program. Finally, no design variable linking is used in this example.

Table 4.13 gives the final cross-sectional areas, value of the cost function, and number of active constraints, maximum constraint

AD-A065 935 IOWA UNIV IOWA CITY DIV OF MATERIALS ENGINEERING F/G 1/3
SUBSTRUCTURING METHODS FOR DESIGN SENSITIVITY ANALYSIS AND STRU--ETC(U)
AUG 77 A K GOVIL, J S ARORA, E J HAU DAAK11-77-C-0023
UNCLASSIFIED TR-34 NL

2 OF 3
AD
A065835

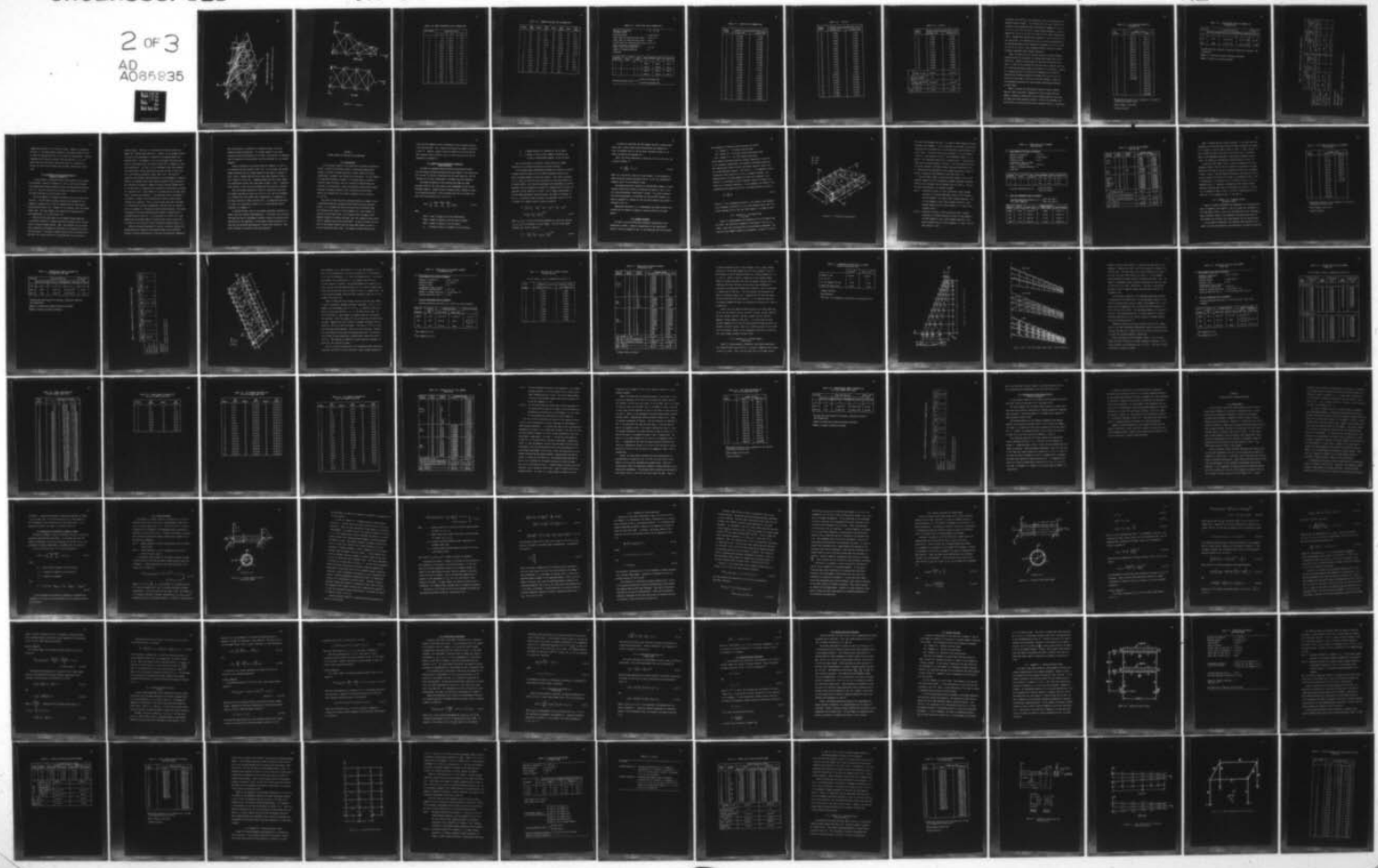

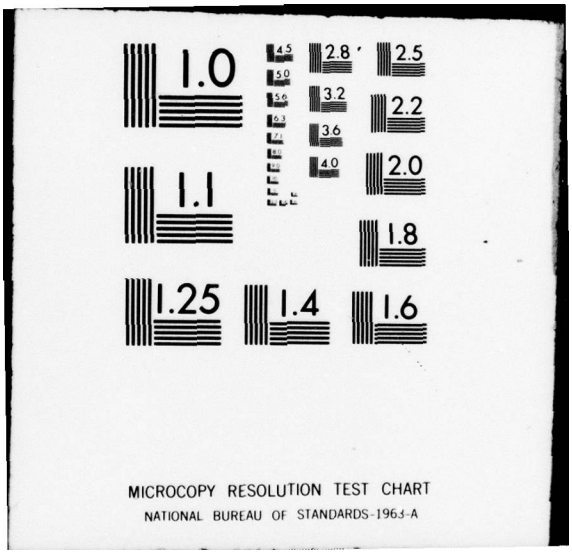
1.0
1.1
1.25
1.4
1.6
1.8
2.0
2.2
2.5
2.8
3.2
3.6
4.0
4.5
5.0
5.6
MICROCOPY RESOLUTION TEST CHART
NATIONAL BUREAU OF STANDARDS-1963-A

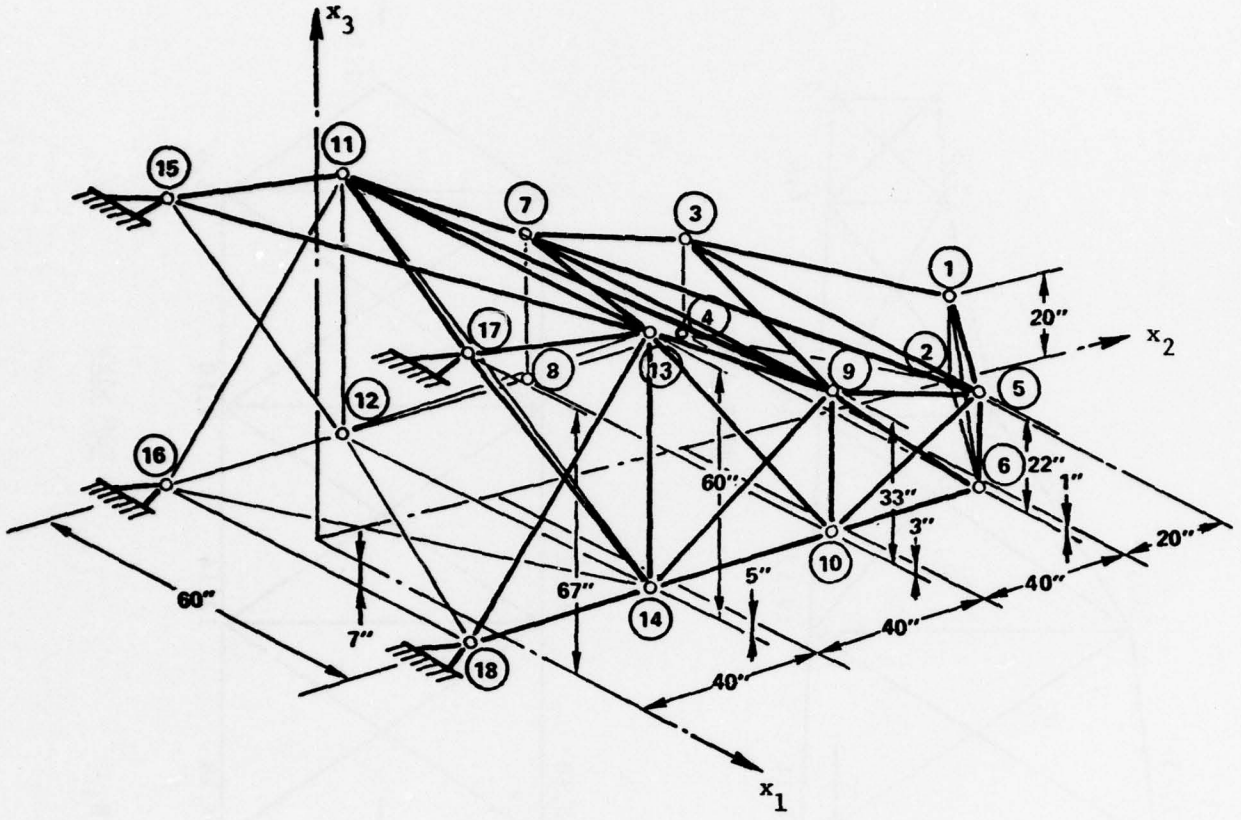

TRUSS IDEALIZATION OF WCTS - 3D VIEW

Figure 4.4. 63 Member Wing-Carry-Through Structure

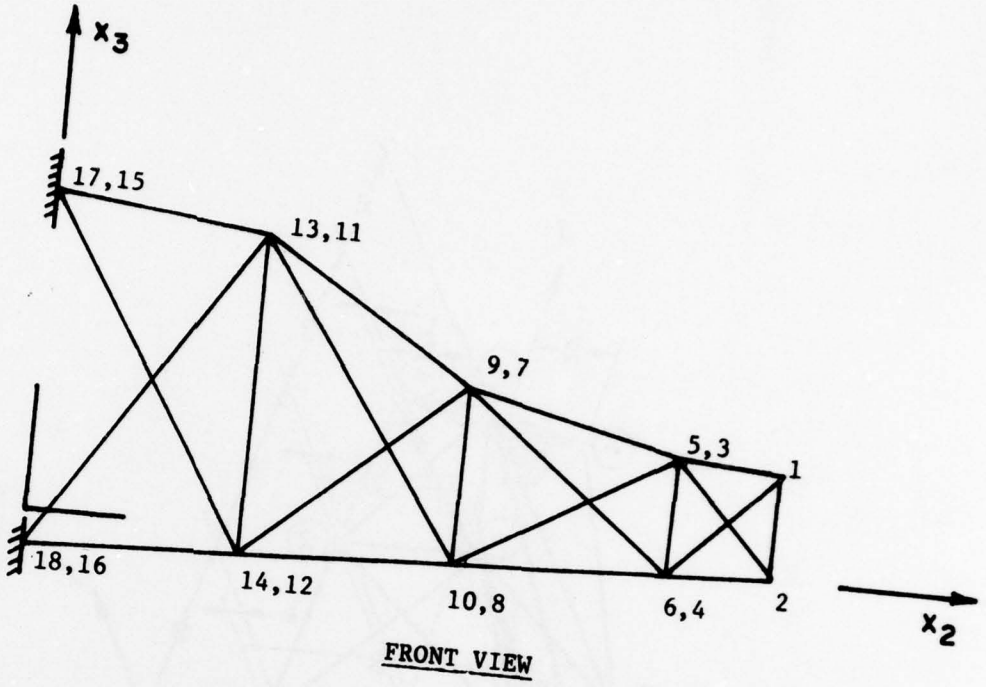

FRONT VIEW

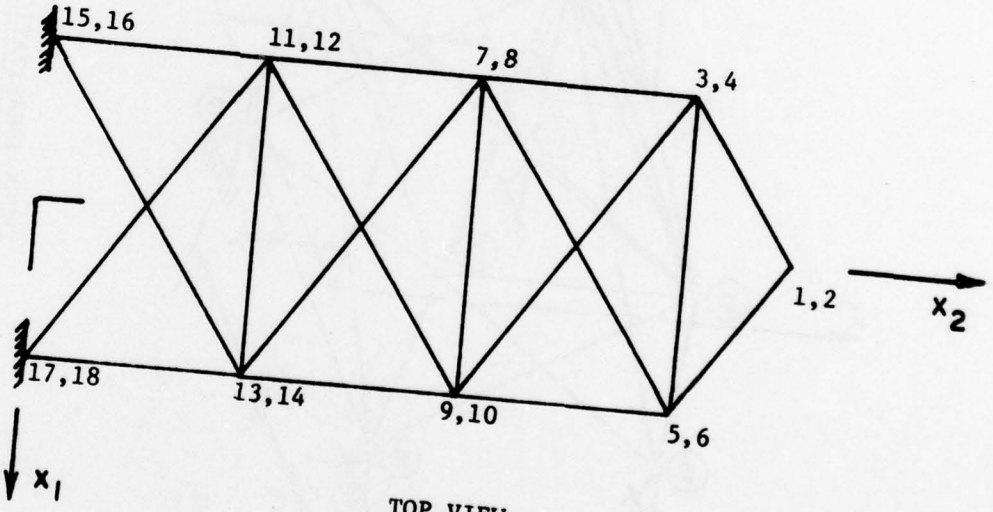

TOP VIEW

Figure 4.4. (cont'd.)

TABLE 4.10. NODAL COORDINATES FOR 63 MEMBER WCTS

Node Number	Coordinate in in.		
	x_1	x_2	x_3
1	0.0	140.0	20.0
2	0.0	140.0	0.0
3	-30.0	120.0	21.0
4	-30.0	120.0	-1.0
5	30.0	120.0	21.0
6	30.0	120.0	-1.0
7	-30.0	80.0	30.0
8	-30.0	80.0	-3.0
9	30.0	80.0	30.0
10	30.0	80.0	-3.0
11	-30.0	40.0	55.0
12	-30.0	40.0	-5.0
13	30.0	40.0	55.0
14	30.0	40.0	-5.0
15	-30.0	0.0	60.0
16	-30.0	0.0	-7.0
17	30.0	0.0	60.0
18	30.0	0.0	-7.0

TABLE 4.11. MEMBER LOCATIONS FOR 63 MEMBER WCTS

Member	End Nodes	Member	End Nodes	Member	End Nodes	Member	End Nodes
1	1,3	17	3,5	33	8,6	49	7,4
2	2,4	18	4,6	34	7,13	50	9,14
3	1,5	19	7,9	35	8,14	51	7,12
4	2,6	20	8,10	36	11,9	52	13,10
5	7,3	21	11,13	37	12,10	53	11,8
6	8,4	22	12,14	38	11,17	54	13,18
7	9,5	23	1,2	39	12,18	55	11,16
8	10,6	24	3,4	40	15,13	56	17,14
9	11,7	25	5,6	41	16,14	57	15,12
10	12,8	26	7,8	42	1,6	58	5,4
11	13,9	27	9,10	43	1,4	59	3,6
12	14,10	28	11,12	44	5,2	60	9,8
13	15,11	29	13,14	45	3,2	61	7,10
14	16,12	30	3,9	46	5,10	62	13,12
15	17,13	31	4,10	47	3,8	63	11,14
16	18,14	32	7,5	48	9,6		

TABLE 4.12. DESIGN DATA FOR 63 MEMBER WCTS

Modulus of elasticity (Titanium alloy)	= 16×10^3 ksi
Material density	= 0.16 lb/in.^{3}
Lower limit on cross-sectional areas	= 0.01 in.^{2}
Upper limit on cross-sectional areas	= None
Initial value of cross-sectional areas	= 20.0 in.^{2}
Limit on relative displacement of nodes 1 and 2 in x_1-direction	= 1.0 in.
Number of loading conditions	= 2

Load data:

Loading Condition	No. of loaded Nodes	Node Number	Load components (kips) in direction		
			x_1	x_2	x_3
1	2	1	2500.0	-5000.0	250.0
		2	-2500.0	5000.0	250.0
2	2	1	5000.0	-2500.0	250.0
		2	-5000.0	2500.0	250.0

Starting reduction ratio, $\bar{r} = \begin{cases} 0.010 \text{ for Problem 3(A)} \\ 0.070 \text{ for Problem 3(B)} \end{cases}$

TABLE 4.13. RESULTS FOR 63 MEMBER WCTS

Member Number	Optimum Cross-Sectional Area in $in.^2$	
	Problem 3(A)	Problem 3(B)
1	38.0780	37.4460
2	36.1020	37.5610
3	51.9230	52.7160
4	54.2430	53.6230
5	25.0690	23.8050
6	28.2220	28.8300
7	17.4610	17.1540
8	20.7660	21.4020
9	24.8100	26.2760
10	26.9370	25.0950
11	7.5854	8.8686
12	9.0049	8.9586
13	24.0470	23.4150
14	20.4880	19.5970
15	4.2966	5.1817
16	2.9538	3.0207
17	37.0600	37.0940
18	37.1710	37.3540
19	0.0100	0.0100
20	0.0100	0.0100
21	0.0470	0.0921
22	0.0100	0.0100
23	0.1048	0.0100
24	1.1187	0.0100
25	0.0312	0.0100

TABLE 4.13. (cont'd.)

Member Number	Optimum Cross-Sectional Area in $in.^2$	
	Problem 3(A)	Problem 3(B)
26	2.9000	4.1985
27	1.3034	0.9148
28	4.7738	3.2278
29	0.8632	0.0100
30	2.6809	8.0127
31	2.7707	8.0586
32	5.8034	9.1997
33	5.6645	9.0427
34	6.0951	9.6634
35	5.6651	9.0430
36	2.8156	8.4160
37	2.7665	8.0605
38	2.6920	7.9197
39	2.7716	8.0652
40	5.7531	9.2645
41	5.6651	9.0417
42	16.0290	24.3540
43	18.3970	26.0850
44	11.4900	19.3100
45	13.8640	21.0440
46	11.7350	17.0110
47	6.1777	12.8530
48	11.7930	18.4540
49	13.9880	19.8470
50	7.3508	6.5775

TABLE 4.13. (cont'd.)

Member Number	Optimum Cross-Sectional Area in $in.^2$	
	Problem 3(A)	Problem 3(B)
51	7.7067	5.6535
52	5.3699	8.4259
53	0.0285	3.8917
54	3.5992	6.1081
55	9.7775	12.1060
56	4.2407	5.7593
57	0.1179	1.5657
58	0.0100	0.0100
59	0.0100	0.0100
60	0.0100	0.0100
61	0.0100	0.0100
62	0.0100	0.0100
63	0.0100	0.0100
At Optimum: Weight in lbs.	4975.06	6117.38
At Optimum: No. of Active Constraints	55	23
At Optimum: Max. Constraint Violation	0.52×10^{-4}	0.34×10^{-3}
At Optimum: $\|\|\delta b^1\|\|_2$	3.68	0.91
Max. $\|\|\delta b^1\|\|_2$	21.64	39.46

violation, and $||\delta b^1||_2$ at the optimum for both the problems and the maximum values of $||\delta b^1||_2$. For Problem 3(A), the set of active constraints at the optimum includes constraints for members 1 to 15, 17, 18, 21, 23 to 25, 28, 50, and 52, under loading condition 1, and for members 26, 30, 32 to 36, 38 to 49, and 54 to 56, under loading condition 2. Minimum size constraints on members 19, 20, 22, and 58 to 63 are also active. For Problem 3(B), the set of active constraints at the optimum includes stress constraints for members 1 to 8, 10 to 18, 21, 28, 29, 50, and 51, under loading conition 1, and the torsional stiffness constraint under loading condition 2.

Table 4.14 gives the cost function history for these problems. Problem 3(A) took 16 iterations to converge and Problem 3(B) took 22 iterations. Details of monitoring the step size are marked in the table. A side run for Problem 3(A) was made with a constant step size ($\bar{r} = 0.09$) and the same optimum was achieved in 34 iterations. Further it is noted here that for Problem 3(B) components of δb^1 and δb^2 associated with design variables for members 19, 20, 22 to 25, 29, and 58 to 63 are equal to zero after the 9th iteration. Hence, in the subsequent iterations for this problem, these design variables are kept fixed.

Table 4.15 gives the computational times for these problems. Finally, Table 4.16 gives a comparison of final weights achieved, number of analyses, average CPU time per design iteration, and total CPU times with other available results. For both the problems, the cost function is practically the same as reported in Ref. 2, whereas in

TABLE 4.14. COST FUNCTION HISTORY FOR 63 MEMBER WCTS

DI† Number	Weight in lbs.	
	3(A)	3(B)
1	4979.82	4977.53
2	4991.27	5593.39
3	4989.77	6067.49
4	4990.27*	6153.84
5	4987.90	6169.71
6	4986.09	6171.36
7	4985.36	6124.21
8	4974.29	6126.13
9	4982.45	6118.17*
10	4982.08	6120.81*
11	4981.20	6117.87
12	4980.56*	6139.43
13	4979.20	6147.08
14	4977.92	6144.55
15	4976.72	6144.69*
16	4975.85	6144.20*
17	4975.06‡	6138.92*
18		6134.22*
19		6128.68*
20		6123.99*
21		6120.99*
22		6118.50*
23		6117.38‡

‡Underlined iteration is not counted as it is used for checking the solution only.

*Means change in step size.

†Design iteration.

TABLE 4.15. COMPUTATIONAL TIMES IN SECONDS FOR 63 MEMBER WCTS

Problem	Total CPU Time For			Total CPU Time (2)+(3)+(4)
	Problem Setup	Stress-Ratio Design	Optimal Design	
1	2	3	4	5
3(A)	1.987	8.955 (10)†	97.242 (16)‡	108.182
3(B)	1.988	11.641 (13)†	62.221 (22)‡	75.850

*Includes CPU time required for analysis, sensitivity analysis, and optimization.

†Number of stress-ratio design iterations performed.

‡Number of design iterations performed.

TABLE 4.16. COMPARISON OF RESULTS FOR 63 MEMBER WCTS

	Problem 3(A)				Problem 3(B)			
	Present‡	Schmit-Miura* [2]	Berke-Khot [6]	Dobbs-Nelson [5]	Present‡	Schmit-Miura* [2]	Berke-Khot [6]	Dobbs-Nelson [5]
Weight in lbs.	4975.06	4976.00	5034.50	5026.40	6117.38	6120.90	6159.30	6646.00
No. of DI†	16	14	50	11	22	13	50	20
Av. CPU Time/DI† in sec.	6.078	6.427	--	--	2.828	6.695	--	--
Total CPU Time in sec.	108.182	90.467	--	--	75.850	87.511	--	--

†Design iteration.

‡IBM 360/65(H).

*IBM 360/91. For comparison, time should be multiplied by 8.

comparison with Ref. 6, it is about 1% lower. Further, in comparison with Ref. 5, the final weight achieved by the present method is about 1% lower for Problem 3(A) and it is 9% lower for Problem 3(B). Finally, comparing the CPU time per design iteration with Ref. 2, it is observed that with the present formulation there is a reduction by factors of 8 and 19 for Problems 3(A) and 3(B), respectively (Table 4.16).

4.5 Discussion and Conclusions Based On Results of Chapter 4

In this section, conclusions based on the results of this chapter are presented. Results of Examples 4.1 and 4.2 are first discussed and compared with results obtained without the substructuring formulation [1]. Then all solutions are discussed and compared with other solutions available in the literature [2-8].

The first example, a 10 member cantilever truss, is a small scale structure. The CPU time per design iteration for problems of this example is reduced by up to 23%, as compared with CPU times without substructuring (Table 4.2). Example 4.2 is a moderate size, 200 member plane truss. For this example, the reduction in computing time is more significant, 6.5 to 66% (Table 4.13).

There are three major phases of any optimal design algorithm: 1) structural analysis, 2) design sensitivity analysis, and 3) calculation of iterative design changes. Thus, the efficiency of any method can be improved by increasing the efficiency of calculations in any of the three phases. The present examples indicate that with substructuring there can be some reduction in computing time of the structural

analysis phase. This fact is also observed by Kirsch, Reiss, and Shamir [9], and Noor and Lowder [10]. However, in the present formulation most of the efficiency is achieved in the design sensitivity analysis phase. For example, if all the constraint violations take place in one substructure, the adjoint matrix λ_I^{sl} is computed for only that substructure. For Case I of the 200 member plane truss example, this means that in design sensitivity analysis one has to solve only a 66 × 66 system of equations, rather than a 150 × 150 system of equations, each having a half band-width of 20 (including the diagonal). Further, an operation count shows that only $(\frac{1}{2}\,nm^2 + \frac{3}{2}\,nm)$ operations are required to decompose a symmetric positive definite banded matrix (n, m) and n(2m + 1) operations are required for the solution of system of n equations [35]. The parameter m is defined here as the half band-width, excluding the diagonal. In the operation count, an operation is defined to consist of one multiplication which is nearly always followed by an addition. Thus, it can be easily seen that the number of calculations is reduced considerably, even with just two substructures, as compared to a formulation without substructuring. The system of equations is further reduced when the number of substructures is increased (Case II and III). It is noted here that Case III of this example has the optimum number of substructures, which is seen from the operation count as well as from the results obtained (Table 4.13).

Based on the above discussion of results, structural analysis and design sensitivity analysis with substructuring is more efficient, because it involves manipulation of matrices having smaller dimensions.

This contributes to a reduction in computation time, as well as computer storage requirements. For optimal design of very large structures with the formulation of the ODPS, the reduction in computing time is expected to be even greater than that achieved for the present examples.

Results obtained by the present method for Examples 4.1 and 4.3 are compared with the results of Refs. 2-6. In all cases, the optimum weights obtained with the present method are the same as obtained in Refs. 2 and 3, whereas they are better than those reported in Refs. 5 and 6 (Tables 4.5 and 4.16). Computing times with the present method are significantly better than those given in Refs. 2 and 3. Computing times in Refs. 5 and 6 are not available and thus cannot be compared.

With the present formulation, there is a reduction in CPU time per design iteration by factors of up to 5.6, 8.3, and 19 for Example 4.1; Problem 3(A); and Problem 3(B), respectively, in comparison to CPU times reported by Schmit and Muira [2]. In comparison with Rizzi [4], there is a reduction by factor of 2.4 in CPU time per design iteration, for Example 4.1.

It should be noted that in the present algorithm, selection of a proper step size requires some experience. A very small step size will slow down the rate of convergence, whereas a large step size may cause oscillation in the algorithm. In the present example problems, the step size was monitored and adjusted to obtain final solutions. More work is needed in the area of step size selection.

CHAPTER 5

OPTIMAL DESIGN OF IDEALIZED WING STRUCTURES

5.1 Introduction

In the previous chapter it was shown that the present formulation offers a reliable and efficient means of obtaining minimum-weight designs for general trusses subjected to static loads with stress, displacement, frequency, and minimum size constraints. In this chapter, the algorithm developed in Chapter 2 for general ODPS is applied to idealized wing structures, with the intention of demonstrating the feasibility of developing a large scale general purpose finite element structural synthesis capability that is practical and efficient. Results are compared with the results available in the literature [2,3,4,7,8].

The class of wing structures considered herein is assumed to have a preassigned geometric configuration and fixed structural material. Further, it is assumed that these structures can be idealized using the following three types of finite elements: (i) truss elements of uniform cross-sectional area, (ii) constant strain triangular (CST) membrane elements of uniform thickness, and (iii) symmetric shear panels (SSP) or symmetric pure shear panels (SPSP). It may be pointed out here that the SSP element differs from the usual SPSP element in that it carries bending and shear loads. The element stiffness matrices for

truss and CST elements are well documented in the literature and will not be derived here. For a complete derivation the reader is referred to Ref. 34. However, element stiffness matrices for the SSP and the SPSP elements cannot be easily found, so their derivation is briefly summarized in Appendix 2.

5.2 Reduction of the Method to Idealized Wing Structures

The ODPS for idealized wing structures is defined as follows: find the design variable associated with each element of the wing structure so that its weight is minimized and the state equations, and the constraints on stress, displacement, and member size are satisfied.

The design variables for the structure are taken as cross-sectional areas of the truss elements and thicknesses of the CST and SSP/SPSP elements. Design variable linking is used, limited of course to pre-specified groups of finite elements that are of the same type. Thus, the cost function of Eq. (2.4-1) is

$$J(b) = \sum_{r=1}^{L} \sum_{k=1}^{TP(r)} \sum_{i=1}^{NG(k)} \sum_{j=1}^{NM(i)} \rho_i \ell_j b_i \qquad (5.2\text{-}1)$$

where

TP(r) = type of element in the rth substructure,

NG(k) = number of groups in the kth type of element,

NM(i) = number of members in the ith group,

ρ_i = material density of elements of the ith group,

b_i = design variable for elements of the ith group,

ℓ_j = length of the jth truss element or surface area of the jth CST/SSP/SPSP element, of the ith group.

The cost function is an explicit linear function of design variables, so its design derivatives are easily obtained.

In the present work, CST/SSP/SPSP elements are required to satisfy a design criterion based on the Von Mises equivalent stress (also known as Maximum Energy of Distortion Theory). This theory, proposed by M. T. Huber in 1904 and later developed by R. Von Mises (1913) and H. Hencky (1925), is in excellent agreement with experiments on ductile materials that are subjected to biaxial or triaxial state of stress, as compared to other theories of failure. For a complete development of the Von Mises equivalent stress criterion, the reader is referred to Ref. 53. According to this criterion, the equivalent stress (σ^c) for an element in a general state of stress is given by

$$\sigma^c = \left[\frac{1}{2}\{(\sigma_{11} - \sigma_{22})^2 + (\sigma_{22} - \sigma_{33})^2 + (\sigma_{33} - \sigma_{11})^2 + 6(\sigma_{12}^2 + \sigma_{23}^2 + \sigma_{31}^2)\}\right]^{1/2} \tag{5.2-2}$$

where σ_{ij} (i,j, = 1,2,3) are stress components at a point of interest (x_1, x_2, x_3) in the domain Ω of the element. For CST or SSP (SPSP) elements, Eq. (5.2-2) reduces to

$$\sigma^c = (\sigma_{11}^2 + \sigma_{22}^2 - \sigma_{11}\sigma_{22} + 3\sigma_{12}^2)^{1/2} \tag{5.2-3}$$

It should be noted that the SSP elements include a uniform shear stress and a linear normal stress distribution (see Appendix II). Thus, the maximum value of the Von Mises equivalent stress in Ω is easily calculated (see Appendix II).

Next, the stress constraint of either Eq. (2.4-3) or (2.4-4), for a typical element, is

$$\phi^s \equiv \left|\frac{\sigma^c}{\sigma^a}\right| - 1.0 \leq 0 \qquad (5.2\text{-}4)$$

where σ^c is the direct stress for truss elements, or the maximum Von Mises equivalent stress calculated from Eq. (5.2-3) for CST/SSP/SPSP elements, and σ^a is an allowable stress.

The design sensitivity analysis for CST/SSP/SPSP elements is quite straight forward and proceeds as explained in Chapters 3 and 4, once the stress-displacement relationship is known. As an easy reference, the stress-displacement relationships for SSP and SPSP elements are given in Appendix II, whereas for CST and truss elements the reader is referred to Ref. 34.

Remaining constraints, i.e., displacement and design variable constraints are the same as in Chapter 4 and are treated in the same manner.

5.3 Example Problems

In order to test the structural synthesis capabilities of the formulation of ODPS, a computer program based on the algorithm of Chapter 2 and flow diagram of Fig. 4.1 was developed and the following

three examples of idealized wing structures are solved:

(i) Example 5.1: 18 Element Wing Box Beam

(ii) Example 5.2: 33 Design Variable Rectangular Wing

(iii) Example 5.3: 150 (130) Element Swept Wing.

These examples have been studied by several researchers [2,3,4,7,8]. In the subsequent subsections, each example is discussed separately. The computational times (in double precision) reported, herein, are for an IBM 360/65(H) computer. The value of ε for imposing ε-active constraints varies from 0.1% to 5% in all example problems. The weighting matrix in these examples is taken to be diagonal, as in Chapter 4, but different from the identity, because the design variables are of different dimensions. In all examples, an element of the weighting matrix associated with the ith design variable is taken as

$$W_i = \frac{\partial J}{\partial b_i} \bar{w}_i \tag{5.3-1}$$

where $\bar{w}_i > 0$ is a weighting multiplier, to be chosen by the designer. In all examples, the value of $\bar{w}_i$ for truss elements varies from 0.50 to 200, whereas for CST, SSP, and SPSP elements it is taken as unity.

5.3.1 Example 5.1: 18 Element Wing Box Beam

Figure 5.1 shows geometry and dimensions of the 18 element wing box beam. The structure is symmetric with respect to the $x_1 - x_2$ plane. Thus, only the upper half of the box beam is idealized. Two cases for this example problem are considered. In Case I, 5 truss, 5

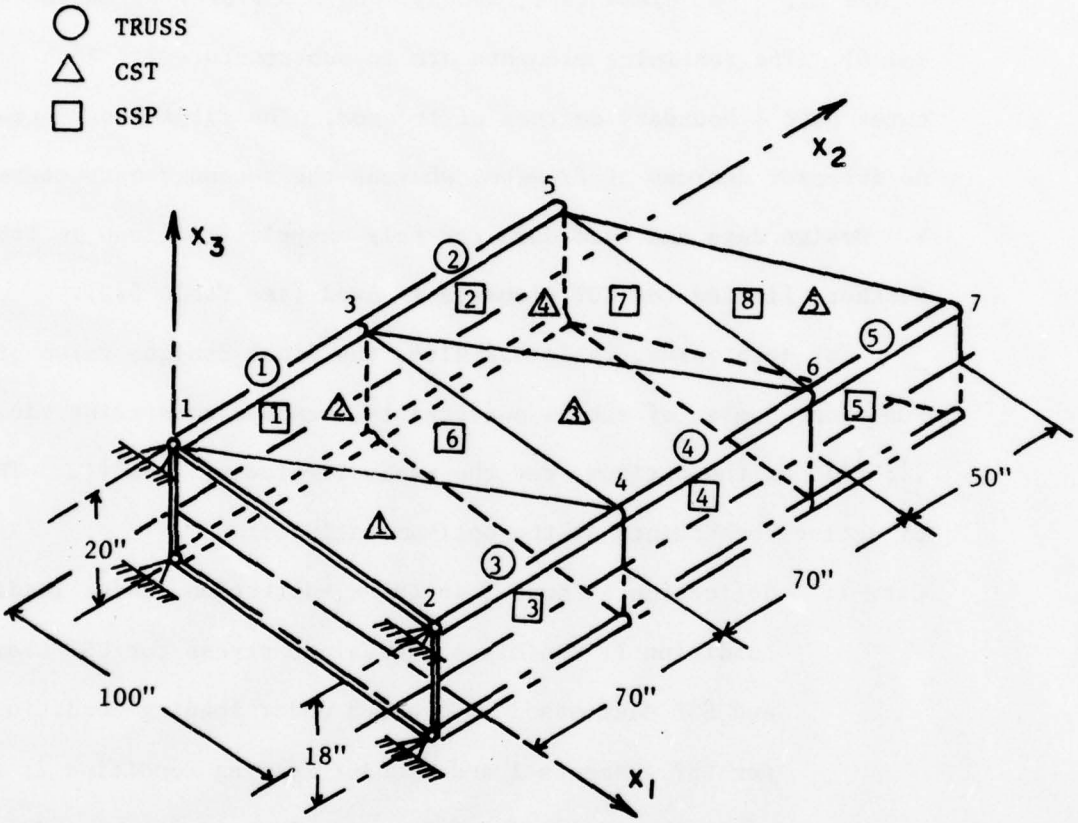

Figure 5.1. 18 Element Wing Box Beam

CST, and 8 SSP elements are used. For Case II, SPSP elements are used, instead of SSP elements. In the formulation of the ODPS, the idealized wing structure is divided into two substructures by partitioning it at nodes 3 and 4. The first substructure consists of 2 truss elements (1 and 3), 2 CST elements (1 and 2), and 3 SSP/SPSP elements (1, 3, and 6). The remaining elements are in substructure 2. Both substructures have 6 boundary degrees of freedom. The first substructure has no interior degrees of freedom, whereas the second substructure has 9. Design data and load data for this example are given in Table 5.1. Further, linking for CST elements is used (see Table 5.2).

For both cases, Table 5.2 gives the final design, value of cost function, number of active constraints, maximum constraint violation, $||\delta b^1||_2$ at the optimum, and the maximum value of $||\delta b^1||_2$. The set of active constraints at the optimum includes:

Case I: deflection at node 5 in the x_3-direction, under loading condition 1; Von Mises equivalent stress for CST element 5 and SSP elements 3 to 5 and 8 under loading condition 1 and for SSP elements 1 and 2 under loading condition 2; and minimum element size for truss elements 2 to 5 and for SSP elements 6 and 7.

Case II: deflection at node 5 in the x_3-direction under loading condition 2; Von Mises equivalent stress for CST element 2 and SPSP elements 1 and 2 under loading condition 2; and minimum element size for truss elements 2, 3, and 5, and for SPSP elements 6 and 7.

TABLE 5.1. DESIGN DATA FOR 18 ELEMENT WING BOX BEAM

A. Data Common to All Type of Elements:

Modulus of elasticity = 10^4 ksi

Material density = 0.10 lb/in.^{3}

Poisson's ratio = 0.30

Displacement limit at nodes 3 to 7 in x_3-direction = ±2.0 in.

Number of loading conditions = 2

Load data:

Loading Condition	No. of Loaded Nodes	Node Number	Load Component (kips) in direction		
			x_1	x_2	x_3
1	1	7	0.0	0.0	5.0
2	1	5	0.0	0.0	10.0

Starting reduction ratio, $\bar{r}$ = {0.027 for Case I; 0.081 for Case II}

B. Data for Individual Type of Elements:

Starting weighting multiplier, $\bar{w}_i$ = {100.0 for Case I; 200.0 for Case II} (for truss elements)

Type of Element	Stress Limit ksi	Design Variable		
		Lower Limit	Upper Limit	Initial Design
TRUSS	±10.0	0.10 in.^{2}	None	0.98 in.^{2}
CST	10.0	0.02 in.	1.0 in.	0.196 in.
SSP	10.0	0.02 in.	1.0 in.	0.196 in.
SPSP	10.0	0.02 in.	1.0 in.	0.196 in.

TABLE 5.2. RESULTS FOR 18 ELEMENT WING BOX BEAM

Type of Element	Group Number	Element Number	Optimum Design Case I	Optimum Design Case II
Truss ($in.^2$)	1	1	3.8682	1.39290
	2	2	0.1000	0.10000
	3	3	0.1000	0.10000
	4	4	0.1000	0.54522
	5	5	0.1000	0.10000
CST (in.)	6	1,2	0.084383	0.122730
	7	3,4	0.053070	0.053830
	8	5	0.037844	0.038444
SSP For Case I And SPSP For Case II (in.)	9	1	0.370500	0.088141
	10	2	0.224470	0.089840
	11	3	0.128540	0.074624
	12	4	0.120750	0.073084
	13	5	0.091634	0.075286
	14	6	0.020000	0.020000
	15	7	0.020000	0.020000
	16	8	0.030954	0.024886
At Optimum: Weight in lbs.			402.73	357.09
At Optimum: No. of Active Constraints			14	9
At Optimum: Max. Constraint Violation			0.53×10^{-3}	0.48×10^{-3}
At Optimum: $\|\|\delta b^1\|\|_2$			17.13	44.18
Max. $\|\|\delta b^1\|\|_2$			1513.00	1204.00

Table 5.3 gives the cost function history. It is noted here that components of δb^1 and δb^2 associated with design variables for elements 2 to 5 (truss), 14 and 15 (SSP) of Case I, and 2, 3, and 5 (truss), 14 and 15 (SPSP) of Case II are equal to zero after the 1st iteration. Hence in the subsequent iterations, these design variables are kept fixed. The details of computational times are given in Table 5.4.

Finally for both cases, Table 5.5 gives a comparison of results. Compared to Refs. 2 and 3, the cost function is practically the same, whereas for the Case II there is a reduction of about 9%, as compared to Refs. 7 and 8. With the present formulation, the total CPU time is less by factors of 2.2 and 3.2 for Case I, as compared to Refs. 2 and 4, respectively. For the Case II, it is less by a factor of 3.5, as compared to Ref. 2. Finally, a comparison of CPU time per design iteration indicates that there are reductions by factors of 4.3 and 3.4, as compared to Refs. 2 and 4, for Case I, respectively and by a factor of 4.6, as compared to Ref. 2, for Case II.

5.3.2 Example 5.2: 33-Design Variable Rectangular Wing

Figure 5.2 shows the geometry and dimensions for a wing structure, which is symmetric with respect to the x_1-x_2 plane and corresponds to the wing middle surface. Thus, only the upper half of the rectangular wing is modeled, using 12 truss elements to represent spar caps, 12 CST elements for the skin, and 15 SSP elements for the vertical webs.

In the present formulation, the idealized wing structure is divided into three substructures by partitioning it at nodes 5-6, and 9-10.

TABLE 5.3 COST FUNCTION HISTORY FOR 18 ELEMENT WING BOX BEAM

DI† Number	Weight in lbs.	
	Case I	Case II
1	401.21	355.90
2	424.42	359.66
3	377.76*	354.07
4	414.38*	360.83*
5	377.00	360.67
6	381.94	360.19*
7	400.95	358.93
8	377.56	358.76
9	399.92	357.12
10	410.36*	357.09‡
11	410.77	
12	406.43	
13	404.04	
14	402.98	
15	402.59	
16	402.73‡	

‡Underlined iteration is not counted as it is used for checking the solution only.

*Means change in step size.

†Design iteration.

TABLE 5.4. COMPUTATIONAL TIMES IN SECONDS FOR 18 ELEMENT WING BOX BEAM

Problem	Total CPU Time for			Total CPU Time (2)+(3)+(4)
	Problem Setup	Stress-Ratio Design	Optimal Design*	
1	2	3	4	5
Case I	0.847	1.505 (4)†	9.80 (15)‡	12.152
Case II	1.015	1.316 (4)†	5.593 (9)‡	7.924

*Includes CPU time required for analysis, sensitivity analysis, and optimization.

†Number of stress-ratio design iterations performed.

‡Number of design iterations performed.

TABLE 5.5. COMPARISON OF RESULTS FOR 18 ELEMENT WING BOX BEAM

	Case I				Case II			
	Weight in lbs	No. of DI†	Av. CPU Time/ DI† in sec	Total CPU Time in sec	Weight in lbs	No. of DI†	Av. CPU Time/ DI† in sec	Total CPU Time in sec
Present‡	402.73	15	0.653	12.152	357.09	9	0.622	7.924
Schmit-Miura* [2]	402.97	8	0.353	3.366	357.82	8	0.360	3.427
Rizzi** [3,4]	402.74	15	0.055	0.973	--	-	--	--
Gellatly-Berke [7]	--	--	--	--	387.67	4	--	--
Gellatly [8]	--	--	--	--	389.80	193	--	--

†Design iteration.

‡IBM 360/65(H).

*IBM 360/91. For comparison, time should be multiplied by 8.

**CDC 7600. For comparison, time should be multiplied by 40.

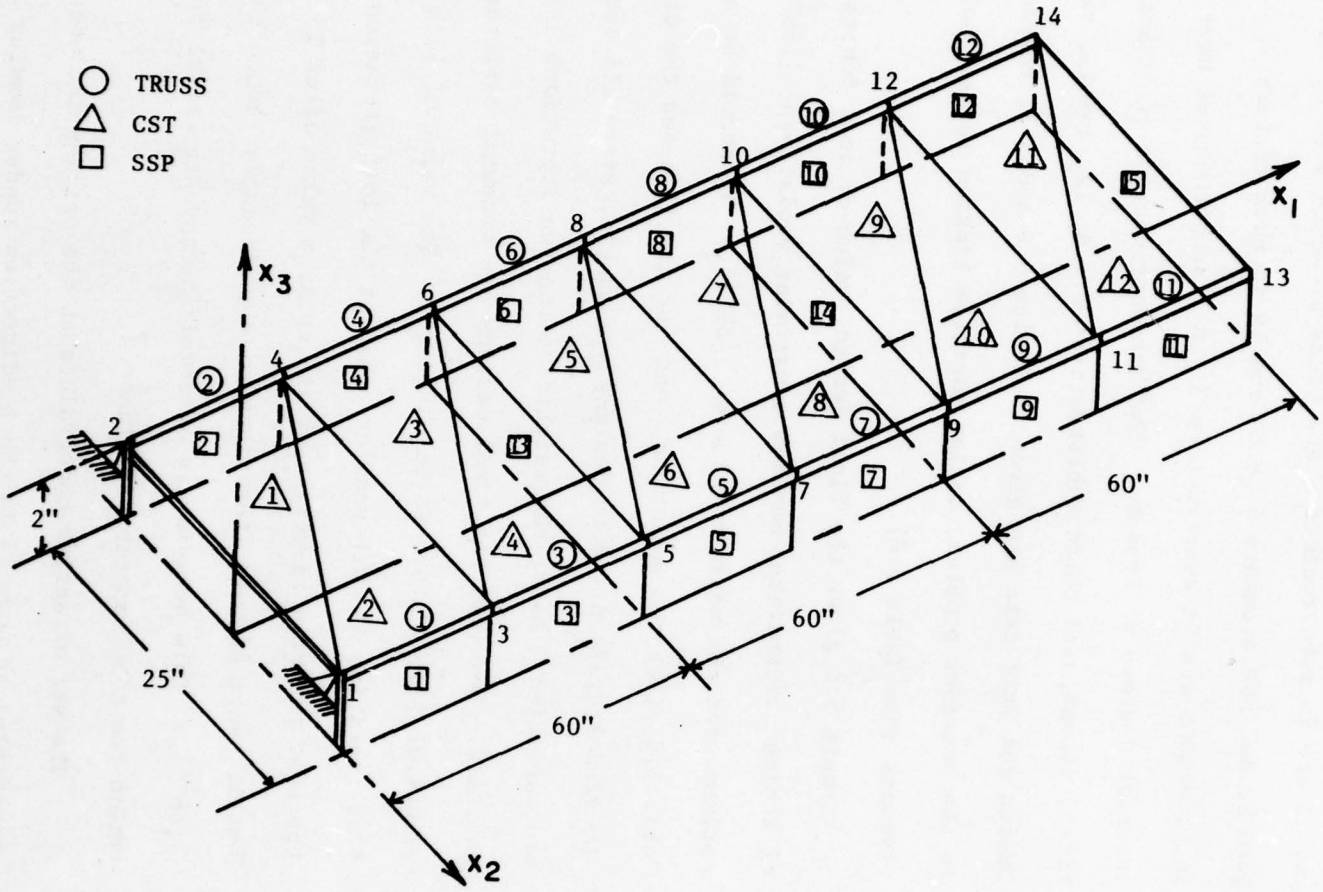

Figure 5.2. 33 Design Variable Rectangular Wing

Truss elements 1 to 4, CST elements 1 to 4, and SSP elements 1 to 4, and 13 are in substructure 1 and truss elements 5 to 8, CST elements 5 to 8, and SSP elements 5 to 8 and 14 in substructure 2. The remaining elements are in substructure 3. All substructures have six interior degrees of freedom. The boundary degrees of freedom for the first, second, and third substructures are 6, 12, and 12, respectively. Design and load data are given in Tables 5.6 and 5.7, respectively. As in the previous problem, design variable linking is used only for CST elements (see Table 5.8).

Table 5.8 gives the final design, value of cost function, number of active constraints, maximum constraint violations, $||\delta b^1||_2$ at the optimum, and the maximum value of $||\delta b^1||_2$. It should be noted that Table 5.8 gives two solutions, one at the 15th and the other at the 42nd iteration. Both designs are usable, since all constraints are satisfied. Also, the weights at the two iterations are practically the same. However, the final designs are somewhat different and the values of $||\delta b^1||_2$ are quite different. The value of $||\delta b^1||_2$ at the 42nd iteration is much smaller than at the 15th iteration. Further, the cost function is very near its optimum value after 15 iterations, but it takes 27 more iterations to significantly reduce the value of $||\delta b^1||_2$. This behavior is observed in many structural problems, in which the cost function is linear.

The set of active constraints at the optimum includes: deflection constraint at node 14 in the x_3-direction under loading condition 2;

TABLE 5.6. DESIGN DATA FOR 33 DESIGN VARIABLE RECTANGULAR WING

A. Data Common to All Type of Elements:

Modulus of elasticity	$= 10.5 \times 10^3$ ksi
Material density	$= 0.1$ lb/in.^{3}
Poisson's ratio	$= 0.3$
Displacement limit at nodes 13 and 14 in x_3-direction	$= \pm 11.0$ in.
Number of loading conditions	= 2 (see Table 5.7)
Starting reduction ratio, $\bar{r}$	$= 0.021$

B. Data for Individual Type of Elements:

Starting weighting multiplier, $\bar{w}_i = 0.667$ (for truss elements)

Type of Element	Stress Limit in ksi	Design Variable		Initial Design
		Lower Limit	Upper Limit	
TRUSS	±25.0	0.10 in.^{2}	1.50 in.^{2}	2.0 in.^{2}
CST	25.0	0.01 in.	None	0.08 in.* 0.04 in.**
SSP	25.0	0.01 in.	None	0.04 in.

*For elements 1 to 12

**For elements 13 to 15

TABLE 5.7. LOAD DATA FOR 33 DESIGN VARIABLE RECTANGULAR WING

For all nodes, x_1 and x_2 components of load = 0.0

Node Number	Component of Load in x_3 direction (kips)	
	Load Condition 1	Load Condition 2
3	0.1658	0.2996
4	0.4144	0.3745
5	0.1426	0.2576
6	0.3564	0.3221
7	0.1311	0.2367
8	0.3274	0.2958
9	0.1177	0.2127
10	0.2943	0.2659
11	0.0978	0.1768
12	0.2445	0.2209
13	0.0381	0.0689
14	0.0953	0.0861

TABLE 5.8. RESULTS FOR 33 DESIGN VARIABLE RECTANGULAR WING

Type of Element	Group Number	Element Numbers	Optimum Design	
			At 15th DI†	At 42nd DI†
Truss ($in.^2$)	1	1	1.32640	1.3063
	2	2	1.37700	1.3713
	3	3	0.83578	0.82372
	4	4	0.91279	0.92373
	5	5	0.49935	0.48875
	6	6	0.52112	0.52810
	7	7	0.24142	0.22519
	8	8	0.24934	0.26079
	9	9	0.10129	0.10
	10	10	0.11074	0.12404
	11	11	0.10	0.10
	12	12	0.10	0.10
CST (in.)	13	1,2	0.123930	0.127470
	14	3,4	0.099328	0.098920
	15	5,6	0.073211	0.072230
	16	7,8	0.047007	0.046674
	17	9,10	0.020752	0.020828
	18	11,12	0.010	0.010
SSP (in.)	19	1	0.059261	0.059019
	20	2	0.080678	0.072716
	21	3	0.041459	0.041699
	22	4	0.064171	0.063083
	23	5	0.031355	0.029265
	24	6	0.047776	0.050518
	25	7	0.026171	0.022464
	26	8	0.038431	0.040775
	27	9	0.018753	0.014846
	28	10	0.028262	0.031025
	29	11	0.010	0.010
	30	12	0.025174	0.013188
	31	13	0.010	0.010
	32	14	0.010	0.010
	33	15	0.010	0.010
At Optimum: Weight in lbs.			100.344	100.212
At Optimum: No. of Active Constraints			10	15
At Optimum: Max. Constraint Violation			0.88×10^{-7}	0.72×10^{-7}
At Optimum: $\|\|\delta b^1\|\|_2$			17.48	1.94
Max. $\|\|\delta b^1\|\|_2$			102.70	102.70

†Optimal Design iteration.

Von Mises equivalent stress in SSP elements 1 and 3, under loading condition 2; and minimum element size for truss elements 11 and 12, CST elements 11 and 12 (design variable 16), and SSP elements 11, 13, 14, and 15. Table 5.9 gives a comparison of final design weight, number of design iterations, CPU time per design iteration, and total computing time which includes initial set-up time (2:086 sec), 4 iterations of stress-ratio design time (3:528 sec), and 15 iterations of design time (17.689 sec). The cost function is practically the same as obtained by Rizzi [3,4]. Comparing the CPU time per design iteration and total CPU time with Ref. 4, it is observed that with the present formulation there is a reduction by factors of 6.4 and 5.4, respectively.

Lastly, the cost function history (in lbs.) for this problem is: 64.476, 82.551, 99.790, 104.314, 104.157*, 102.071, 101.095, 100.797*, 100.279, 100.185, 100.121*, 100.359, 100.360, 100.359, 100.365, 100.344 (* means change in step size). It is noted that for this problem components of δb^1 and δb^2 associated with design variables for elements 11 and 12 (truss), and 31 to 33 (SSP) are equal to zero after the 4th iteration. Hence, in the subsequent iterations for the problem, these design variables are kept fixed.

5.3.3 Example 5.3: 150(130) Element Swept Wing

Figure 5.3 shows geometry, dimensions, and element numbering of the idealized swept wing structure. The wing is symmetric with respect to the x_1-x_2 plane. Thus, only the upper half of the swept wing is

TABLE 5.9. COMPARISON OF RESULTS FOR 33 DESIGN VARIABLE RECTANGULAR WING

	Present‡	Rizzi [3,4]**
Weight in lbs.	100.344	100.542
No. of DI†	15	15
Av. CPU Time/DI† in sec	1.179	0.189
Total CPU Time in sec	23.303	3.142

†Design iteration

‡IBM 360/65(H)

**CDC 7600. For comparison, time should be multiplied by 40.

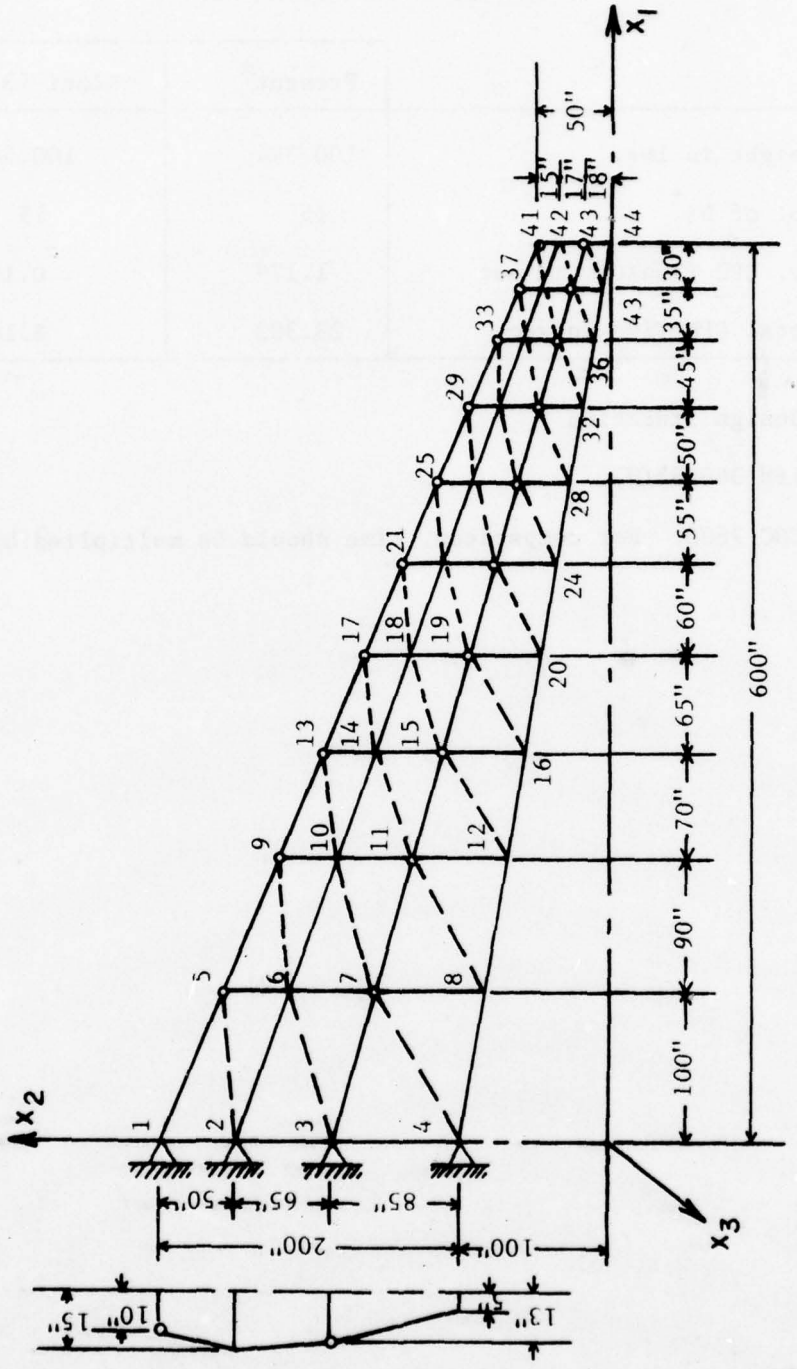

Figure 5.3(a) 150 (130) Element Swept Wing

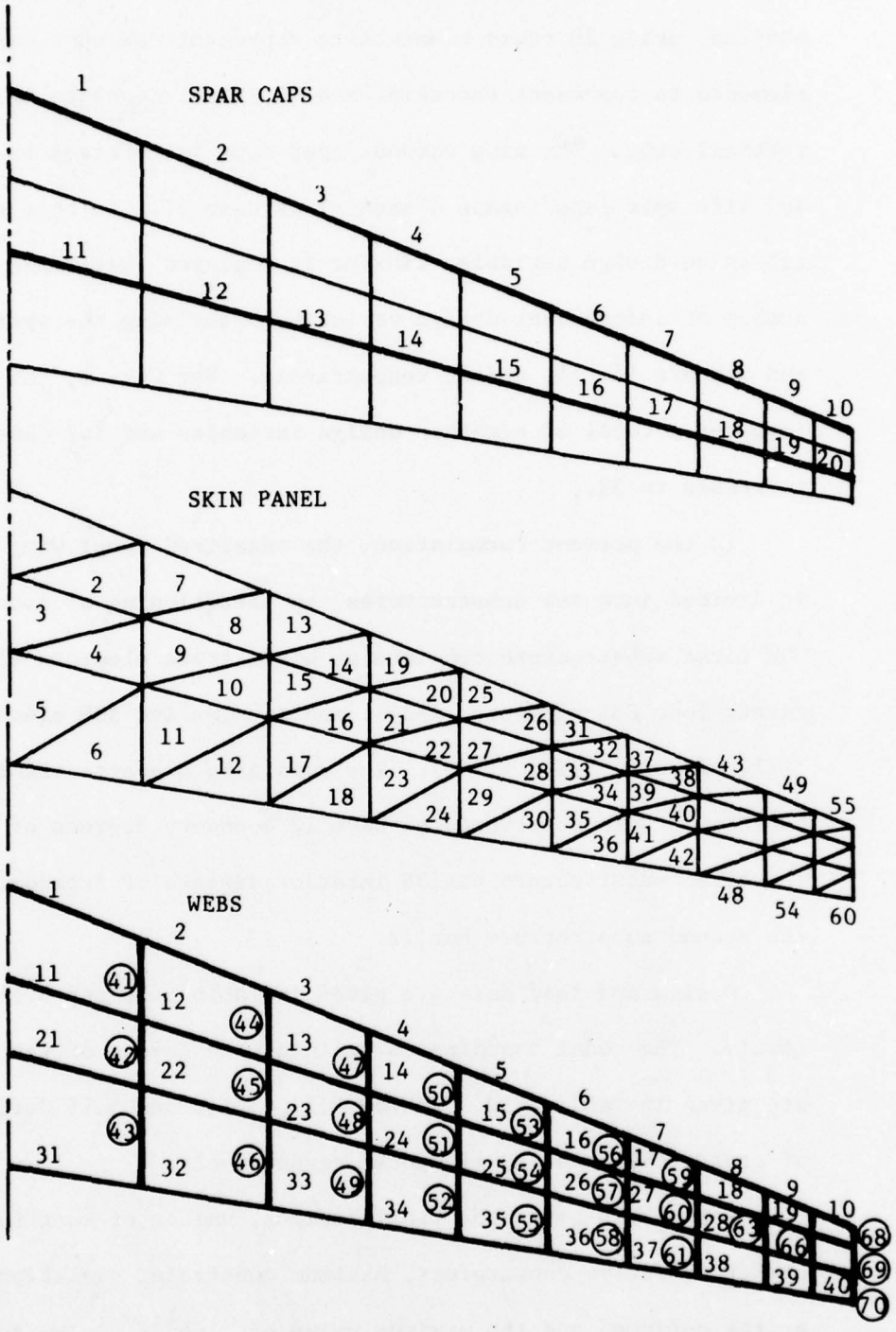

Figure 5.3(b). 150 (130) Element Swept Wing. Element Numbering

modeled, using 20 truss elements to represent the spar caps, 60 CST elements to represent the skin, and 70 SSP elements to represent the vertical webs. The wing without spar caps is referred to as Case I, and with spar caps (truss elements) as Case II. In this example, extensive design variables linking is employed (see Table 5.16). The number of independent design variables describing the spar cap, skin, and web are 14, 11, and 7, respectively. For Case I, the problem involves a total of eighteen design variables and for Case II, it increases to 32.

In the present formulation, the idealized swept wing structure is divided into two substructures by partitioning at nodes 17 to 20. The first substructure consists of eight truss elements (1-4, 11-14), twenty four CST elements (1-24), and twenty-five SSP elements (1-4, 11-14, 21-24, 31-34, 41-49). The remaining elements are in substructure two. Both substructures have 12 boundary degrees of freedom. The first substructure has 36 interior degrees of freedom, whereas the second substructure has 72.

Design and load data are given in Table 5.10 and 5.11, respectively. The nodal coordinates defining the layout of the swept wing are given in Table 5.12. Tables 5.13, 5.14, and 5.15 define locations of truss, CST, and SSP elements, respectively.

Table 5.16 gives the final designs, values of cost function, number of active constraints, maximum constraint violations, $||\delta b^1||_2$ at the optimum, and the maximum value of $||\delta b^1||_2$. The set of active constraints at optimum includes:

TABLE 5.10. DESIGN DATA FOR 150 (130) ELEMENT SWEPT WING

A. Data Common to All Type of Elements:

Modulus of elasticity (Aluminum alloy)	$= 10.6 \times 10^3$ ksi
Material density	$= 0.096$ lb/in.^{3}
Poisson's ratio	$= 0.30$
Displacement limit at nodes 41 and 44 in x_3-direction	$= \pm 60.0$ in.
Number of loading conditions	= 2 (see Table 5.11)
Starting reduction ratio, $\bar{r}$	= 0.054 for both Case I and II

B. Data for Individual Type of Elements:

Starting weighting multiplier, $\bar{w}_1 = 20.0$ for Case II (for truss elements)

Type of Element	Stress Limit in ksi	Design Variable		Initial Design	
		Lower Limit	Upper Limit	With Spar Caps	Without Spar Caps
TRUSS	±25.0	0.01 in.^{2}	1.50 in.^{2}	0.02 in.^{2}	--
CST	25.0	0.02 in.	None	{0.20* in.* / 0.10 in.**}	0.30 in.
SSP	25.0	0.02 in.	None	0.20 in.	0.15 in.

*For elements 1 to 24.

**For elements 25 to 60.

TABLE 5.11. LOAD DATA FOR 150 (130) ELEMENT SWEPT WING

For all nodes, x_1 and x_2 components of load = 0.0

Node Number	Load in x_3 direction kips	Node Number	Load in x_3 direction kips	Node Number	Load in x_3 Direction kips
Load Condition 1					
5	1.282	19	1.453	33	0.206
6	2.581	20	1.057	34	0.431
7	3.398	21	0.459	35	0.563
8	2.380	22	0.958	36	0.383
9	0.978	23	1.251	37	0.144
10	2.013	24	0.852	38	0.302
11	2.593	25	0.362	39	0.395
12	1.764	26	0.756	40	0.269
13	0.727	27	0.986	41	0.620
14	1.386	28	0.671	42	0.129
15	1.906	29	0.282	43	0.169
16	1.297	30	0.589	44	0.116
17	0.570	31	0.768		
18	1.190	32	0.522		
Load Condition 2					
5	2.361	19	1.025	33	0.402
6	3.876	20	0.355	34	0.646
7	2.308	21	0.843	35	0.398
8	0.793	22	1.374	36	0.154
9	1.772	23	0.825	37	0.311
10	2.895	24	0.284	38	0.482
11	1.705	25	0.665	39	0.306
12	0.582	26	1.092	40	0.135
13	1.310	27	0.651	41	0.133
14	2.135	28	0.224	42	0.206
15	1.258	29	0.518	43	0.131
16	0.433	30	0.851	44	0.580
17	1.047	31	0.508		
18	1.719	32	0.175		

TABLE 5.12. NODAL COORDINATES FOR 150(130) ELEMENT SWEPT WING

Node Number	Coordinate in inches		
	x_1	x_2	x_3
1	0.0	300.00	10.00
2	0.0	250.00	15.00
3	0.0	185.00	13.00
4	0.0	100.00	5.00
5	100.0	258.3332	8.5833
6	100.0	214.1667	12.8333
7	100.0	157.1667	11.0833
8	100.0	83.3333	4.3333
9	190.0	220.8333	7.3083
10	190.0	181.9167	10.8833
11	190.0	132.1167	9.3583
12	190.0	68.3333	3.7333
13	260.0	191.6667	6.3167
14	260.0	156.8333	9.3667
15	260.0	112.6333	8.0167
16	260.0	56.6667	3.2667
17	325.0	164.5833	5.3958
18	325.0	133.5416	7.9583
19	325.0	94.5417	6.7708
20	325.0	45.8333	2.8333
21	385.0	139.5833	4.5458
22	385.0	112.0416	6.6583
23	385.0	77.8417	5.6208
24	385.0	35.8333	2.4333
25	440.0	116.6666	3.7667
26	440.0	92.3333	5.4667
27	440.0	62.5333	4.5667
28	440.0	26.6667	2.0667
29	490.0	95.8333	3.0583
30	490.0	74.4167	4.3833
31	490.0	48.6166	3.6083
32	490.0	18.3333	1.7333
33	535.0	77.0833	2.4208
34	535.0	58.2917	3.4083
35	535.0	36.0917	2.7458
36	535.0	10.8333	1.4333
37	570.0	62.50	1.9250
38	570.0	45.75	2.6500
39	570.0	26.35	2.0750
40	570.0	5.00	1.20
41	600.0	50.00	1.50
42	600.0	35.00	2.00
43	600.0	18.00	1.50
44	600.0	0.00	1.00

TABLE 5.13. TRUSS ELEMENT LOCATIONS FOR 150 (130) ELEMENT SWEPT WING

Member	End Nodes	Member	End Nodes
1	1,5	11	3,7
2	5,9	12	7,11
3	9,13	13	11,15
4	13,17	14	15,19
5	17,21	15	19,23
6	21,25	16	23,27
7	25,29	17	27,31
8	29,33	18	31,35
9	33,37	19	35,39
10	37,41	20	39,43

TABLE 5.14. CST ELEMENT LOCATIONS FOR
150 (130) ELEMENT SWEPT WING

Member	End Nodes	Member	End Nodes	Member	End Nodes
1	1,2,5	21	14,15,18	41	27,28,31
2	6,5,2	22	19,18,15	42	32,31,28
3	2,3,6	23	15,16,19	43	29,30,33
4	7,6,3	24	20,19,16	44	34,33,30
5	3,4,7	25	17,18,21	45	30,31,34
6	8,7,4	26	22,21,18	46	35,34,31
7	5,6,9	27	18,19,22	47	31,32,35
8	10,9,6	28	23,22,19	48	36,35,32
9	6,7,10	29	19,20,23	49	33,34,37
10	11,10,7	30	24,23,20	50	38,37,34
11	7,8,11	31	21,22,25	51	34,35,38
12	12,11,8	32	26,25,22	52	39,38,35
13	9,10,13	33	22,23,26	53	35,36,39
14	14,13,10	34	27,26,23	54	40,39,36
15	10,11,14	35	23,24,27	55	37,38,41
16	15,14,11	36	28,27,24	56	42,41,38
17	11,12,15	37	25,26,29	57	38,39,42
18	16,15,12	38	30,29,26	58	43,42,39
19	13,14,17	39	26,27,30	59	39,40,43
20	18,17,14	40	31,30,27	60	44,43,44

TABLE 5.15. SSP ELEMENT LOCATIONS FOR
150 (130) ELEMENT SWEPT WING

Member	End Nodes	Member	End Nodes	Member	End Nodes
1	1,5	25	19,23	49	15,16
2	5,9	26	23,27	50	17,18
3	9,13	27	27,31	51	18,19
4	13,17	28	31,35	52	19,20
5	17,21	29	35,39	53	21,22
6	21,25	30	39,43	54	22,23
7	25,29	31	4,8	55	23,24
8	29,33	32	8,12	56	25,26
9	33,37	33	12,16	57	26,27
10	37,41	34	16,20	58	27,28
11	2,6	35	20,24	59	29,30
12	6,10	36	24,28	60	30,31
13	10,14	37	28,32	61	31,32
14	14,18	38	32,36	62	33,34
15	18,22	39	36,40	63	34,35
16	22,26	40	40,44	64	35,36
17	26,30	41	5,6	65	37,38
18	30,34	42	6,7	66	38,39
19	34,38	43	7,8	67	39,40
20	38,42	44	9,10	68	41,42
21	3,7	45	10,11	69	42,43
22	7,11	46	11,12	70	43,44
23	11,15	47	13,14		
24	15,19	48	14,15		

TABLE 5.16. RESULTS FOR 150 (130) ELEMENT SWEPT WING

Type of Element	Group Number	Element Numbers	Optimum Design	
			Case I	Case II
Truss ($in.^2$)	1	1		0.010000
	2	2		0.010000
	3	3		0.010000
	4	4		0.010000
	5	5,6		0.010000
	6	7,8		0.010000
	7	9,10		0.010000
	8	11		1.500000
	9	12		0.637270
	10	13		0.339730
	11	14		0.716110
	12	15,16		1.002900
	13	17,18		0.389730
	14	19,20		0.010000
CST (in.)	15	1-6	0.203340	0.191260
	16	7-12	0.177250	0.171290
	17	13-18	0.156250	0.151740
	18	19-24	0.129290	0.123110
	19	25-36	0.110810	0.099201
	20	37-48	0.094851	0.087910
	21	49-60	0.020000	0.020000
SSP (in.)	22	1-4	0.032631	0.032648
	23	5-10	0.020000	0.020000
	24	11-14	0.033091	0.031825
	25	15-20	0.046713	0.047229
	26	21-24	0.221400	0.228710
	27	25-30	0.097980	0.115860
	28	31-34	0.088411	0.084393
	29	35-40	0.060872	0.055557
	30	41-49	0.035310	0.035857
	31	50-58	0.061103	0.068786
	32	59-70	0.105600	0.099396
At Optimum	Weight in lbs.		2462.34	2442.06
	No. of Active Constraints		13	22
	Max. Constraint Violations		0.28×10^{-3}	0.59×10^{-4}
	$\|\|\delta b^1\|\|_2$		33.12	35.11
Max. $\|\|\delta b^1\|\|_2$			2647.00	3263.00

Case I: Von Mises equivalent stress for CST element 8, 14, 20 under loading condition 1, for SSP elements 20, 21, 30,58, and 61 under loading condition 1, and 3, 11, and 42 under loading condition 2; and minimum element size for CST elements 49 to 60 and SSP elements 5 to 10.

Case II: For the final design with spar caps, active constraints at the optimum are the same as for Case I, with the addition of minimum area constraints for truss elements 1 to 10, 19 and 20, and maximum area constraint for truss element 11.

The set of active constraints is found to be the same as in Refs. 2 and 3, with the exception of stress constraint for SSP element 11 under loading condition 2. It is noted that none of the tip deflection constraints are active. It is noted that for Case II the spar cap, web, and skin materials account for 3.57%, 12.61%, and 83.82% of the final wing weight, respectively. For Case I, the web and skin materials account for 13.11% and 86.89% of the final wing weight, respectively. In Ref. 2, spar cap material accounts for less than 0.5% of the final wing weight, while the web material accounts for approximately 12.5% of the final wing weight in both cases. Thus, the distribution of the material achieved by the present method is approximately the same as in Ref. 2, except for the spar caps. The optimum design reported in Table 5.16 is obtained in 15 design iterations for both the cases. Also, it is noted that for Case I, a usable design is found at the 10th iteration with a weight of 2469.36 lbs., which is within 0.3% of the minimum achieved. For Case II, a usable design is found at the 7th

iteration, with a weight of 2459.52 lbs, which is within 0.7% of the minimum achieved.

Table 5.17 gives the cost function history for both cases. It is noted that components of δb^1 and δb^2 associated with design variables for elements 1 to 10, 19 to 20 (Truss), 49 to 60 (CST), and 5 to 10 (SSP) for Case II; and 49 to 60 (CST), and 5 to 10 (SSP) for Case I are equal to zero after the 8th iteration for Case II and after the 9th iteration for Case I. Hence, in the subsequent iterations these design variables are kept fixed. Computational times are given in Table 5.18. Table 5.19 gives a comparison of results. The cost function, as compared to Ref. 3, is practically the same for both cases. It is the same for Case I, as compared to Ref. 2, but about 0.9% less for Case II. With the present formulation, the total CPU time is less by factors of 2.1 and 6.4 for Case I, as compared to Refs. 2 and 4, respectively. For Case II, it is less by factors of 3.1 and 9.1, as compared to Refs. 2 and 4. A comparison of CPU time per design iteration indicates that there is a reduction by factors of 4.4 and 6.5 for the Case I; and by factors of 6.0 and 9.4 for the Case II, as compared to Refs. 2 and 4, respectively.

Lastly, the swept wing is divided into five substructures by partitioning it at nodes 9 to 12, 17 to 20, 25 to 28, and 33 to 36. Nodes 41 to 44 are also considered as boundary nodes. With this partitioning, there is considerable linking of design variables across substructure boundaries. The optimum results obtained are the same for both Cases I and II. The total CPU time is also the same. This is

TABLE 5.17. COST FUNCTION HISTORY FOR
150 (130) ELEMENT SWEPT WING

DI† Number	Weight in lbs.	
	Case I	Case II
1	2360.13	2360.76
2	2432.72	2413.35
3	2471.54	2465.10
4	2460.06	2422.09
5	2459.76	2429.75
6	2457.30	2455.01
7	2452.68	2459.52
8	2467.41	2456.99
9	2463.20	2454.11*
10	2469.36*	2448.68
11	2466.98*	2443.93*
12	2465.37*	2443.44
13	2464.16*	2442.74*
14	2463.24*	2442.62
15	2462.67*	2442.46*
16	2462.34‡	2442.06‡

‡Underlined iteration is not counted as it is used for checking the solution only.

*Means change in step size.

†Design iteration.

TABLE 5.18. COMPUTATIONAL TIMES IN SECONDS FOR 150 (130) ELEMENT SWEPT WING

Problem	Total CPU Time for			Total CPU Time (2)+(3)+(4)
	Problem Setup	Stress-Ratio Design	Optimal Design*	
1	2	3	4	5
Case I	3.101	9.800 (4)†	69.118 (15)‡	82.019
Case II	3.717	10.584 (4)†	74.067 (15)‡	88.368

*Includes CPU time required for analysis, sensitivity analysis, and optimization.

†Number of stress-ratio design iterations performed.

‡Number of design iterations performed.

TABLE 5.19. COMPARISON OF RESULTS FOR 150 (130) ELEMENT SWEPT WING

	Case I				Case II			
	Weight in lbs	No. of DI†	Av. CPU Time/ DI† in sec	Total CPU Time in sec	Weight in lbs	No. of DI	Av. CPU Time/ DI† in sec	Total CPU Time in sec
Present‡	2462.34	15	4.608	82.118	2442.06	15	4.938	88.368
Schmit-Miura* [2]	2462.82	8	2.527	21.496	2460.84	9	3.692	34.647
Rizzi** [3,4]	2461.76	16	0.747	13.194	2445.76	16	1.156	20.208

†Design iteration.

‡IBM 360/65(H).

*IBM 360/91. For comparison, time should be multiplied by 8.

**CDC 7600. For comparison, time should be multipled by 40.

due to the fact that the total number of calculations with two and five substructures is approximately the same (see Section 4.5).

5.4 Discussion and Conclusions Based on Results of Chapter 5

In this section results of all examples are discussed and compared with other solutions available in the literature [2-8].

The first example, the 18 element wing box beam, is a small scale structure and is used for developing the computer program for idealized wing structures. The second example is of medium scale, whereas the third problem is fairly large.

The optimum weights for all examples, obtained by the present method, are the same as obtained in Refs. 2 to 4, except for Example 5.3 (Case II), in which the final weight achieved is 0.9% less than in Ref. 2. Further, as compared to Refs. 7 and 8, there is a reduction of about 9% in the cost function for Example 5.1 (Case I).

The computing times with the present method are significantly better than given in Refs. 2 to 4. This fact is also observed in Chapter 4. Computing times in Refs. 7 and 8 are not available and thus cannot be compared. With the present formulation, there is a reduction in CPU times per design iteration by factors of 4.3, 4.6, 4.4, and 6.0 for both the cases of Examples 5.1 and 5.3, respectively, as compared with CPU times reported by Schmit and Miura [2]. In comparison with Rizzi [4], there are reductions by factors of 3.4, 6.4, 6.5, and 9.4 for Case I of Example 5.1, Example 5.2, and both cases of Example 5.3, respectively.

It should be noted that in the present method, as applied to idealized wing structures, selection of a proper weighting multiplier $\bar{w}_i$ associated with ith design variable is essential for fast convergence. In the present examples this multiplier is monitored and adjusted to obtain final solutions. As a test example, side computation for the Case II of 150 (130) Element Swept Wing was made keeping the weighting multiplier to be unity for all design variables. The same optimum as reported in Table 5.16 was achieved in 40 iterations as compared to 15 iterations reported in Table 5.17. This shows that proper selection of a weighting matrix is essential for rapid convergence.

Numerical results presented in this chapter indicate that the present formulation is quite efficient to serve as a practical structural synthesis method. However, more research work is needed in the area of selection of a proper weighting matrix.

CHAPTER 6

OPTIMAL DESIGN OF FRAMED STRUCTURES

6.1 Introduction

In this chapter, the optimal design method developed with substructuring in Chapter 2 is applied to framed structures. Framed structures are found quite frequently in practical situations, including some buildings, transmission towers, bridges, airplane hangers, and wing structures. Members of a framed structure usually consist of beams and columns and the connections between them are classified according to their rotational characteristics as rigid (Type I), flexible (Type II), and semi-rigid (Type III) [54]. In the present work, optimal design of plane and general three-dimensional framed structures using hollow circular sections is considered, under the assumption that the connections between members are Type I. Such framed structures are called "rigid frames".

The use of hollow circular sections (hereafter also called tubes) as structural components is not new, but this usage has increased considerably in recent years. In the past, use of tubes was restricted because of connection difficulties. These difficulties have been overcome with the development of fully automatic oxyacetylene tube-cutting machines. A cost comparison of tubular and rolled sections indicates that the increased unit cost for tubular members is usually offset by the increase in weight required for rolled shapes [55]. In many

instances, steel tubing is unsurpassed in its efficiency, especially where weight as well as appearance becomes an important design consideration (arenas, stadiums, etc.), or where weight savings may be a very substantial economical consideration (bridge, derrick, tower cranes, etc.). For a complete discussion on hollow circular sections, the reader is referred to Ref. 55.

The class of framed structures considered herein is assumed to have preassigned geometric configurations and structural materials. The mean radius and thickness of tubes are treated as design variables. Quite often in structural problems, it is possible to obtain a single parameter that completely characterizes a member, thus allowing one to treat only one design variable for each member. This point, however, is not central to the present application and two design variables are used for each member. It should also be noted here that a clear distinction is made between the elements and the members of a frame, in order to adequately represent the static behavior of the structure with long members. In other words, a member of the frame may be divided into many elements for the purpose of structural analysis. However, only uniform members are treated in optimal design. Therefore, all elements of a member have the same design variables. Provision of design variable linking is also incorporated.

In modeling the structure, points of application of concentrated loads are treated as nodal points. Constraints are imposed on member stresses, displacements, and design variables. Multiple loading conditions for the structure are treated in the same way as explained

in Chapter 3. Equations developed for structural analysis in Chapter 2 are also used here. The stiffness matrix for a frame element is well documented in the literature and is not derived here. For a complete derivation, the reader is referred to Ref. 34.

6.2 Reduction of the Method to Design of Frames

The ODPS for design of frames is defined as follows: find design variables associated with each member of the frame such that its weight is minimized and the state equations (2.3-2) and (2.3-7), and constraints on stress, displacement, and member size are satisfied.

The cost function of Eq. (2.4-1) can be expressed as:

$$J(b) = 2\pi \sum_{r=1}^{L} \sum_{i=1}^{NG(r)} \sum_{j=1}^{NM(i)} \rho_i R_i t_i \ell_j \qquad (6.2\text{-}1)$$

where

R_i = mean radius of members of the ith group,

t_i = thickness of members of the ith group,

ℓ_j = length of jth member,

and

$$b = \{R_1, R_2, \ldots, R_{NG(1)}, t_1 t_2, \ldots t_{NG(1)}, \ldots, t_{NG(L)}\}^T \qquad (6.2\text{-}2)$$

In the subsequent three sections, treatment of constraints is presented, and in the last section results for three example problems are presented.

6.3 Stress Constraint

The members of a framed structure are subjected to a state of combined stress due to axial force, bending moment, shear force, and/or torsional moment (Fig. 6.1). Thus, the effect of combined stresses must be considered in implementing stress constraints of either Eq. (2.4-3) or Eq. (2.4-4). Further, the nature of the axial force distinctly divides the design criterion for a member in the following two categories:

Case 1: member subjected to direct tensile force with (or without) lateral loads.

Case 2: member subjected to direct compressive force with (or without) lateral loads.

In the present work, members are required to satisfy a design criterion based on Von Mises equivalent stress, which is also used in Chapter 5. Using this approach, the stress constraint for an element can be written as:

$$\left.\begin{aligned} \phi^s(x_1,x_2,x_3,z_B,z_I,b) = \alpha\{\sigma^2 + 3\tau^2\}^{1/2} - 1.0 \leq 0 , \\ \text{for all } x_1,\ x_2,\ x_3 . \end{aligned}\right\} \qquad (6.3\text{-}1)$$

where $\alpha = 1/\sigma^a$, $\sigma^a = \frac{\sigma_y}{FS}$, σ_y = yield stress, σ^a = allowable stress, FS = factor of safety, and σ and τ are direct and shear stresses, respectively. It may be pointed out here that σ and τ are assumed to be continuous functions of spatial coordinates x_1, x_2, and x_3, state variables z_B and z_I, and design variable b. Further, in this research

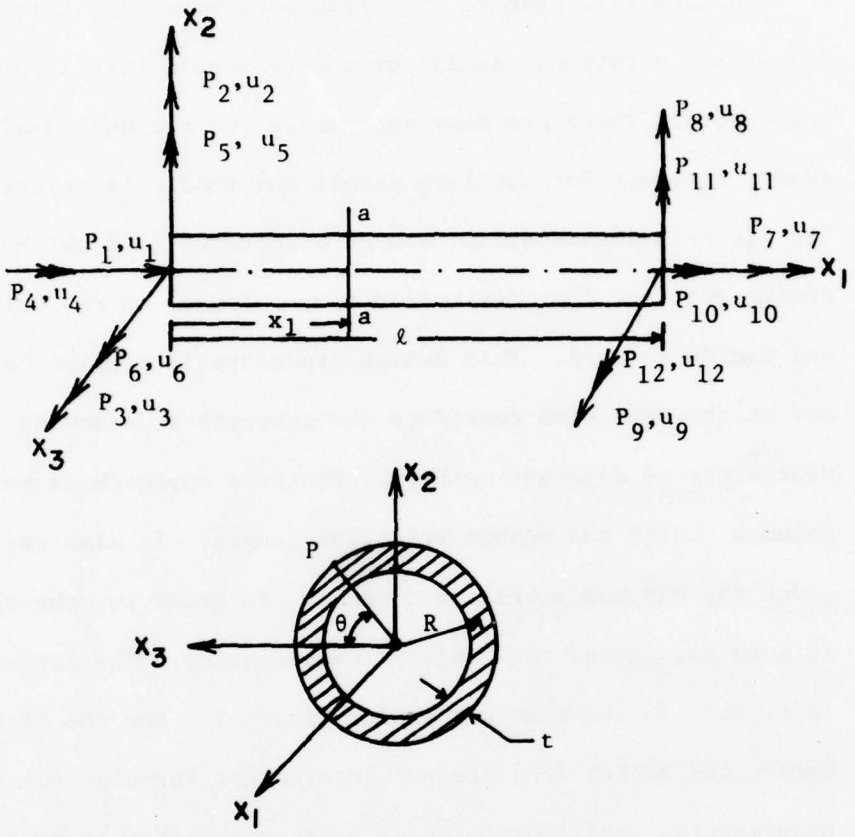

Figure 6.1. A Frame Element in Local Coordinate System

the thickness t of the tube is assumed to be small in comparison with the mean radius R.

In Case (2), members of a framework behave as beam columns. Therefore, a rational design procedure should take into account end restraints. There are many approaches for the design of restrained frame members. For complete detail the reader is referred to the Ref. 56. In this dissertation, Winter's approach [57] which is a current design practice (for restrained beam-columns) in the United States and Canada is used. This design procedure is simple, conservative, and at the same time considers the strength afforded by the end restraints of adjacent members. Winter's approach is to check beam-columns, using the member effective length. It also requires one to check the maximum stress in a member, in order to make certain that it does not exceed the basic allowable value. The latter requirement is treated in the same way as for Case (1). For the first requirement, Gerard and Becker [58] present interaction formulas together with experimental verification under various combined loading conditions; including 1) axial compression and bending, 2) axial compression and torsion, 3) axial compression, bending and torsion, 4) bending and torsion, and 5) bending and transverse shear. Although a slightly different interaction equation is proposed for each case, Schilling [59] suggests that a single formula can be conservatively applied to all the above mentioned loading combinations. For details the reader is referred to Refs. 56 and 59.

Using Schilling's approach, an additional stress constraint for Case (2) is written as

$$\left.\begin{aligned} \phi^s(x_1,x_2,x_3,z_B,z_I,b) \equiv \frac{\sigma}{\sigma_{cr}} + \left(\frac{\tau}{\tau_{cr}}\right)^2 - 1.0 \leq 0 \ , \\ \text{for all } x_1,x_2,x_3 \end{aligned}\right\} \quad (6.3\text{-}2)$$

where σ = normal stress due to axial force and/or bending moment at point (x_1, x_2, x_3)

τ = shear stress due to shear force and/or twisting moment at a point (x_1, x_2, x_3)

σ_{cr} = critical buckling stress for axial compression (or bending) alone, and

τ_{cr} = critical shear buckling stress for torsion (or transverse shear) alone.

The values of σ_{cr} and τ_{cr} for a member are given in Appendix 3.

As pointed out earlier, a member of the frame may be divided into many elements for the purpose of structural analysis. On the other hand, the critical compressive stress for all elements making up a member is the same because the axial loads are assumed to be acting only at the end of a member. Hence, the effective length factor k, required in the computation of σ_{cr}, is to be calculated for each member of the frame. In rigid frames, two cases of interest must be considered: (a) frames without sidesway, and (b) frames with sidesway.

The value of k for Cases (a) and (b) are obtained by solving the following transcendental equations, respectively [54]:

$$\left[\frac{1}{2}(\bar{G}_A + \bar{G}_B) + \frac{1}{4}\bar{G}_A\bar{G}_B\left(\frac{\pi}{k}\right)^2 - 1\right]\frac{\pi}{k}\sin\left(\frac{\pi}{k}\right)$$

$$-\left[\frac{1}{2}(\bar{G}_A + \bar{G}_B)\left(\frac{\pi}{k}\right)^2 + 2\right]\cos\left(\frac{\pi}{k}\right) + 2 = 0 \qquad (6.3\text{-}3)$$

and

$$\left[\bar{G}_A\bar{G}_B\left(\frac{\pi}{k}\right)^2 - 36\right]\sin\left(\frac{\pi}{k}\right) - 6(\bar{G}_A + \bar{G}_B)\frac{\pi}{k}\cos\left(\frac{\pi}{k}\right) = 0 \qquad (6.3\text{-}4)$$

The subscripts A and B on $\bar{G}$ in Eqs. (6.3-3) and (6.3-4) refer to the joints at the ends of the member under consideration. The parameter $\bar{G}$ is given by

$$\bar{G} = \frac{\sum \frac{I_c}{\ell_c}}{\sum \frac{I_g}{\ell_g}} \qquad (6.3\text{-}5)$$

where $\sum$ indicates a summation for all members rigidly connected to that joint and lying in the plane in which buckling of the member is being considered, I_c is the moment of inertia, and ℓ_c is the corresponding unbraced length of the compressed members. Also, I_g is the moment of inertia, and ℓ_g the corresponding unbraced length of the restraining members, and I_c and I_g are taken about axes perpendicular to the plane of buckling. In the present work, the secant method of nonlinear algebraic equations is used in finding the lowest root of Eqs. (6.3-3) and (6.3-4).

6.3.1 Treatment of Stress Constraint

Functions in the stress constraints of Eqs. (6.3-1) and (6.3-2) are assumed to be continuous in the spatial coordinates x_1, x_2, and x_3, state variables z_B and z_I, and design variable b. It is required that maximum normalized equivalent stresses for all members of a frame be within the specified limit. In general, the stress constraint for Cases (1) and (2) of the previous section can be expressed as (Fig. 6.1)

$$\max_{\Omega} \phi^s(x_1,\theta,z_B,z_I,b) \leq 0 \tag{6.3-6}$$

where

$$\Omega = \{x_1,\theta \mid 0 \leq x_1 \leq \ell,\ 0 \leq \theta \leq 2\pi\} \tag{6.3-7}$$

and

$$\theta = \theta(x_2,x_3) \tag{6.3-8}$$

For notational convenience, Eq. (6.3-6) represents a stress constraint for a typical frame element. Therefore, no subscript for the constraint function ϕ^s will be used.

The treatment of a max-value constraint defined by Eq. (6.3-6) in the general minimization problem is mathematically quite tedious and computationally quite time consuming. This type of constraint function may not even be differentiable. There are two basically different techniques [33,47] that can be used in treating this type of constraint, which are briefly reviewed here.

Recently, Kwak [47] has treated a very general class of such min-max problems. He has developed and evaluated several algorithms for such problems. His First Order Algorithm is quite efficient and reliable [47]. Briefly, the First Order Algorithm is a two-step procedure. For the ODPS, in the first step, points that give max-value to the constraint function of Eq. (6.3-6) are solved for a given design variable $b^{(0)}$ and state variables $z_B^{(0)}$ and $z_I^{(0)}$. This is called the inner optimization problem, i.e., find $x_1, \theta \in \Omega$ such that ϕ^s is maximized. Then, the constraint Eq. (6.3-6) is replaced by constraints at these points only. In the second step, points that give max-value to constraint of Eq. (6.3-6) are kept fixed and the general minimization problem, known as an outer problem, is solved. The entire procecure is repeated until desired convergence is obtained. There are also procedures which account for changes in the solution points of the inner problem, known as higher order or hybrid methods [47].

Feng [33], on the other hand, first converted the max-value constraint of Eq. (6.3-6) into the pointwise constraint

$$\phi^s(x_1, \theta, z_B, z_I, b) \leq 0 \ , \quad \text{for all } x_1, \theta \in \Omega \tag{6.3-9}$$

and then replaced the constraint Eq. (6.3-9) by the equivalent functional constraint

$$\tilde{\phi}^s(z_B, z_I, b) = \int_\Omega \left[|\phi^s(x_1, \theta, z_B, z_I, b)| + \phi^s(x_1, \theta, z_B . z_I, b) \right]^2 d\Omega = 0 \tag{6.3-10}$$

Since $\phi^s(x_1,\theta,z_B,z_I,b)$ is continuous with respect to x_1 and θ, the integrand in Eq. (6.3-10) is also continuous with respect to x_1 and θ and it is always non-negative. If any constraint in the expression (6.3-9) is violated, the corresponding functional constraint in Eq. (6.3-10) is also violated, and vice-versa. Thus, constraint Eqs. (6.3-9) and (6.3-10) are equivalent. In Feng's approach, the domain Ω of the functional constraint is discretized by introducing grid points in the x_1 direction and the θ direction of the element (Fig. 6.1). The integrand of Eq. (6.3-10) is calculated at each of the grid points and violations in the constraint are noted. In order to correct this constraint error, design sensitivity analysis of the functional must first be developed. This involves calculation of an adjoint matrix at each of the grid points where the constraint is violated. Finally, numerical integration must be done to calculate $\frac{d\phi^s}{db}$. This procedure must be followed for each functional constraint.

Selection of a technique to treat the max-value constraint of the Eq. (6.3-6) appears to be problem dependent. In the case of frame problems, Feng's approach will be numerically inefficient, because of the large number of grid points that will have to be introduced to discretize the domain Ω. On the other hand, Kwak's First Order Algorithm may be quite efficient, since analytic solution of the inner problem for frames is possible. Thus, Kwak's approach is adopted in this dissertation. Details of stress constraint treatment for plane and space frame members are presented separately in the following two subsections.

6.3.2 Stress Constraint For Plane Frames

Figure 6.2 shows a plane frame elment and its local coordinate system, with the sign convention to be used on element forces P_i's and deformations u_i's. The element is assumed to be subjected to in-plane loading only. As pointed out earlier, the points of application of concentrated loads are treated as nodes, so there is no discontinuity in the shear force or bending moment in an element.

Consider a section at x_1 and let axial force, shear force, and bending moment at this section be $F_1(x_1)$, $F_2(x_1)$, and $F_3(x_1)$, respectively. Since no axial load is applied inside the element, F_1 is assumed to be constant over the length of the element. Further, the thickness t of the tube is assumed to be small in comparison with mean radius R. Thus, the shear stress distribution can be assumed constant over the thickness t. Now the direct stress $\sigma(x_1,x_2)$ and shear stress $\tau(x_1,x_2)$ at a point (x_1,x_2) can be respectively expressed as

$$\sigma(x_1,x_2) = \frac{F_3(x_1)}{I} x_2 + \frac{F_1}{A} \tag{6.3-11}$$

and

$$\tau(x_1,x_2) = \frac{F_2(x_1)Q(x_2)}{I\,\bar{b}\,(x_2)} \tag{6.3-12}$$

where

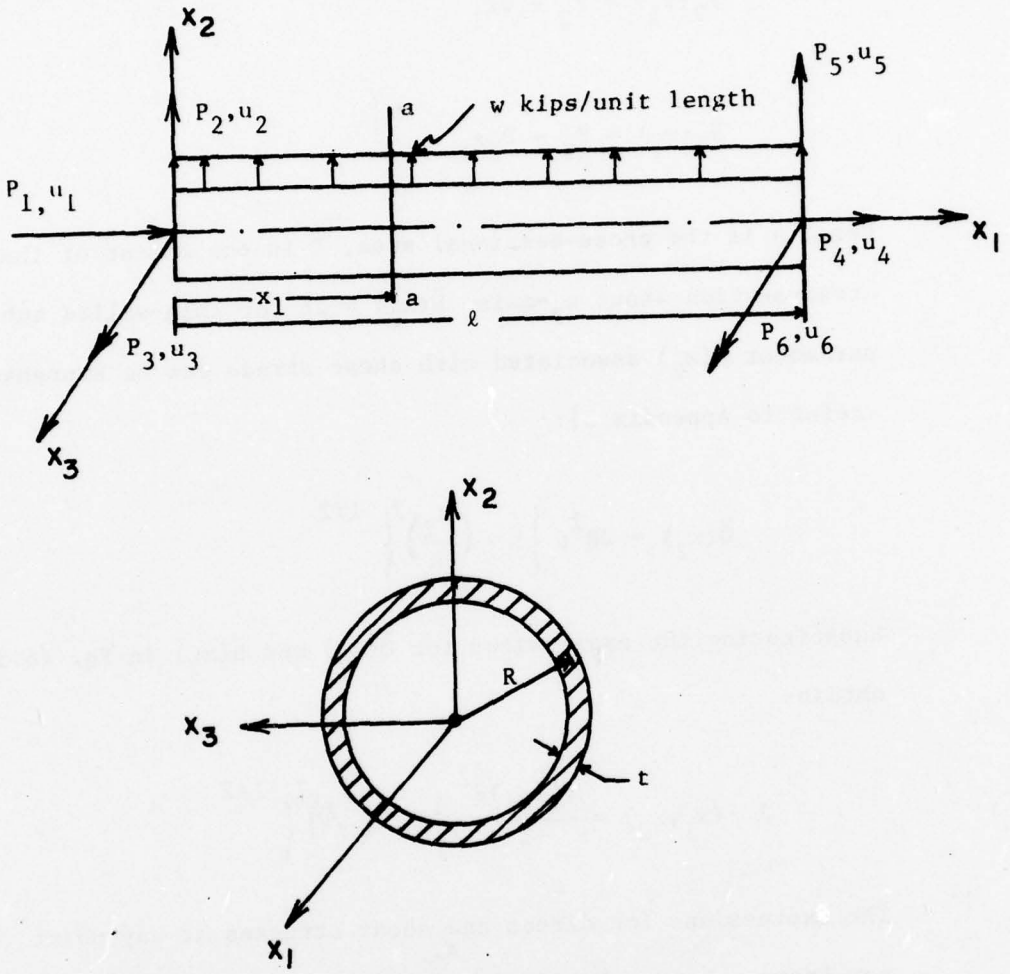

Section at a-a

Figure 6.2. A Typical Plane Frame Element

$$F_1 = P_1 \tag{6.3-13}$$

$$F_2(x_1) = P_2 + wx_1 \tag{6.3-14}$$

$$F_3(x_1) = P_3 - P_2x_1 - \frac{wx_1^2}{2} \tag{6.3-15}$$

Here, A is the cross-sectional area, I is the moment of inertia of the cross-section about x_3-axis, $\bar{b}(x_2) \approx 2t$ for thin-walled tubes, and the parameter $\bar{Q}(x_2)$ associated with shear stress can be expressed as [refer to Appendix 3]:

$$\bar{Q}(x_2) = 2R^2t \left\{1 - \left(\frac{x_2}{R}\right)^2\right\}^{1/2} \tag{6.3-16}$$

Substituting the expressions for $\bar{Q}(x_2)$ and $\bar{b}(x_2)$ in Eq. (6.3-12), one obtains

$$\tau(x_1,x_2) = \frac{F_2(x_1)R^2}{I} \left\{1 - \left(\frac{x_2}{R}\right)^2\right\}^{1/2} \tag{6.3-17}$$

The expressions for direct and shear stresses at any point (x_1,x_2) are now known. Using the First Order Algorithm of Kwak [47], stress constraints for Cases (1) and (2) of Section 6.3 are now considered separately.

6.3.2.1 Case (1)

The stress constraint Eq. (6.3-1) for a plane frame element reduces to

$$\phi^s(x_1,x_2,z_B,z_I,b) = \alpha \left\{\sigma^2(x_1,x_2) + 3\tau^2(x_1,x_2)\right\}^{1/2}$$

$$- 1.0 \leq 0 \ , \quad \text{for all } x_1 \text{ and } x_2 \qquad (6.3\text{-}18)$$

where $\sigma(x_1,x_2)$ and $\tau(x_1,x_2)$ are given by Eqs. (6.3-11) and (6.3-17), respectively. Equation (6.3-18) can be rewritten as a max-value constraint (see Eq. (6.3-6)) and the domain Ω for the constraint is given as

$$\Omega = \{x_1,x_2 \mid 0 \leq x_1 \leq \ell \ , \ -R \leq x_2 \leq R\} \qquad (6.3\text{-}19)$$

This constraint function has a continuous derivative in the neighborhood of a point $(\bar{x}_1,\bar{x}_2)$ which is in the interior of domain Ω. The necessary condition for a stationary point $(\bar{x}_1,\bar{x}_2)$ of the constraint function defined by Eq. (6.3-18) is

$$\nabla\left[\alpha\left\{\sigma^2(\bar{x}_1,\bar{x}_2) + 3\tau^2(\bar{x}_1,\bar{x}_2)\right\}^{1/2} - 1.0\right] = 0 \qquad (6.3\text{-}20)$$

Thus, from Eq. (6.3-20) one obtains, after simplification,

$$F_2(\bar{x}_1)\left[\{F_3(\bar{x}_1) + 3wR^2\}\,\bar{x}_2^2 + \frac{F_1 I}{A}\,\bar{x}_2 - 3wR^4\right] = 0 \qquad (6.3\text{-}21)$$

and

$$A\,\{3R^2F_2^2(\bar{x}_1) - F_3^2(\bar{x}_1)\}\,\bar{x}_2 - IF_1F_3(\bar{x}_1) = 0 \qquad (6.3\text{-}22)$$

Equation (6.3-21) implies that either $F_2(\bar{x}_1) = 0$, i.e. $\bar{x}_1 = -\frac{P_2}{w}$ if $w \neq 0$, or

$$\{F_3(\bar{x}_1) + 3wR^2\}\,\bar{x}_2^2 + \frac{F_1 I}{A}\,\bar{x}_2 - 3wR^4 = 0 \ . \qquad (6.3\text{-}23)$$

Solving Eq. (6.3-22), one obtains

$$\bar{x}_2 = \frac{(\frac{I}{A})\ F_1 F_3(\bar{x}_1)}{3R^2 F_2^2(\bar{x}_1) - F_3^2(\bar{x}_1)} \quad , \ -R < \bar{x}_2 < R \qquad (6.3\text{-}24)$$

Substituting the expressions for $\bar{x}_2$, $F_2(\bar{x}_1)$, and $F_3(\bar{x}_1)$ from Eqs. (6.3-24), (6.3-14), and (6.3-15), respectively, in Eq. (6.3-23); one obtains an 8th degree polynomial in $\bar{x}_1$:

$$a_8\bar{x}_1^8 + a_7\bar{x}_1^7 + \ldots + a_1\bar{x} + a_o = 0 \qquad (6.3\text{-}25)$$

where the coefficients (a_i, $i = 0$ to 8) are given in Appendix 3. Using the permissible zeroes of Eq. (6.3-25) and $\bar{x}_1 = -\frac{P_2}{w}$ if $w \neq 0$, corresponding values of $\bar{x}_2$ from Eq. (6.3-24) are calculated. Thus, one obtains a set of stationary points at which the stress constraint of Eq. (6.3-18) needs to be evaluated.

In case $w = 0$, the 8th order polynomial defined by Eq. (6.3-25) reduces to a linear equation (see Appendix 3 for coefficient a_i's) and the stationary point along the x_1-axis is given by $\bar{x}_1 = (P_3/P_2)$, which implies that the point at which the bending moment is zero (refer to Eq. (6.3-15)) is a stationary point and from Eq. (6.3-24) one obtains $\bar{x}_2 = 0$. Thus, in this case, the necessary condition gives only one stationary point. It may be noted that whether $w = 0$ or $w \neq 0$, one also needs to evaluate the Von Mises equivalent stress at the boundary

points. Finally, knowing the value of stresses at stationary points and at boundary points, one obtains a global maximum for the constraint of Eq. (6.3-18), which should be satisfied.

6.3.2.2 Case (2)

For a plane frame, the buckling constraint given by Eq. (6.3-2) reduces to

$$\phi^s(x_1,x_2,z_B,z_I,b) = \frac{\sigma(x_1,x_2)}{\sigma_{cr}} + \frac{\tau^2(x_1,x_2)}{\tau_{cr}^2} - 1.0 \leq 0 \ ,$$

$$\text{for all } x_1 \text{ and } x_2 \qquad (6.3\text{-}26)$$

Following the same approach as in Section 6.3.2.1, after simplification, one obtains the following necessary conditions for the stationary points $(\bar{x}_1,\bar{x}_2)$ of constraint Eq. (6.3-26):

$$F_2(\bar{x}_1)\ (\beta w\bar{x}_2^2 + \bar{x}_2 - \beta wR^2) = 0 \qquad (6.3\text{-}27)$$

and

$$F_3(\bar{x}_1) - \beta F_2^2(\bar{x}_1)\bar{x}_2 = 0 \qquad (6.3\text{-}28)$$

where $\beta = \dfrac{2R^2\sigma_{cr}}{I\tau_{cr}^2}$. Equation (6.3-27) implies either $F_2(\bar{x}_1) = 0$,

i.e. $\bar{x}_1 = -\dfrac{P_2}{w}$ if $w \neq 0$, or

$$\beta w\ \bar{x}_2^2 + \bar{x}_2 - \beta wR^2 = 0 \ . \qquad (6.3\text{-}29)$$

Substituting the values of $F_3(\bar{x}_1)$, and $F_2(\bar{x}_1)$ in Eq. (6.3-28), after simplification, one obtains

$$(\frac{w}{2} - \beta w^2 \bar{x}_2)\bar{x}_1^2 + (P_2 + 2\beta w P_2 \bar{x}_2)\bar{x}_1 + \beta \bar{x}_2 P_2^2 - P_3 = 0 \qquad (6.3\text{-}30)$$

Now the zeroes of quadratic Eq. (6.3-29) are obtained and then, for each permissible value of $\bar{x}_2$, the quadratic Eq. (6.3-30) is solved for $\bar{x}_1$. Thus, one obtains a set of stationary points. In case $w = 0$, then Eq. (6.3-29) yields $\bar{x}_2 = 0$ and, from Eq. (6.3-30), $\bar{x}_1 = \left(\frac{P_3}{P_2}\right)$. Thus, the stationary point for the stress constraint of Case (2), when $w = 0$, is the same as obtained in Section 6.3.2.1. The remainder of the procedure for obtaining the global maximum of the stress constraint defined by Eq. (6.3-26) is exactly the same as in Section 6.3.2.1.

6.3.3 Stress Constraint for Space Frames

A typical three dimensional frame element and its local coordinate system, with the sign convention to be used for element forces P_i's and deformations u_i's, is shown in Fig. 6.1. The element is assumed to be subjected to only nodal loads that pass through the shear center. Hence, $x_1 = 0$ and $x_1 = \ell$ are the only critical points along the x_1-axis at which one needs to impose the stress constraint.

Consider a section at either $x_1 = 0$ or $x_1 = \ell$ and let axial force F_1, shear forces F_2 and F_3, twisting moment F_4, and bending moments F_5 and F_6 be the force components at that section. As in

Section 6.3.2, the thickness t of the hollow circular section is assumed to be small in comparison to mean radius R. The direct stress $\sigma(\theta)$ and shear stress $\tau(\theta)$ at a point P (see Fig. 6.1) are expressed as

$$\sigma(\theta) = \frac{F_1}{A} + \frac{F_5 R}{I} \cos\theta + \frac{F_6 R}{I} \sin\theta \qquad (6.3\text{-}31)$$

and

$$\tau(\theta) = \frac{F_4 R}{2I} + \frac{F_2 R^2}{I} \cos\theta + \frac{F_3 R^2}{I} \sin\theta \qquad (6.3\text{-}32)$$

As in Section 6.3.2, stress constraints for Cases (1) and (2) of Section 6.3 are considered separately.

6.3.3.1 Case (1)

The stress constraint of Eq. (6.3-1) for a space frame element reduces to

$$\phi^s(\theta, z_B, z_I, b) \equiv \alpha \{ \sigma^2(\theta) + 3\tau^2(\theta) \}^{1/2} - 1.0 \leq 0 \,, \quad \text{for all } \theta \,. \qquad (6.3\text{-}33)$$

where $\sigma(\theta)$ and $\tau(\theta)$ are given by Eqs. (6.3-31) and (6.3-32), respectively. Equation (6.3-33) can be rewritten as a max-value constraint (see Eq. (6.3-6)), with the domain Ω given as

$$\Omega = \{\theta \mid 0 \leq \theta \leq 2\pi\} \qquad (6.3\text{-}34)$$

Following the same approach as in the previous section, after simplification, one obtains the following necessary condition for the

stationary points ($\bar{\theta}$) of constraint Eq. (6.3-33):

$$a_3 \cot 2\bar{\theta} + a_2 \sec \bar{\theta} + a_1 \operatorname{cosec} \bar{\theta} + a_o = 0 \qquad (6.3\text{-}35)$$

where the coefficients (a_i, i = 0 to 3) are given in Appendix 3.

From the transcendental Eq. (6.3-35), one obtains a set of stationary points at which the stress constraint of Eq. (6.3-33) needs to be evaluated. Finally, one obtains a global maximum of this constraint, which should be satisfied.

6.3.3.2 Case (2)

For a space frame, the buckling constraint given by Eq. (6.3-2) reduces to

$$\phi^s(\theta, z_B, z_I, b) \equiv \frac{\sigma(\theta)}{\sigma_{cr}} + \frac{\tau^2(\theta)}{\tau_{cr}^2} - 1.0 \leq 0 \text{ , for all } \theta. \qquad (6.3\text{-}36)$$

Using the same approach as in Section 6.3.3.1, one obtains the following transcendental equation for stationary points ($\bar{\theta}$) at which the above buckling constraint needs to be evaluated:

$$a_3 \cot 2\bar{\theta} + a_2 \sec \bar{\theta} + a_1 \operatorname{cosec} \bar{\theta} + a_0 = 0 \qquad (6.3\text{-}37)$$

where the coefficients (a_i, i = 0 to 3) are given in Appendix 3. Finally, one obtains a global maximum of this constraint which should be satisfied.

6.4 Displacement Constraints

In earlier work [28], displacement constraints for a frame were imposed at the nodal points only. If the constraint was to be imposed at an interior point of a member, due to practical and/or design considerations, then that point was treated as a node. In the above treatment, the displacement constraint does not depend upon spatial coordinates x_1, x_2, or x_3, so it can be implemented in a way exactly similar to the case of trusses or idealized wing structures (see Chapters 4 or 5). For large framed structures, this approach greatly increases the dimensionality of the problem, as well as computing time.

In the present work, displacement constraints are imposed on the maximum value of displacement in the x_2 and x_3 directions, in the interior of the element (see Fig. 6.1), along with constraints on nodal displacements. The max-value displacement constraint is treated like the stress constraints of Section 6.3, since both constraints are of the same form. For implementation of the constraints on nodal displacements the reader is referred to (developments of) Chapter 4.

Neglecting deformation due to shear, the displacement constraint in a lateral direction is imposed along the x_1-axis, and for a typical element is written as

$$\phi^s(x_1, z_B, z_I, b) \equiv \bar{\beta} \frac{\xi(x_1)}{\xi^a} - 1.0 \leq 0 \text{ , for all } x_1 \qquad (6.4\text{-}1)$$

where $\xi(x_1)$ is the lateral displacement at a point x_1, ξ^a is the allowable displacement, and $\bar{\beta}$ is an amplification factor [60]. In general, $\bar{\beta}$ will depend on the ratio $\frac{P}{P_{cr}}$ (where P is the applied

compressive axial force and P_{cr} is the Euler critical load) and the type of lateral load. In the present work $\bar{\beta}$ is taken to be unity for tensile axial force, which is somewhat conservative. For compressive axial force, a simplified expression for $\bar{\beta} = 1/(1-\frac{P}{P_{cr}})$ is used with good accuracy, if the ratio $\frac{P}{P_{cr}}$ is not large. For complete details the reader is referred to Ref. 60. Further, Eq. (6.4-1) is rewritten as a max-value constraint

$$\underset{\Omega}{\text{Max}} \left\{ \bar{\beta} \frac{\xi(x_1)}{\xi^a} - 1.0 \right\} \leq 0 \tag{6.4-2}$$

where

$$\Omega = \{x_1 \mid 0 \leq x_1 \leq \ell\} \tag{6.4-3}$$

In subsequent sections, the displacement constraint is considered for plane frames and space frames, separately.

6.4.1 Displacement Constraint for Plane Frame

Using the Euler-Bernoulli equation, the general expression for elastic curve of a plane frame element (Fig. 6.2) can be written as

$$\xi_2(x_1) = \frac{w\, x_1^4}{24EI} + \frac{1}{6} c_3 x_1^3 + \frac{1}{2} c_2 x_1^2 + c_1 x_1 + c_0 \tag{6.4-4}$$

where $\xi_2(x_1)$ is displacement in the x_2-direction and c_i, i = 0 to 3 are constants of integration (see Appendix 3). Using the necessary conditions of Section 6.3, one obtains a 3rd order polynomial in $\bar{x}_1$ $(0 < \bar{x}_1 < \ell)$

$$\frac{1}{6}\frac{w\,\bar{x}_1^3}{EI} + \frac{1}{2}\,c_3\bar{x}_1^2 + c_2\bar{x}_1^2 + c_1 = 0 \qquad (6.4\text{-}5)$$

The zeroes of the above cubic equation can easily be obtained as a closed form solution [61]. Further treatment of this constraint is exactly the same as in Section 6.3.

6.4.2 Displacement Constraint for Space Frame

Let $\xi_2(x_1)$ and $\xi_3(x_1)$ be displacements in the x_2 and x_3 directions, respectively. The total displacement $\xi(x_1)$ can be expressed as

$$\xi(x_1) = \{\xi_2^2(x_1) + \xi_3^2(x_1)\}^{1/2} \qquad (6.4\text{-}6)$$

Using the same approach as in previous section, the general expressions for elastic curves in the x_2 and x_3 directions can be expressed as (Fig. 6.1)

$$\xi_2(x_1) = \frac{1}{6}\,c_3x_1^3 + \frac{1}{2}\,c_2x_1^2 + c_1x_1 + c_0 \qquad (6.4\text{-}7)$$

and

$$\xi_3(x_1) = \frac{1}{6}\,d_3x_1^3 + \frac{1}{2}\,d_2x_1^2 + d_1x_1 + d_0 \qquad (6.4\text{-}8)$$

where c_i and d_i ($i = 0$ to 3) are constants of integration and are given in Appendix 3. Using the necessary conditions for stationary points of the displacement $\xi(x_1)$, one obtains a 5th order polynomial in $\bar{x}_1$

$$a_5 \bar{x}_1^5 + \ldots + a_1 \bar{x}_1 + a_0 = 0 \qquad (6.4\text{-}9)$$

where the coefficients a_i (i = 0 to 5) are given in Appendix 3. One can solve this 5th order polynomial for stationary values, in order to implement the constraint.

6.5 Design Variable Constraint

In this research, mean radius (R) and thickness (t) of a hollow circular member are treated as design variables. Thus, the design variable constraints of Eq. (2.2-5) are expressed as

$$R^L \leq R \leq R^U \qquad (6.5\text{-}1)$$

and

$$t^L \leq t \leq t^U \qquad (6.5\text{-}2)$$

where R^U, R^L, t^U, and t^L are the upper and lower bounds on R and t, respectively. These bounds on design variables are to be furnished by the designer. In the present work, bounds on mean radius are provided by the designer, whereas bounds on thickness are selected as

$$t^U = 0.1\ R\ , \qquad (6.5\text{-}3)$$

for a thin circular section [62] and

$$t^L = \left(\frac{\sigma_y}{1650}\right) R\ , \qquad (6.5\text{-}4)$$

to avoid local buckling of a member [56].

6.6 Design Sensitivity Analysis

The cost function J(b) given by Eq. (6.2-1) depends only on design variables and is nonlinear. Thus, the design sensitivity vector of J(b) is easily calculated as $\delta J = \frac{\partial J}{\partial b} \delta b$.

The stress constraints for Cases (1) and (2) of Section 6.3 at a stationary point are continuous functions of state variables z_B and z_I and design variable b. The violated stress constraints at a desired point are first expressed in terms of nodal forces by using Eqs. (6.3-13) to (6.3-15) for plane frames, and Eqs. (6.3-31) and (6.3-32) for space frames. These equations are then expressed in terms of nodal displacements in a global coordinate system by using Eq. (2.3-14). The sensitivity coefficients $\frac{\partial \phi}{\partial z_B}$, $\frac{\partial \phi}{\partial z_I}$, and $\frac{\partial \phi}{\partial b}$ are then routinely evaluated. The computations are somewhat lengthy but are straightforward. In the present work, the effective length factor k, defined by Eq. (6.3-3) or (6.3-4), is treated as constant in a particular design cycle. This assumption is reasonable, since the value of k does not change appreciably from one design cycle to another, which was also observed in Ref. 28. However, at the start of each design cycle, k values for members subjected to axial compression are recomputed, or read in.

Lastly, the design sensitivity analysis for displacement and design variable constraints is straightforward and can easily be performed. Further, bounds on design variables are calculated at the beginning of each design cycle. At this stage, all necessary information is available to assemble the matrix Λ of Eq. (2.6-6).

6.7 Example Problems

A computer program based on the algorithm of Chapter 2 and the flow diagram of Chapter 4 is developed for optimal design of plane and space frames. The following structures are optimized as examples:

(i) Example 6.1: One-Bay Two-Story Frame

(ii) Example 6.2: Two-Bay Six-Story Frame

(iii) Example 6.3: Helicopter Tail Boom Structure

The first two examples are plane frames that were solved in Refs. 28 and 41 by treating the moment of inertia of each member as a design variable. In the present formulation, the mean radius (R) and thickness (t) of each member are considered as design variables. Further, the constraints imposed here are different than those imposed in Refs. 28 and 41. Therefore, direct comparisons of final results are not possible.

The last example is a space frame. This example is new and has not been solved earlier. A truss idealization of this structure was optimized in Ref. 63. Here, a frame idealization of the same structure is optimized and the final solution analyzed.

In the following subsections each example is discussed separately and the final results are presented. The computation times reported herein are for an IBM 360/65(H) computer (double precision). The value of ε for imposing ε-active constraints varies from 1 to 5% for all example problems. The weighting matrix is selected as explained in Chapter 5. For all examples, the value of weighting multiplier ($\bar{w}_i$) for mean radius (R) varies from 2 to 100, whereas for thickness

(t) it is taken as unity. The factor of safety (FS) associated with Eq. (6.3-1), for evaluating allowable stress (σ^a), is selected based on the recommendations of Ref. 64. Further, the bound (ξ^a) used in imposing the displacement constraint in the interior of an element (see Eq. (6.4-1)) is taken as $\frac{\ell_m}{360}$, where ℓ_m is the length of the member to which the element belongs. Finally, the allowable nodal displacements are taken in accordance with Refs. 65 and 66, such that the deflection index (ratio of deflection to height) is restricted to 0.002.

6.7.1 Example 6.1: One-Bay Two-Story Frame

This small scale frame serves as a good example for testing the computer program based on the present algorithm. Figure 6.3 shows the dimensions and the loading conditions for this structure. In the present formulation the frame is divided into two substructures by partitioning it at nodes 2, 6, and 7. Thus, the first substructure consists of elements 1, 5, 6, and 8 and has 9 boundary degrees of freedom. The remaining elements are in the second substructure, which has 6 boundary and 9 interior degrees of freedom. Table 6.1 gives the design data for this example. It may be noted that in Refs. 28 and 41 symmetry in the structural design was guaranteed by imposing an additional loading condition. In the present work design variable linking is used in order to provide symmetry in the frame (see Table 6.2). This feature, as pointed out in Chapter 3, is more efficient since it reduces the number of loading conditions as well as design variables.

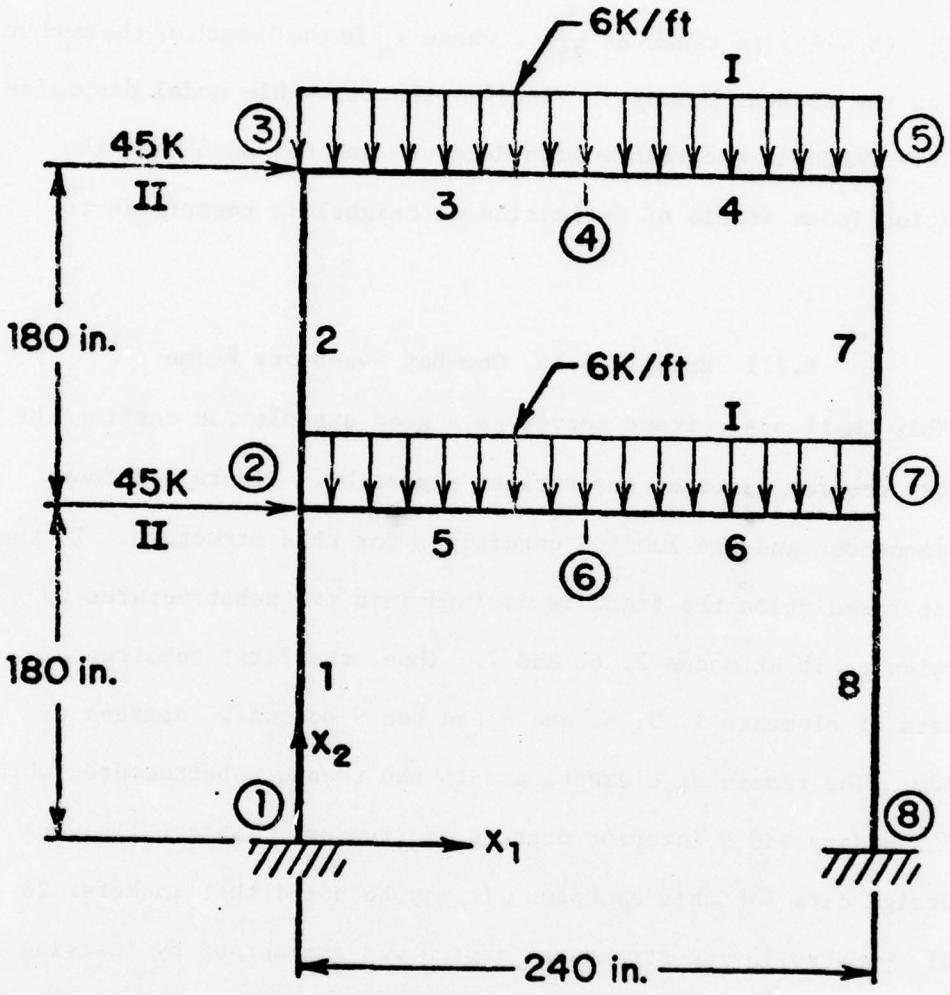

Figure 6.3. One-Bay Two-Story Frame

TABLE 6.1. DESIGN DATA FOR ONE-BAY TWO-STORY FRAME

Modulus of elasticity	$= 3 \times 10^4$ ksi
Material density	$= 0.2836$ lb/in.^{3}
Yield stress	= 36.0 ksi
Factor of safety	= 1.51
Initial value of mean rad., R	= 16.610 in.
Initial value of thickness, t	= 0.450 in.
Lower limit on mean rad., R	= 1.0 in.
Upper limit on mean rad., R	= None
Displacement limits in x_1 and x_2 directions	= ±0.72 in. for nodes 3 to 5 ±0.36 in. for nodes 2, 6, & 7 ±0.67 in. for elements 3 to 6
Starting reduction ratio, $\bar{r}$	= 0.037
Starting weighting multiplier, $\bar{w}_i$	= 0.04
Number of loading conditions (see Fig. 6.3)	= 2

The above data is same for both the cases.

The framed structure is optimized under two separate constraint conditions: stress constraint only (Case I); and stress and displacement constraints (Case II). Table 6.2 gives the final designs, values of cost function, number of active constraints, maximum constraint violations, $||\delta b^1||_2$ at the optimum, the maximum value of $||\delta b^1||_2$, and the total CPU time. The set of active constraints at the optimum design includes:

Case I: Buckling constraint for elements 3, 5, 7, and 9 under loading condition 2, and minimum element thickness for all elements.

Case II. Buckling constraint for element 8 under loading condition 2, displacement constraint at node 3 in x_1-direction under loading condition 2, and minimum element thickness for all elements.

The total CPU time reported in Table 6.2 includes initial set-up time (0.707 sec for both cases), and 15 and 21 iterations of design time (10.017 sec and 14.135 sec) for Case I and II, respectively.

Table 6.3 gives the cost function history for both cases. As pointed out in Section 6.6, the effective length factor (k) does not change appreciably from one design cycle to another. This fact is also observed numerically by evaluating k at each design iteration. A side computation was made by keeping k fixed after 2 design iterations and essentially the same optimum design was achieved. The CPU time per design iteration was reduced by 12% for this run.

The Von Mises equivalent stress constraint is imposed at the relative maximum points $(\bar{x}_1, \bar{x}_2)$ obtained from solutions of Eqs. (6.3-25)

TABLE 6.2. RESULTS FOR ONE-BAY TWO-STORY FRAME

Group Number	Element Numbers	Optimum Design in inches			
		Case I		Case II	
		Mean Rad.	Thickness	Mean Rad.	Thickness
1	1,8	16.099	0.3513	15.658	0.3416
2	2,7	11.825	0.2580	13.206	0.2881
3	3,4	11.427	0.2493	13.072	0.2852
4	5,6	15.277	0.3333	17.011	0.3711
At Optimum	Weight in lbs	8980.73		10166.63	
	No. of Active Constraints	8		6	
	Max. Constraint Violation	0.64×10^{-3}		0.68×10^{-3}	
	$\|\|\delta b^1\|\|_2$	0.30×10^{-11}		194.4	
Max. $\|\|\delta b^1\|\|_2$		25140.0		25140.0	
Total CPU Time in sec.		10.724		14.842	

TABLE 6.3. COST FUNCTION HISTORY FOR ONE-BAY TWO-STORY FRAME

DI† Number	Weight in lbs.	
	Case I	Case II
1	15805.09	15805.09
2	8895.28*	8895.28*
3	8054.98	10534.66
4	8432.11	11383.10
5	8137.61	11213.80
6	8369.07	10820.25
7	8642.53	10420.79
8	8741.71	10391.42
9	8863.67*	9902.82*
10	8924.57	10335.22
11	8954.21	8015.05
12	8968.43	8270.03
13	8975.21	9142.02
14	8978.44	10141.47
15	8979.99	10162.23
16	8980.73‡	10162.35*
17		10175.35
18		10176.06
19		10169.92
20		10166.22
21		10166.48
22		10166.63‡

‡Underlined iteration is not counted as it is used for checking the solution only.

*Means change in step size.

†Design iteration.

and (6.3-24), the ends of the element, and the point of maximum bending moment. The Von Mises equivalent stress constraint was not active at any of the relative maximum points obtained from the necessary conditions of Eq. (6.3-25), during the entire design process. Thus, the computing times reported in Table 6.2 are for the case in which stress constraints are imposed only at the end points and at the point of maximum bending moment. When critical points arise in the necessary condition (solutions of Eqs. (6.3-25) and (6.3-24)) and the Von Mises equivalent stress constraint is checked at these points, the computational times are increased by 30%.

Based on the foregoing, the polynomial defined by Eq. (6.3-25) is not solved in the subsequent examples and stress constraints defined by Eq. (6.3-18) are imposed along the x_1-axis, at the ends of the elements and at the point of maximum bending moment. The remainder of the procedure is the same as explained in Section 6.3.2. Also, the effective length factor (k) is not evaluated in each design iteration. Rather, it is kept constant after the first few design iterations. These simplifications are reasonable from a practical standpoint and considerable efficiencies result from them, especially for large scale problems.

6.7.2 Example 6.2: Two-Bay Six-Story Frame

Figure 6.4 shows the geometry and dimensions of a two-bay six-story structure. In the present formulation, the frame is divided into three substructures by partitioning it at joints 7 to 9 and

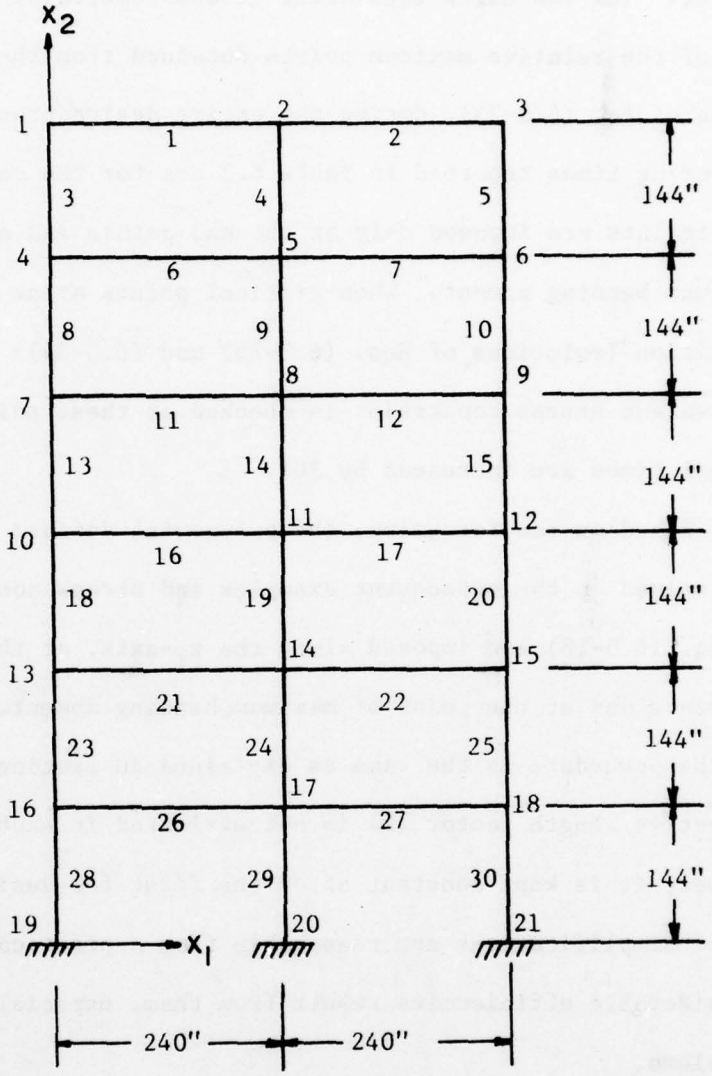

Figure 6.4. Two-Bay Six-Story Frame

13 to 15. Joints 1 to 3 are also treated as boundary nodes, in order to provide a minimum upper bandwidth for $K_{II}^{(1)}$. Members 1 to 10 are in substructure 1 and members 11 to 20 in substructure 2. The remaining 10 members (21 to 30) are in substructure 3. The first two substructures have 18 boundary degrees of freedom and the third has only 9. Further, all substructures have 9 interior degrees of freedom.

Table 6.4 gives design data for this example. Design variable linking is used in order to provide symmetry in the frame (see Table 6.5). This reduces the number of loading conditions from 4 (used in Refs. 28 and 41) to 2, as well as design variables from 60 to 36. As in the previous example, this framed structure is optimized under two separate constraint conditions: stress constraint only (Case I); and stress and displacement constraints (Case II).

Table 6.5 gives the final designs, values of cost functions, number of active constraints, maximum constraint violations, $||\delta b^1||_2$ at the optimum, the maximum value of $||\delta b^1||_2$ and the total CPU time. The set of active constraints at the optimum design includes:

Case I: Buckling constraint for elements 1, 3, 10, 11, 13, and 20 under loading condition 1 and for elements 9, 16, 19, 21, 24 to 26, and 29 under loading condition 2, Von Mises equivalent stress constraint for element 7 under loading condition 1, and minimum element thickness for all elements.

Case II: Buckling constraint for elements 1, 3, 4 under loading condition 1, Von Mises equivalent stress constraint for element 7 under loading condition 1, displacement constraint

TABLE 6.4 DESIGN DATA FOR TWO-BAY SIX-STORY FRAME

Modulus of elasticity = 3×10^4 ksi

Material density = 0.2836 lb/in.^{3}

Yield stress = 36.0 ksi

Factor of safety = 1.51

Elements	Initial values of design variables for (in.)			
	Case I		Case II	
	R	t	R	t
1-10	9.0	0.20	9.0	0.20
11-20	10.0	0.22	11.0	0.24
21-30	12.0	0.26	14.0	0.31

Lower limit on R = 1.0 in.

Upper limit on R = None

Displacement limits in x_1 and x_2 directions =
- 1.728 in. for nodes 1-3
- 1.440 in. for nodes 4-6
- 1.152 in. for nodes 7-9
- 0.864 in. for nodes 10-12
- 0.576 in. for nodes 13-15
- 0.288 in. for nodes 16-18
- 0.670 in. for all beam elements

Starting reduction ratio, $\bar{r}$ =
- 0.081 Case I
- 0.054 Case II

Starting weighting multiplier, $\bar{w}_i$ = 0.05 for both the cases

Number of loading conditions = 2

TABLE 6.4. (cont'd)

Load data:	
Loading Condition 1.	Uniformly distributed load (in negative x_2-direction) of 4.0 kip/ft. on elements, 1, 7, 11, 17, 21 and 27; and 1.0 kip/ft. on elements 2, 6, 12, 16, 22 and 26.
Loading Condition 2.	Uniformly distributed load (in negative x_2-direction) of 1.0 kip/ft. on elements 1, 2, 6, 7, 11, 12, 16, 17, 21, 22, 26, and 27; and loads of 9.0 kips each at nodes 1, 4, 7, 10, 13 and 16 in x_1-direction.

TABLE 6.5. RESULTS FOR TWO-BAY SIX-STORY FRAME

Group Number	Element Numbers	Optimum Design in inches			
		Case I		Case II	
		Mean Rad.	Thickness	Mean Rad.	Thickness
1	1,2	10.235	0.2233	10.009	0.2183
2	3,5	10.571	0.2306	10.361	0.2261
3	4	5.547	0.1210	6.322	0.1379
4	6,7	9.808	0.2140	9.682	0.2112
5	8,10	7.208	0.1573	7.825	0.1707
6	9	9.140	0.1994	10.953	0.2390
7	11,12	10.082	0.2200	10.639	0.2321
8	13,15	10.535	0.2298	9.891	0.2158
9	14	9.233	0.2014	10.763	0.2348
10	16,17	10.395	0.2268	11.406	0.2488
11	18,20	8.973	0.1958	8.687	0.1895
12	19	11.336	0.2473	13.104	0.2859
13	21,22	11.076	0.2417	12.114	0.2643
14	23,25	10.619	0.2317	10.690	0.2332
15	24	11.236	0.2452	11.919	0.2601
16	26,27	10.986	0.2397	11.707	0.2554
17	28,30	10.687	0.2332	11.413	0.2490
18	29	15.021	0.3277	13.915	0.3036
At Optimum: Weight in lbs		22530.52		24405.38	
At Optimum: No. of Active Constraints		33		23	
At Optimum: Max. Constraint Violation		0.56×10^{-2}		0.52×10^{-2}	
At Optimum: $\|\|\delta b^1\|\|_2$		2764.0		4223.0	
Max. $\|\|\delta b^1\|\|_2$		34120.0		43020.0	
Total CPU Time in sec.		87.766		87.077	

at node 7 in the x_1-direction under loading condition 2,

and minimum element thickness for all elements.

The total CPU time reported in Table 6.5 includes initial set-up time (2.100 sec for both cases), and 22 and 26 iterations of design time (85.666 sec and 84.977 sec) for Case I and II, respectively. The total computing time reported herein also includes the computation time required for calculation of the effective length factors (k's) at each design iteration. This calculation takes 10% of total computing time.

Table 6.6 gives the cost function history for this example. For Case I, the final design is achieved in 22 design iterations and for Case II in 26 iterations. As pointed out in chapters 4 and 5, the rate of convergence is highly dependent on step size and the weighting matrix. Lastly, two additional runs were made when critical points from the necessary conditions (solutions of Eqs. (6.3-25) and (6.3-24)) were also calculated. The Von Mises equivalent stress constraint was not active at any of the above critical points. However, the computational time per design iteration was increased by 30% when the critical points were evaluated.

6.7.3 Example 6.3: Helicopter Tail Boom Structure

The helicopter tail boom structure shown in Fig. 6.5 is idealized using 48 frame elements (see Fig. 6.6). The total number of degrees of freedom is 144. The element numbering system for a typical panel is given in Fig. 6.7. For convenience, the joint coordinates and element locations are given in Tables 6.7 and 6.8, respectively.

TABLE 6.6. COST FUNCTION HISTORY FOR TWO-BAY SIX-STORY FRAME

DI† Number	Weight in lbs.	
	Case I	Case II
1	23336.48	28536.81
2	22723.48	26286.30
3	21441.48	25000.70
4	21819.70*	24901.38
5	22216.96	24423.88
6	22153.72	23176.56
7	22253.80*	24313.63
8	22321.84	22661.77*
9	22416.93	24325.53
10	22414.44*	24420.39
11	22474.35	23644.30
12	22499.20	24397.14
13	22517.74	23833.90
14	22529.27	24532.80
15	22540.89	23797.65*
16	22541.22	24429.36*
17	22546.73	24547.51
18	22545.92*	24214.25
19	22540.41	24458.22
20	22540.69	24280.10
21	22524.64	24505.66
22	22530.48	24178.72
23	22530.52‡	24459.04*
24		24335.72
25		24416.48
26		24305.77
27		24405.38‡

‡Underlined iteration is not counted as it is used for checking the solution only.

*Means change in step size.

†Design iteration.

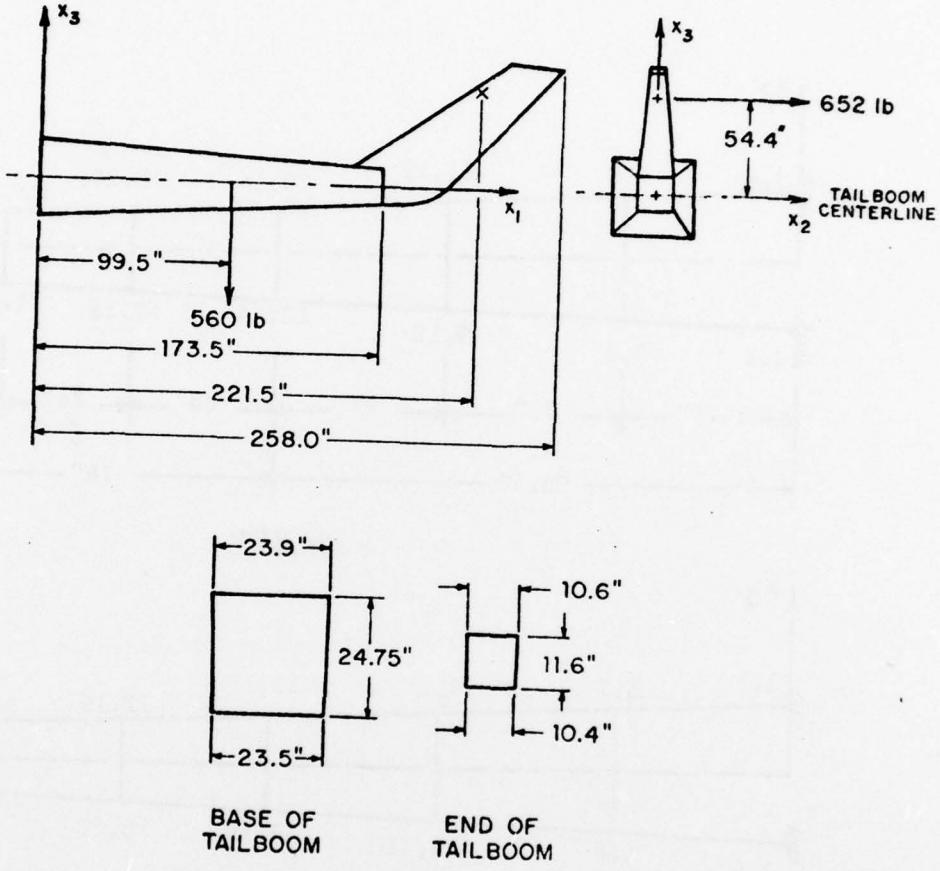

Figure 6.5. Geometry of Helicopter Tail Boom Structure

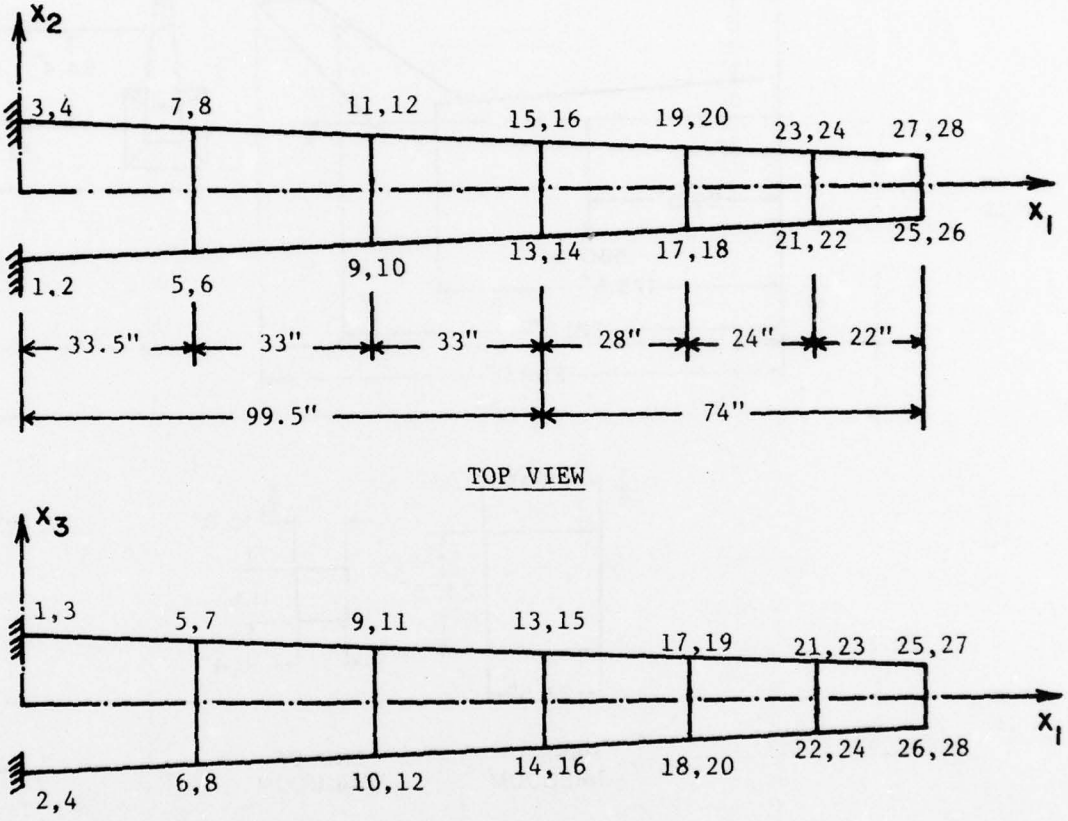

Figure 6.6. Frame Idealization of Helicopter Tail Boom Structure

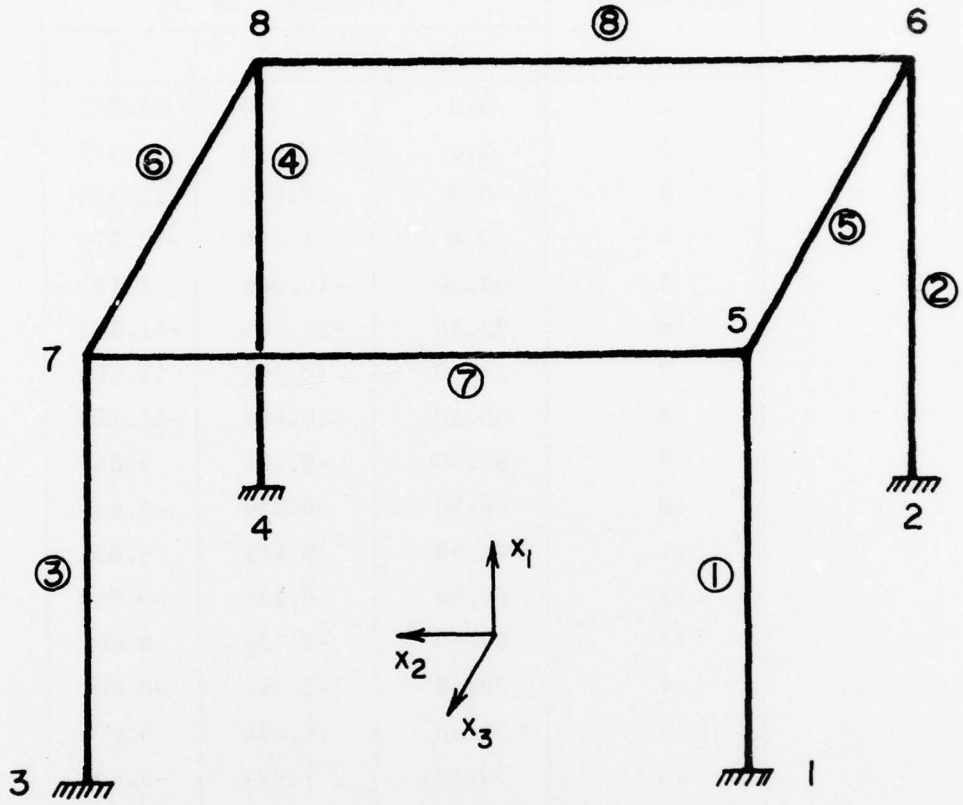

Figure 6.7. Element Numbering for the First Panel

TABLE 6.7. NODAL COORDINATES FOR HELICOPTER TAIL BOOM STRUCTURE

Node Number	Coordinate in in.		
	x_1	x_2	x_3
1	0.0	-11.950	12.375
2	0.0	-11.750	-12.375
3	0.0	11.950	12.375
4	0.0	11.750	-12.375
5	33.50	-10.666	11.105
6	33.50	-10.485	-11.105
7	33.50	10.666	11.105
8	33.50	10.485	-11.105
9	66.50	-9.401	9.855
10	66.50	-9.239	-9.855
11	66.50	9.401	9.855
12	66.50	9.239	-9.855
13	99.50	-8.136	8.604
14	99.50	-7.994	-8.604
15	99.50	8.136	8.604
16	99.50	7.994	-8.604
17	127.50	-7.063	7.543
18	127.50	-6.937	-7.543
19	127.50	7.063	7.543
20	127.50	6.937	-7.543
21	151.50	-6.143	6.634
22	151.50	-6.030	-6.634
23	151.50	6.143	6.634
24	151.50	6.030	-6.634
25	173.50	-5.30	5.80
26	173.50	-5.20	-5.80
27	173.50	5.30	5.80
28	173.50	5.20	-5.80

AD-A065 935 IOWA UNIV IOWA CITY DIV OF MATERIALS ENGINEERING F/G 1/3
SUBSTRUCTURING METHODS FOR DESIGN SENSITIVITY ANALYSIS AND STRU--ETC(U)
AUG 77 A K GOVIL, J S ARORA, E J HAU DAAK11-77-C-0023
UNCLASSIFIED TR-34 NL

3 OF 3
AD
A065935

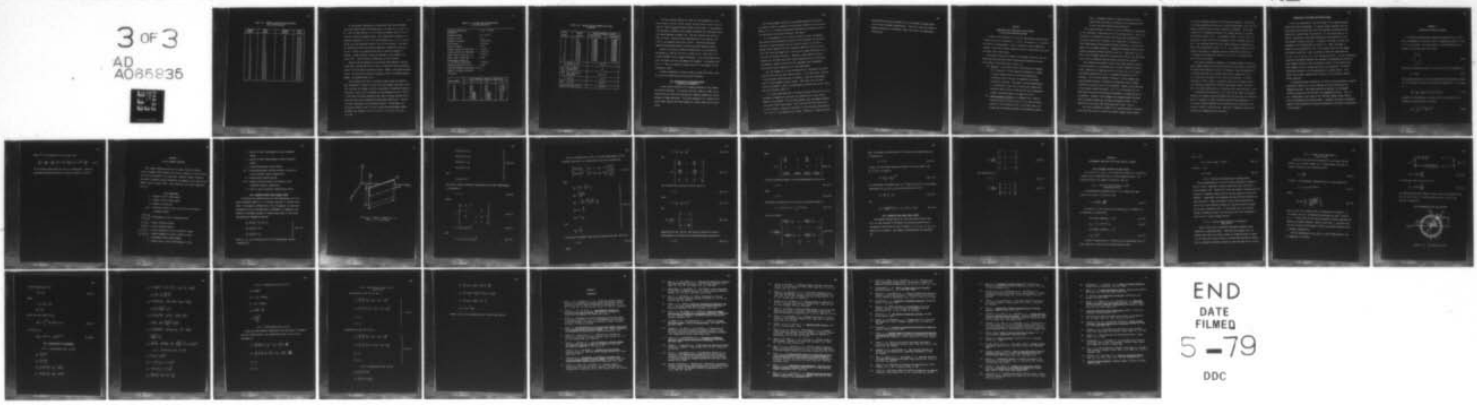

END
DATE FILMED
5-79
DDC

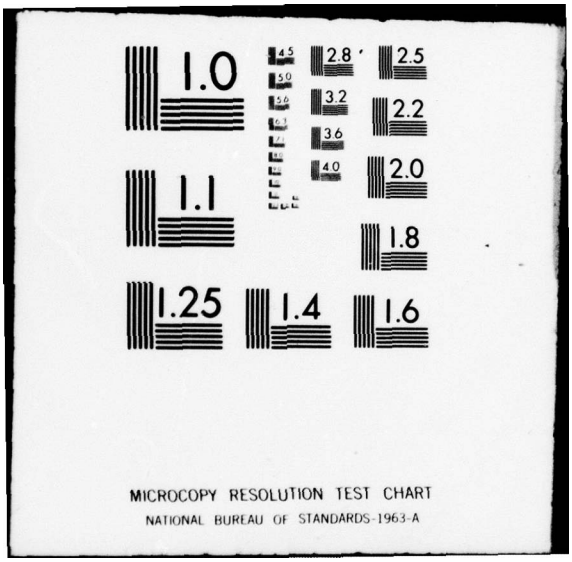
1.0
1.1
1.25
1.4
1.6
1.8
2.0
2.2
2.5
2.8
3.2
3.6
4.0
4.5
5.0
5.6
MICROCOPY RESOLUTION TEST CHART
NATIONAL BUREAU OF STANDARDS-1963-A

TABLE 6.8. ELEMENT LOCATIONS FOR HELICOPTER TAIL BOOM STRUCTURE

Element Number	End Nodes	Element Number	End Nodes
1	1,5	25	13,17
2	2,6	26	14,18
3	3,7	27	15,19
4	4,8	28	16,20
5	5,6	29	17,18
6	7,8	30	19,20
7	5,7	31	17,19
8	6,8	32	18,20
9	5,9	33	17,21
10	6,10	34	18,22
11	7,11	35	19,23
12	8,12	36	20,24
13	9,10	37	21,22
14	11,12	38	23,24
15	9,11	39	21,23
16	10,12	40	22,24
17	9,13	41	21,25
18	10,14	42	22,26
19	11,15	43	23,27
20	12,16	44	24,28
21	13,14	45	25,26
22	15,16	46	27,28
23	13,15	47	25,27
24	14,16	48	26,28

In the present formulation, the idealized tail boom is divided into three substructures by partitioning it at nodes 9 to 12 and 17 to 20. For the same reasons as in the previous example, nodes 25 to 28 are also treated as boundary nodes. Each substructure consists of 16 elements; elements 1 to 16 in the first substructure, 17 to 32 in the second, and the remaining elements 33 to 48 in the third. The first two substructures have 48 boundary degrees of freedom and the third has 24. Further, all substructures have 24 interior degrees of freedom. Design variable linking is employed in this example (see Table 6.10). Table 6.9 gives design data for this problem.

Based on the conclusions of the previous two examples, transcendental Eqs. (6.3-35) and (6.3-37) are not solved for relative maximum points of the Von Mises equivalent stress. Rather, constraints defined by Eqs. (6.3-33) and (6.3-36) are imposed at points of maximum bending moment and maximum shear force.

The idealized tail boom is optimized under stress and displacement constraints. Table 6.10 gives the final design, the value of the cost function, the number of active constraints, the maximum constraint violation, $||\delta b^1||_2$ at the optimum, and the maximum value of $||\delta b^1||_2$. It also gives the total computing time, which includes problem set-up time (3.44 sec) and 12 design iterations time (108.58 sec). The set of active constraints at the optimum includes: displacement constraints at nodes 25 and 27 in the x_2-direction and minimum element thickness for elements 5 to 8, 13 to 16, 21 to 24, 29 to 32, and 33 to 48.

TABLE 6.9. DESIGN DATA FOR HELICOPTER TAIL BOOM STRUCTURE

Modulus of elasticity (Aluminum)	= 10.5×10^3 ksi
Material density	= 0.1 lb/in.^{3}
Poisson's ratio	= 0.3
Modulus of rigidity	= 4038.46 ksi
Yield stress	= 42.0 ksi
Factor of safety	= 1.25
Initial values for mean rad., R	= 2.0 in.
Initial values for thickness, t	= 0.051 in.
Lower limit on mean rad., R	= 0.25 in.
Upper limit on mean rad., R	= None
Displacement limits in x_1, x_2, and x_3 directions	= ±0.50 in.
Starting reduction ratio, $\bar{r}$	= 0.081
Starting weighting multiplier, $\bar{w}_i$	= 0.1
Number of loading conditions	= 1

Load data:

Node Number	Load Component (kips) in direction		
	x_1	x_2	x_3
13	0.0	0.0	-0.140
14	0.0	0.0	-0.140
15	0.0	0.0	-0.140
16	0.0	0.0	-0.140
25	1.4903	1.6918	0.0
26	1.4903	-1.3658	0.0
27	-1.4903	1.6918	0.0
28	-1.4903	-1.3658	0.0

TABLE 6.10. RESULTS FOR HELICOPTER TAIL BOOM STRUCTURE

Group Number	Element Numbers	Optimum Design in inches	
		Mean Radius	Thickness
1	1-4	2.6695	0.0880
2	5-8	1.9152	0.0487
3	9-12	2.6530	0.0829
4	13-16	2.1035	0.0535
5	17-20	2.6784	0.0753
6	21-24	2.1488	0.0547
7	25-28	2.6238	0.0673
8	29-32	2.1569	0.0549
9	33-36	2.5038	0.0637
10	37-40	2.1730	0.0553
11	41-44	2.3748	0.0604
12	45-48	1.9707	0.0502

At Optimum	Weight in lbs.	111.20
	No. of Active Constraints	10
	Max. Constraint Violation	0.92×10^{-4}
	$\|\|\delta b^1\|\|_2$	44.42
Max. $\|\|\delta b^1\|\|_2$		618.30
Total CPU Time in sec.		112.02

The cost function history (in lbs) for this problem is: 69.11, 86.23, 105.78, 112.36, 112.40, 100.32, 110.49, 111.46, 111.23, 111.16, 105.23*, 110.96, 111.20 (* means change in step size). A side computation was made, in which 16 more design iterations were performed beyond the result reported in Table 6.10. The cost function was reduced by 0.6% to 110.64. There was some redistribution of the material and $||\delta b^1||_2$ was reduced from 44.42 to 36.75. This slow convergence behavior was observed earlier in some structural design problems.

Lastly, the value of effective length factor (k) required for evaluating σ_{cr} (see Eq. (6.3-2)) is taken as 2.0. This value of k is held constant for all design iterations. In the last design iteration, the value of k for each member was computed. Its maximum value was 1.7. Thus, the effective length factor of 2 is slightly on the conservative side.

A direct comparison of results cannot be made with those of Ref. 63, as the two idealizations are entirely different.

6.8 Discussion and Conclusions Based on Results of Chapter 6

In this section results of all example problems of this chapter are briefly discussed. The one-bay two-story frame is a small scale structure and is used for developing the computer program for optimal design of framed structures. The second example is of a medium scale plane frame, whereas the third example is a space frame and is fairly large.

The optimum weight obtained by the present method for the first two examples cannot be compared with available results in the literature [28,41], but it is noted that material distribution follows practically the same pattern as in the references cited above.

It is interesting to note from the results of these two examples that during the entire design process for both problems, the Von Mises equivalent stress constraint was not active at any of the relative maximum points obtained from the necessary conditions of Eq. (6.3-25). Also, the effective length factor (k) does not change appreciably after the first few design iterations. Therefore, some simplifications in imposing the Von Mises equivalent stress constraint and in evaluating the effective length factors (k's) are reasonable and considerable efficiencies result, especially for large structures.

The last example is a frame idealization of a helicopter tail boom structure that has not been treated earlier. It is noted here, contrary to the idealized wing structures of Chapter 5, that the displacement limit for this example is quite severe. Thus apart from the lower bound on thickness t, only the displacement constraint was active, which was also observed in Ref. 63.

It is also noted here that all design variables associated with the thickness of members for the first two examples are at their lower bounds at the optimum. For the third example, many thickness variables also attain their lower bounds. This indicates that the lower bound on the thickness, selected on the basis of local buckling consideration (Eq. (6.5-4)), will generally be optimum. Therefore, in many practical

design problem it may be possible to fix the member thickness based on just local buckling considerations. This will reduce the number of design variables for the problem, which will result in considerable efficiencies.

CHAPTER 7

CONCLUSIONS AND EXTENSIONS OF THE METHOD TO FAIL-SAFE STRUCTURAL DESIGN

A number of key features of the method and problem solutions have already been noted in Chapters 4, 5, and 6. Sections 4.5, 5.4, and 6.8 are devoted to discussions of results obtained in their respective chapters. This final chapter summarizes some of these points and cites areas that need further study.

The general conclusions, based on the present study are that the sensitivity analysis and optimal design method developed with substructuring, in the state space setting, is:

(a) general; in the sense that no restrictions are imposed on the type(s) of finite element(s) employed, on design variable linking within or across the substructure boundaries, and on the type of behavioral and design constraints included. This aspect has been demonstrated by considering a large class of structural optimization problems, which consist of both two and three dimensional trusses, idealized wings, and framed structures.

(b) computationally efficient; as compared with a similar algorithm without substructuring [1] and other available methods in the literature [2-4], in the sense that computing time per design iteration is considerably reduced.

Also, a comparable number of design iterations [2-4] are needed with the present formulation in an interactive mode of step size and weighting matrix selection.

The example problems of Chapter 4 serve to measure the performance of the algorithm, by employing the substructuring concept. Results are obtained for optimization problems involving truss idealization of structures under static loadings, with constraints on stresses and nodal displacements under multiple loading conditions, on natural frequency, and on design variables. Comparing the present results with a similar formulation without substructuring [1], reductions of up to 23% for the 10 member cantilever truss and up to 66% for the 200 member plane truss in computing time per design iteration are achieved.

Also comparing the present results with other available results in the literature, it is observed that for the 10 member cantilever truss reductions in computing time by factors of up to 5.6 compared with Schmit and Miura [2] and 2.4 compared with Rizzi [3,4] are achieved. For the third example of Chapter 4, the 63 member wing-carry-through structure, a reduction in computing time per design iteration by factors of up to 19 is achieved. Based on the comparison of the present results with Refs. 1 to 4, it is concluded that for large scale structures still greater efficiency in computing time can be achieved. Further, in all examples the optimum weights obtained with the present method are the same as obtained in Refs. 1 to 4, whereas they are better than those reported in Refs. 5 and 6.

The results obtained in Chapter 5 for optimal design of idealized wing structures serve to confirm the general purpose finite element

structural synthesis capability of the present algorithm. Constraints on Von Mises equivalent stress and on nodal displacements under multiple loading conditions and on design variables are imposed. The optimum weights for all examples obtained by the present method are the same as obtained in Refs. 2 to 4. As compared to Refs. 7 and 8, there is a reduction of about 9% in the final weight for the 18 element wing box beam. The computing times with the present method are significantly better than those given in Refs. 2 to 4. For example problems of this chapter, reductions in computing time per iteration by factors up to 6.0 compared with Schmit and Miura [2], and up to 9.4 compared with Rizzi [3,4] are achieved.

The results obtained in Chapter 6 for optimal design of plane and space frames present a practical application of the present formulation. The constraints imposed are same as in Chapter 5, with the addition of a buckling constraint for elements under direct compressive force and a deflection constraint in the interior of elements. No direct comparison of final results is possible, since in the present formulation constraints imposed are different than those in Refs. 28 and 41. Also, the frame idealization of a helicopter tail boom structure is new.

As mentioned in Sections 4.5, 5.4, and 6.8 the number of analyses needed in the present algorithm depends upon the step size and weighting matrix. Selection of these parameters requires some experience. In the present example problems, these parameters were monitored and adjusted to obtain a final solution. More work is needed in the area of step size and weighting matrix selection.

Extensions to Fail-Safe Structural Design

So far, the objectives of the first phase of the ongoing research project have been accomplished. An optimal design technique with substructuring has been developed, with the associated design sensitivity analysis for various types of structures. In the second phase of the project, extensions of the method developed will be applied for fail-safe design of large structures. In doing so, one needs to modify the statement of the problem given in Section 2.4. Here, one needs to impose all the constraints of Eqs. (2.4-2) and (2.2-6), for all damage and loading conditions. Also, one needs to solve the state equations (2.3-2), (2.3-7) and (2.2-3) for all damaged structures. The real advantage of substructuring becomes apparent now, because in reanalyzing the structure under damage conditions, only the matrices related to the substructure where damage occurs are changed and need to be recomputed. The design sensitivity analysis is also accomplished in a similar manner. This feature will enhance computational efficiency of the fail-safe optimal design algorithm.

In imposing various constraints, the worst violated constraint concepts, explained in Section 3.4, can be extended to include constraints for damaged structures. The design sensitivity analysis for the damaged structure proceeds as for the case of an undamaged structure. Thus, in the second phase of the project, the fail-safe optimal design problem will be formulated with substructuring. A computer code will be developed, based on this formulation and several problems will be solved to demonstrate its efficiency.

APPENDIX 1

APPROXIMATE EIGENVALUE PROBLEM

In defining the approximate eigenvalue problem of Eq. (2.3-16), static condensation of the mass matrix, as explained in Refs. 34, and 44 to 46 is utilized. For this purpose, y is partitioned into its boundary and interior parts as follows:

$$y = \begin{bmatrix} y_B \\ \\ y_I \end{bmatrix} \tag{A1-1}$$

Using the transformation matrix Q in Eq. (2.3-5), y_I is expressed as:

$$y_I = Q y_B \tag{A1-2}$$

The boundary mass matrix is then determined by writing kinetic energy of the structure in terms of the boundary coordinates y_B. It is given as

$$M_B = M_{BB} + M_{BI} Q + Q^T M_{IB} + Q^T M_{II} Q \tag{A1-3}$$

Assembly of the matrix M_B is carried out in a way similar to the boundary stiffness matrix, as follows:

$$M_B = \sum_{r=1}^{L} \beta^{(r)^T} M_B^{(r)} \beta^{(r)} \tag{A1-4}$$

where $\beta^{(r)}$ is the same as in Eq. (2.3-12), and

$$M_B^{(r)} = M_{BB}^{(r)} + M_{BI}^{(r)} Q^{(r)} + Q^{(r)^T} M_{II}^{(r)} Q^{(r)} + Q^{(r)^T} M_{IB}^{(r)} \qquad \text{(A1-5)}$$

is the boundary mass matrix for the rth substructure. Then the approximate eigenvalue problem is defined by the Eq. (2.3-16).

APPENDIX 2

FINITE ELEMENTS EMPLOYED

The element stiffness matrices for truss, frame and constant strain triangular (CST) elements are readily available in the literature [34], and are therefore not given here. However, element stiffness matrices for symmetric shear panels (SSP) and symmetric pure shear panels (SPSP) cannot be easily found. Their derivation is briefly summarized here [2].

A2.1 Notations

a = length of SSP or SPSP element

b = height of SSP or SPSP element

E = modulus of elasticity

ℓ_1, m_1 = direction cosines of the local $\tilde{x}_1$ axis in the datum coordinate system

$\left.\begin{matrix}\tilde{u}(\tilde{x}_1,\tilde{x}_2)\\ \tilde{v}(\tilde{x}_1,\tilde{x}_2)\end{matrix}\right\}$ = displacement in local coordinate system

x_1, x_2, x_3 = datum coordinate system

$\tilde{x}_1, \tilde{x}_2, \tilde{x}_3$ = local coordinate system

$\varepsilon_{11}, \varepsilon_{22}, \varepsilon_{12}$ = strain components in local coordinate system

$\sigma_{11}, \sigma_{22}, \sigma_{12}$ = stress components in local coordinate system

t = thickness of SSP or SPSP element

Θ = aspect ratio of SSP or SPSP element ($\Theta = \frac{a}{b}$)

$\tilde{r}$ = vector of nodal displacement in local coordinate system

r = vector of nodal displacements in datum coordinate system

B = strain-displacement relation matrix

$C, \tilde{C}$ = stress-displacement relation matrices in datum and local coordinate system, respectively

D = stress-strain relation matrix

$k, \tilde{k}$ = element stiffness matrices in datum and local coordinate systems, respectively

Λ = local to datum coordinate transformation matrix

A2.2 Symmetric Shear Panel Element (SSP)

In deriving the stiffness matrix for SSP elements (Fig. A2.1), the basic assumptions made are: 1) isotropic material, 2) uniform thickness, 3) rectangular configuration; if not rectangular, an equivalent rectangular plate of the same area is considered, 4) symmetric with respect to the middle surface, 5) plane stress state, 6) the stress distribution is assumed as follows:

$$\left.\begin{aligned} \sigma_{11}\ (\tilde{x}_1, \tilde{x}_2) &= \alpha_1\ \tilde{x}_2 + \alpha_2 \\ \sigma_{22}\ (\tilde{x}_1, \tilde{x}_2) &= 0.0 \\ \sigma_{12}\ (\tilde{x}_1, \tilde{x}_2) &= \alpha_3 \end{aligned}\right\} \quad \text{(A2.2-1)}$$

where α_1, α_2, α_3 are constants, and 7) the displacement boundary conditions are

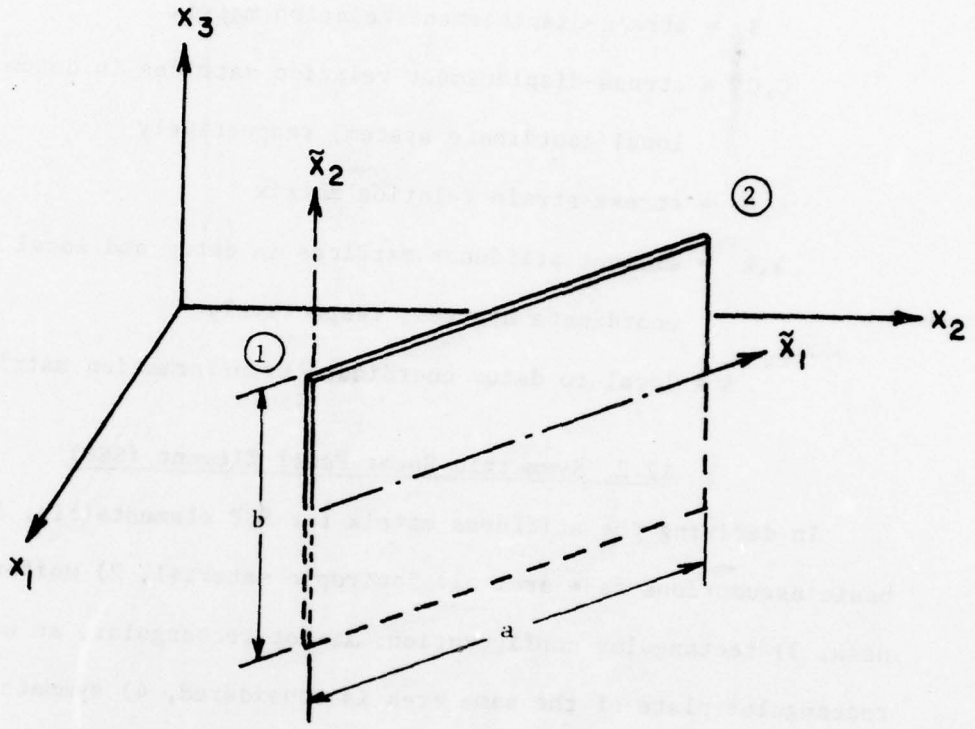

Figure A2.1. Symmetric Shear Panel, or
Symmetric Pure Shear Panel

$$\left.\begin{aligned} \tilde{u}(0,1/2\ b) &= \tilde{r}_1 \\ \tilde{u}(a,1/2\ b) &= \tilde{r}_3 \\ \tilde{v}(0,1/2\ b) &= \tilde{r}_2 \\ \tilde{v}(a,1/2\ b) &= \tilde{r}_4 \end{aligned}\right\} \quad \text{(A2.2-2)}$$

and

$$\tilde{u}(\tilde{x}_1,0) = 0.0 \quad .$$

The local to datum coordinate transformation for nodal displacements is expressed as

$$\tilde{r} = \Lambda\, r \quad \text{(A2.2-3)}$$

where

$$\Lambda = \begin{bmatrix} \ell_1 & m_1 & 0 & & & \\ 0 & 0 & 1 & & \underline{0} & \\ & & & & & \\ & \underline{0} & & \ell_1 & m_1 & 0 \\ & & & 0 & 0 & 1 \end{bmatrix} \quad \text{(A2.2-4)}$$

$$r = \{\tilde{r}_1\ \tilde{r}_2\ \tilde{r}_3\ \tilde{r}_4\}^T \quad \text{(A2.2-5)}$$

and

$$r = \{r_1\ r_2\ r_3\ r_4\ r_5\ r_6\}^T \quad \text{(A2.2-6)}$$

From the assumed stress state, the strain-displacement and the boundary conditions, the displacement state can be obtained as:

$$\begin{Bmatrix} \tilde{u}(\tilde{x}_1,\tilde{x}_2) \\ \tilde{v}(\tilde{x}_1,\tilde{x}_2) \end{Bmatrix} = \begin{bmatrix} A_{11} & 0 & A_{13} & 0 \\ A_{21} & A_{22} & A_{23} & A_{24} \end{bmatrix} \begin{Bmatrix} \tilde{r}_1 \\ \tilde{r}_2 \\ \tilde{r}_3 \\ \tilde{r}_4 \end{Bmatrix} \qquad \text{(A2.2-7)}$$

where

$$\left.\begin{aligned} A_{11} &= \frac{2}{b}\left(1 - \frac{\tilde{x}_1}{a}\right)\tilde{x}_2 \\ A_{13} &= \frac{2\,\tilde{x}_1\,\tilde{x}_2}{ab} \\ A_{21} &= -\frac{\tilde{x}_1}{b} + \frac{\tilde{x}_1^2 + \nu\tilde{x}_2^2}{ab} - \frac{\nu b}{4a} \\ A_{22} &= 1 - \frac{\tilde{x}_1}{a} \\ A_{23} &= -A_{21} \end{aligned}\right\} \qquad \text{(A2.2-8)}$$

and

$$A_{24} = \frac{\tilde{x}_1}{a}$$

The strain displacement relations are obtained using Eq. (A2-5) as:

$$\varepsilon = B\,\tilde{r} \qquad \text{(A2.2-9)}$$

where

$$\varepsilon = \{\varepsilon_{11} \quad \varepsilon_{22} \quad \varepsilon_{12}\}^T \tag{A2.2-10}$$

and

$$B = \begin{bmatrix} -\frac{2\tilde{x}_2}{ab} & 0 & \frac{2\tilde{x}_2}{ab} & 0 \\ \frac{2\nu\tilde{x}_2}{ab} & 0 & -\frac{2\nu\tilde{x}_2}{ab} & 0 \\ \frac{1}{b} & -\frac{1}{a} & \frac{1}{b} & \frac{1}{a} \end{bmatrix} \tag{A2.2-11}$$

The stress-strain relation for plane stress is:

$$\sigma = D\,\varepsilon \tag{A2.2-12}$$

where

$$\sigma = \{\sigma_{11} \quad \sigma_{22} \quad \sigma_{12}\}^T \tag{A2.2-13}$$

and

$$D = \frac{E}{1-\nu^2} \begin{bmatrix} 1 & \nu & 0 \\ \nu & 1 & 0 \\ 0 & 0 & \frac{1-\nu}{2} \end{bmatrix} \tag{A2.2-14}$$

Substituting in Eq. (A2-12) the values of strains in terms of displacements, one obtains the stress-displacement relation as:

$$\sigma = \tilde{C}\,\tilde{r} \tag{A2.2-15}$$

where

$$\tilde{C} = E \begin{bmatrix} -\frac{2\tilde{x}_2}{ab} & 0 & \frac{2\tilde{x}_2}{ab} & 0 \\ 0 & 0 & 0 & 0 \\ \frac{1}{2(1+\nu)b} & -\frac{1}{2(1+\nu)a} & \frac{1}{2(1+\nu)b} & \frac{1}{2(1+\nu)a} \end{bmatrix} \quad \text{(A2.2-16)}$$

In datum coordinate system, the stress-displacement relation is:

$$\sigma = C\, r \quad \text{(A2.2-17)}$$

where

$$C = \tilde{C}\, \Lambda \quad \text{(A2.2-18)}$$

The element stiffness matrix in the local coordinate system is

$$\tilde{k} = \int_v B^T D\, B\, dv = t \int_s B^T D\, B\, ds \quad \text{(A2.2-19)}$$

Thus, one obtains

$$\tilde{k} = \frac{Et}{12(1+\nu)} \begin{bmatrix} \frac{2(1+\nu)}{\theta} + 3\theta & -3 & -\frac{2(1+\nu)}{\theta} + 3\theta & 3 \\ -3 & \frac{3}{\theta} & -3 & -\frac{3}{\theta} \\ -\frac{2(1+\nu)}{\theta} + 3\theta & -3 & \frac{2(1+\nu)}{\theta} + 3\theta & 3 \\ 3 & -\frac{3}{\theta} & 3 & \frac{3}{\theta} \end{bmatrix} \quad \text{(A2.2-20)}$$

Thus, the element stiffness matrix in the datum coordinate system can be expressed as:

$$k = \Lambda^T \tilde{k} \Lambda \tag{A2.2-21}$$

Finally, the Von Mises equivalent stress σ^c for this element (see Eq. (5.2-3)) is given as

$$\sigma^c = (\sigma_{11}^2 + 3\sigma_{12}^2)^{1/2} \tag{A2.2-22}$$

For calculating the maximum value of σ^c from Eq. (A2.2-22) the following expressions for σ_{11} and σ_{12} are used (from Eq. (A2.2-15)):

$$\sigma_{11} = \frac{E}{a} (\tilde{r}_3 - \tilde{r}_1) \tag{A2.2-23}$$

and

$$\sigma_{12} = \frac{E}{2(1+\nu)} \left\{ \frac{1}{a} (\tilde{r}_4 - \tilde{r}_2) + \frac{1}{b} (\tilde{r}_3 + \tilde{r}_1) \right\} \tag{A2.2-24}$$

A2.3 Symmetric Pure Shear Panel (SPSP)

The element stiffnes matrix for this pure shear element (Fig. A2.1) is also obtained by following the previous procedure and by assuming the stress state to be as follows: $\sigma_{11} = 0$, $\sigma_{22} = 0$, $\sigma_{12} = \beta_1$, where β_1 is a constant. The element stiffness matrix is then given as:

$$\tilde{k} = \frac{Et}{4(1+\nu)} \begin{bmatrix} \Theta & -1 & \Theta & 1 \\ -1 & \frac{1}{\Theta} & -1 & -\frac{1}{\Theta} \\ \Theta & -1 & \Theta & 1 \\ 1 & -\frac{1}{\Theta} & 1 & \frac{1}{\Theta} \end{bmatrix} \qquad \text{(A2.3-1)}$$

The stress state is

$$\sigma = \tilde{C}\,\tilde{r} \qquad \text{(A2.3-2)}$$

$$\tilde{C} = \frac{E}{2(1+\nu)} \begin{bmatrix} 0 & 0 & 0 & 0 \\ 0 & 0 & 0 & 0 \\ \frac{1}{b} & -\frac{1}{a} & \frac{1}{b} & \frac{1}{a} \end{bmatrix} \qquad \text{(A2.3-3)}$$

APPENDIX 3

SUPPLEMENTAL EQUATIONS FOR OPTIMAL DESIGN OF FRAMES

A3.1 Critical Stresses for Eq. (6.3-2)

The values of σ_{cr} and τ_{cr} for a member are obtained by considering a single force acting alone and are briefly summarized here. For complete details, the reader is referred to Ref. 56.

A3.1.1 Circular Tube Subjected to Axial Compression Alone

A nondimensional slenderness ratio λ for a member with mean radius R and length ℓ is given as [56]:

$$\lambda = 0.450 \frac{k\ell}{R} \sqrt{\frac{\sigma_y}{E}} \tag{A3.1-1}$$

In terms of λ, the critical axial stress (σ_{ca}) of a member can be expressed as follows [56]:

for elastic behavior, $\lambda \leq \sqrt{2}$ (A3.1-2)

$$\sigma_{ca} = (1 - 0.25\,\lambda^2)\,\sigma_y \tag{A3.1-2}$$

for elastic behavior, $\lambda > \sqrt{2}$

$$\sigma_{ca} = \sigma_y/\lambda^2 \tag{A3.1-3}$$

A factor of safety that is a function of the slenderness ratio is often used and is given by the following equation [56]:

For $\lambda < \sqrt{2}$,

$$FS = 1.67 + 0.265\lambda - 0.044\lambda^3 \qquad \text{(A3.1-4)}$$

and for $\lambda \geq \sqrt{2}$,

$$FS = 1.92 \qquad \text{(A3.1-5)}$$

A3.1.2 Circular Tubes Subjected to Bending Alone

The buckling behavior of circular tubes in bending is similar to that of axially compressed cylinders except that bent tubes have a stress gradient [56]. Donnell [67] found the elastic buckling stress in bending to be somewhat higher than the critical stress for axial compression. Flügge [68], and Timoshenko and Gere [60] have reached the same conclusion. Other investigators [69-71] have indicated that there is not much difference between the critical stress in bending and in axial compression [56]. In the present work, the critical stress in bending is taken to be the same as for axial compression. This is also a current design practice.

A3.1.3 Circular Tubes Subjected to Transverse Shear Alone

There is very little information available regarding tubes subjected to transverse shear. Schilling [48] suggests that for manufactured tubes the critical stress in transverse shear be taken as 1.25 times the critical stress in torsion when buckling is elastic, and for inelastic buckling it should be taken the same as for torsion.

A3.1.4 Circular Tubes Subjected to Torsion Alone

Using the Alcoa Structural Handbook [72], the shear buckling stress (τ_{ct}) in elastic range, for a tubular member subjected to torsion is given by the following equation:

$$\tau_{ct} = \frac{\pi^2 E}{\lambda^2} \tag{A3.1-6}$$

in which λ, the equivalent slenderness ratio, is approximated by

$$\lambda = 3.73\ (D/t)^{0.75}\ \overset{*}{W}\ 0.5 \tag{A3.1-7}$$

where

$$\overset{*}{W} = \text{Min}\left\{1,\ \frac{0.561\left(\frac{\ell_f}{2R}\right)^{0.5}}{\left(\frac{2R}{t}\right)^{0.25}}\right\}\ , \tag{A3.1-8}$$

and ℓ_f is the clear length between circumferential stiffeners. In the present work, no circumferential stiffeners are used, therefore, $\ell_f = \ell$. Further there is not much information available regarding the inelastic torsional buckling. Hence in this work, τ_{ct} defined by Eq. (A3.1-6) is used for both elastic as well as inelastic behavior which is slightly conservative.

Now the expressions for σ_{cr} and τ_{cr}, after simplification, can be summarized as follows:

$$\sigma_{cr} = \begin{cases} 4.9383 \frac{E}{FS} \left(\frac{R}{k\ell}\right)^2 , & \text{for } \lambda > \sqrt{2} \\ \left\{1 - 0.0506 \left(\frac{k\ell}{R}\right)^2 \left(\frac{\sigma_y}{E}\right)\right\} \frac{\sigma_y}{FS} , & \text{for } \lambda \leq \sqrt{2} \end{cases} \qquad \text{(A3.1-9)}$$

$$\tau_{cr}^2 = 0.0983 \frac{E^2 t^3}{R^3 \overset{*}{W}^2} , \qquad \text{(A3.1-10)}$$

for transverse shear acting along, and

$$\tau_{cr}^2 = 0.0629 \frac{E^2 t^3}{R^3 \overset{*}{W}^2} , \qquad \text{(A3.1-11)}$$

for combined torsion and transverse shear, where FS is defined by Eqs. (A3.1-4) and (A3.1-5); λ and $\overset{*}{W}$ are defined by Eqs. (A3.1-1) and (A3.1-8), respectively.

A3.2 Computation of $\bar{Q}$, Eq. (6.3-20)

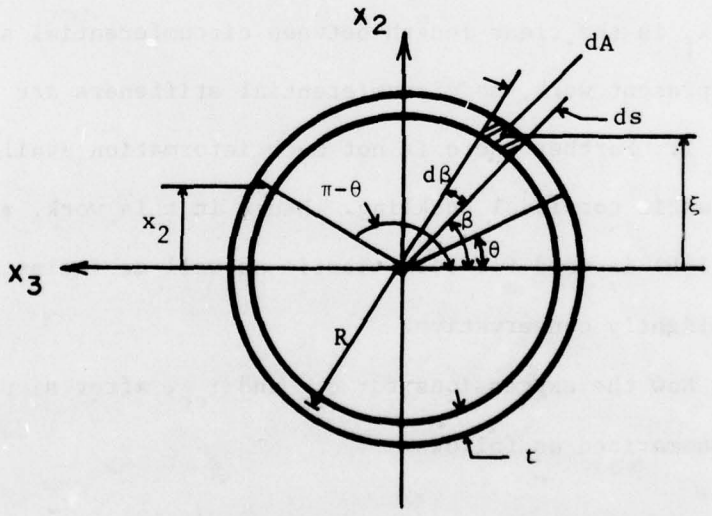

Figure A3.1 Cross-Section of Tube

From the definition of $\bar{Q}$,

$$d\bar{Q} = \xi dA \tag{A3.2-1}$$

where

$$\xi = R \sin \theta, \text{ and}$$

$$dA = Rtd\theta$$

Hence the total value of $\bar{Q}$ is

$$\bar{Q}(\theta) = \int_{\theta}^{\pi-\theta} d\bar{Q} = 2R^2 t \cos \theta \tag{A3.2-2}$$

In terms of x_2,

$$\bar{Q}(x_2) = 2R^2 t \{1 - (x_2/R)^2\}^{1/2} \tag{6.3-20R}$$

A3.3 Coefficients of Polynomials

A3.3.1 Coefficients in Eq. (6.3-25)

$$a_8 = \frac{1}{16} R^2 w^5$$

$$a_7 = \frac{1}{2} R^2 P_2 w^4$$

$$a_6 = \frac{1}{2} R^2 w^3 (3P_2^2 - P_3 w - 3R^2 w^2)$$

$$a_5 = R^2 w^2 P_2 (2P_2^2 - 3P_3 w - 9R^2 w^2)$$

$$a_4 = R^2w\left\{9R^4w^4 - 6R^2w^2\left(\frac{13}{4}P_2^2 - P_3w\right) + P_2^4 - 6P_3P_2^2w + \frac{3}{2}P_3^2w^2 + \left(\frac{1}{2}\frac{P_1Iw}{RA}\right)^2\right\}$$

$$a_3 = R^2w\left\{36R^4P_2w^3 - 6R^2P_2w(3P_2^2 - 4P_3w) + 6P_3^2P_2w - 4P_3P_2^3 + \left(\frac{P_1I}{AR}\right)^2 P_2w\right\}$$

$$a_2 = R^2w\left\{54R^4P_2^2w^2 - 6R^2(P_2^4 - 5P_3P_2^2w + P_3^2w^2) + 6P_3^2P_2^2 - 2P_3^3w + \left(\frac{P_1I}{AR}\right)^2\left(\frac{3}{2}P_2^2\right)\right\}$$

$$a_1 = R^2\left\{36R^4P_2^3w^2 - 12R^2wP_3P_2(P_3w - P_2^2) - 4P_3^3P_2w + \left(\frac{P_1I}{AR}\right)^2 P_2^3\right\}$$

$$a_0 = \left\{9R^4P_2^4w - 6R^2P_2^2P_3^2w + P_3^4w - \left(\frac{P_1I}{AR}\right)^2(P_2^2 + P_3w)P_3\right\}R^2$$

A3.3.2 Coefficients in Eq. (6.3-35)

$$a_3 = R(F_5F_6 + F_2F_3R^2)$$

$$a_2 = -(I/A)\,F_1F_5 - 1.5\,F_2F_4R^2$$

$$a_1 = (I/A)\,F_1F_6 + 1.5\,F_3F_4R^2$$

$$a_0 = \frac{R}{2}\left\{R^2(F_3^2 - F_2^2) + F_6^2 - F_5^2\right\}$$

A3.3.3 Coefficients in Eq. (6.3-37)

$$a_3 = F_2 F_3 R\beta$$

$$a_2 = - F_5 - 0.5\beta F_2 F_4$$

$$a_1 = F_6 + 0.5\beta F_3 F_4$$

$$a_0 = \beta R(F_3^2 - F_2^2)$$

$$\beta = \frac{2\sigma_{cr} R^2}{I\tau_{cr}^2}$$

A3.3.4 Coefficients in Eq. (6.4-4)

Using the known boundary conditions at the two ends of an element and after simplification, the coefficients in Eq. (6.4-4) can be expressed as:

$$c_3 = \frac{12}{\ell^3} \left\{ \frac{\ell}{2} (u_6 + u_3) - (u_5 - u_2) \right\} - \frac{w\ell}{2EI}$$

$$c_2 = \frac{6}{\ell^2} \left\{ - \frac{\ell}{3} (u_6 + 2u_3) + (u_5 - u_2) \right\} + \frac{w\ell^2}{12EI}$$

$$c_1 = u_3$$

$$c_0 = u_2$$

A3.3.5 Coefficients in Eqs. (6.4-7) and (6.4-8)

Coefficients in Eq. (6.4-7) are:

$$\left.\begin{aligned} c_3 &= \frac{12}{\ell^3}\left\{\frac{\ell}{2}(u_{12}+u_6)-(u_5-u_2)\right\} \\ c_2 &= \frac{6}{\ell^2}\left\{-\frac{\ell}{3}(u_{12}+2u_6)+(u_5-u_2)\right\} \\ c_1 &= u_6 \\ c_0 &= u_2 \end{aligned}\right\} \quad \text{(A3.3-1)}$$

Coefficients in Eq. (6.4-8) are:

$$\left.\begin{aligned} d_3 &= \frac{12}{\ell^3}\left\{\frac{\ell}{2}(u_{11}+u_5)-(u_9-u_3)\right\} \\ d_2 &= \frac{6}{\ell^2}\left\{-\frac{\ell}{3}(u_{11}+2u_5)+(u_9-u_3)\right\} \\ d_1 &= u_5 \\ d_0 &= u_3 \end{aligned}\right\} \quad \text{(A3.3-2)}$$

A3.3.6 Coefficients in Eq. (6.4-9)

$$a_5 = \frac{1}{3}(c_3^2 + d_3^2)$$

$$a_4 = \frac{5}{6}(c_2c_3 + d_2d_3)$$

$$a_3 = \frac{4}{3}\,(c_3c_1 + d_3d_1) + \frac{1}{2}\,(c_2^2 + d_2^2)$$

$$a_2 = \frac{1}{3}\,(c_3c_0) + d_3d_0) + \frac{3}{2}\,(c_1c_2 + d_1d_2)$$

$$a_1 = \frac{1}{2}\,(c_2c_0 + d_2d_0) + c_1^2 + d_1^2$$

$$a_0 = c_1c_0 + d_1d_0$$

where c's and d's are defined by Eqs. (A3.3-1) and (A3.3-2).

APPENDIX 4

REFERENCES

1. Arora, J. S., and Haug, E. J., Jr., "Efficient Optimal Design of Structures by Generalized Steepest Descent Programming," International Journal for Numerical Methods in Engineering, Vol. 10, No. 4, 1976, pp. 747-766, and Vol. 10, No. 6, 1976, pp. 1420-1426.

2. Schmit, A., Jr., and Miura, H., Approximation Concepts for Efficient Structural Synthesis, NASA CR-2552, University of California, Los Angeles, CA. 90024, March 1976.

3. Rizzi, P., "Optimization of Multi-Constrained Structures Based on Optimality Criteria," Proc. of AIAA/ASME/SAE 17th Structures, Structural Dynamics, and Material Conference, Kings of Prussia, PA, May 5-7, 1976, pp. 448-462.

4. Rizzi, P., The Optimization of Structures with Complex Constraints Via a General Optimality Criteria Method, Ph.D. Thesis, Department of Aeronautics and Astronautics, Stanford University, 1976.

5. Dobbs, M. W. and Nelson, R. B., "Application of Optimality Criteria to Automated Structural Design", AIAA Journal, Vol. 14, No. 10, October 1976, pp. 1436-1443.

6. Berke, L., and Khot, N. S., Use of Optimality Criteria Methods for Large Scale Systems, AGARD Lecture Series on Structural Optimization, AGARD-LS-70, 1974, pp. 1-29.

7. Gellatly, R. A., and Berke, L., Optimal Structural Design, Technical Report No. AFFDL-TR-70-165, Wright-Patterson Air Force Base, Ohio, 1971.

8. Gellatly, R. A., Development of Procedures for Large Scale Automated Minimum Weight Structural Design, Technical Report No. AFFDL-TR-66-180, Wright-Patterson Air Force Base, Ohio, 1966.

9. Kirsch, U., Reiss, M., and Shamir, U., "Optimum Design by Partitioning into Substructures," Journal of the Structural Division, Proc. ASCE, Vol. 98, No. ST1, January 1972, pp. 249-267.

10. Noor, A. K., and Lowder, H. E., "Approximate Reanalysis Techniques with Substructuring," Journal of the Structural Division, Proc. ASCE, Vol. 101, No. ST8, August 1975, pp. 1687-1698.

11. Wasiutynski, Z. and Brandt, A., "The Present State of Knowledge in the Field of Optimum Design of Structures," Applied Mechanics Reviews, Vol. 16, No. 5, May 1963, pp. 341-350.

12. Sheu, C. Y. and Prager, W., "Recent Development in Optimal Structural Design," Applied Mechanics Reviews, Vol. 21, No. 10, October 1968, pp. 985-992.

13. Schmit, L. A., (Editor), Structural Optimization Symposium, AMD-Vol. 7, The Winter Annual Meeting of the American Society of Mechanical Engineers, New York, November 17-21, 1974.

14. Pope, G. G., and Schmit, L. A. (Editors), Structural Design Applications of Mathematical Programming Techniques, AGARDograph No. 149, National Technical Information Service, Springfield, Virginia, February 1972.

15. Gallagher, R. H., and Zienkiewicz, O. C. (Editors), Optimum Structural Design: Theory and Applications, John Wiley & Sons, New York, 1973.

16. Venkayya, V. B., Khot, N. S., and Berke, L., "Application of Optimality Criteria Approaches to Automated Design of Large Practical Structures," Second Symposium on Structural Optimization, AGARD-CP-123, Milan, Italy, April 1973.

17. Fiacco, A. V. and McCormick, G. P., Nonlinear Programming: Sequential Unconstrained Minimization Techniques, John Wiley, New York, 1968.

18. Schmit, L. A. and Miura, H., "A New Structural Analysis/Synthesis Capability - ACCESS 1," AIAA Journal, Vol. 14, No. 5, May 1976, pp. 661-671.

19. Fox, R. L., and Kapoor, M. P., "A Minimization Method for the Solution of the Eigenproblem Arising in Structural Dynamics," presented at the Air Force Second Conference on Matrix Methods in Structural Mechanics, Wright-Patterson Air Force Base, Ohio, October 15-17, 1968.

20. Kavlie, D., and Moe, J., "Application of Nonlinear Programming to Optimum Grillage Design with Nonconvex Sets of Variables," International Journal for Numerical Methods in Engineering, Vol. 1, No. 4, 1969, pp. 351-378.

21. Kavlie, D., and Moe, J., "Automated Design of Frame Structures," Journal of the Structural Division, Proc. ASCE, Vol. 97, No. ST1, January 1971, pp. 33-62.

22. Brown, D. M., and Ang, A. H. S., "Structural Optimization by Nonlinear Programming," Journal of the Structural Division, Proc. ASCE, Vol. 92, No. ST6, December 1966, pp. 319-340 and Vol. 93, No. ST5, October 1967, pp. 618-619.

23. Romstad, K. M. and Wang, C. K., "Optimum Design of Framed Structures," Journal of the Structural Division, Proc. ASCE, Vol. 94, No. ST12, December 1968, pp. 2817-2845.

24. Moses, F. and Onoda, S. "Minimum Weight Design of Structures with Application to Elastic Grillages," International Journal for Numerical Methods in Engineering, Vol. 1, No. 4, 1969, pp. 311-331.

25. Ridha, R. A. and Wright, R. N., "Minimum Cost Design of Frames," Journal of the Structural Division, Proc. ASCE, Vol. 93, No. ST4, Auguat 1967, pp. 165-183.

26. Bryson, A. E., Jr., and Ho, Y. C., Applied Optimal Control, Ginn and Co., Waltham, Mass., 1969.

27. Haug, E. J., Jr., Pan, K. C., and Streeter, T. D., "A Computational Method for Optimal Structural Design: I Piecewise Uniform Structures," International Journal for Numerical Methods in Engineering, Vol. 5, 1972, pp. 171-184.

28. Arora, J. S., Haug, E. J., Jr., and Rim, K., "Optimal Design of Plane Frames," Journal of the Structural Division, Proc. ASCE, Vol. 101, No. ST10, October 1975.

29. Haug, E. J., Jr., and Arora, J. S., "Optimal Design Techniques Based on Optimal Control Methods," Proc. of the First ASME Design Technology Transfer Conference, New York, October 1974, pp. 65-74.

30. Arora, J. S., On Improving Efficiency of An Algorithm for Structural Optimization and A User's Manual for Program TRUSSOPT3, Technical Report No. 12, Department of Mechanics and Hydraulics, University of Iowa, Iowa City, IA. 52242, June 1974, (Revised, September, 1976).

31. Haug, E. J., Jr., Engineering Design Handbook: Computer Aided Design of Mechanical Systems, AMCP-706-192, U.S. Army Materiel Command, Washington, D.C., July 1973.

32. Haug, E. J., Jr., and Arora, J. S., Engineering Design Handbook: Computer-Aided Design of Mechanical Systems, AMCP-706-193, Army Material Command, to be published, 1977.

33. Feng, T-T., Arora, J. S., and Haug, E. J., Jr., "Optimal Structural Design Under Dynamic Loads," International Journal for Numerical Methods in Engineering, Vol. 11, No. 1, 1977, pp. 39-52.

34. Przemieniecki, J. S., Theory of Matrix Structural Analysis, McGraw-Hill Book Co., Inc., New York, 1968.

35. Bathe, K. J., and Wilson, E. L., "Solution Methods for Eigenvalue Problems in Structural Mechanics," International Journal for Numerical Methods in Engineering, Vol. 6, No. 2, 1973, pp. 213-226.

36. Householder, A. S., Principles of Numerical Analysis, McGraw-Hill Book Co., New York, 1953.

37. Gupta, K. K., "Free Vibrations of Single-Branch Structural Systems," Journal of the Institute of Mathematics and Its Applications, Vol. 5, No. 3, 1969, pp. 351-362.

38. Wilkinson, J. H., The Algebraic Eigenvalue Problem, Claredon Press, Oxford, 1965.

39. Peters, G., and Wilkinson, J. H., "Eigenvalues of $Ax = \lambda Bx$ with Band Symmetric A and B," Computer Journal, Vol. 12, 1969, pp. 398-404.

40. Ostrowski, A. M., Solution of Equations and Systems of Equations, Academic Press, New York, 1960.

41. Arora, J. S., Optimal Design of Elastic Structures Under Multiple Constraint Conditions, Ph.D. Dissertation, Department of Mechanics and Hydraulics, University of Iowa, Iowa City, IA. 52242, August, 1971.

42. Arora, J. S., "Survey of Structural Reanalysis Techniques," Journal of the Structural Division, Proc. ASCE, Vol. 102, No. ST4, April 1976, pp. 783-802.

43. Bradbury, W. W., and Fletcher, R., "New Iterative Methods for Solution of the Eigenproblem," Numerishce Mathematik 9, 1966, pp. 259-267.

44. Appa, K., Smith, G. C. C., and Hughes, J. T., "Rational Reduction of Large-Scale Eigenvalue Problems," AIAA Journal, Vol. 10, No. 2, July 1972, pp. 964-965.

45. Guyan, R. J., "Reduction of Stiffness and Mass Matrices," AIAA Journal, Vol. 3, No. 2, February 1965, p. 380.

46. Irons, B., "Structural Eigenvalue Problem: Elimination of Unwanted Variables," AIAA Journal, Vol. 5, No. 5, May 1965, pp. 961-962.

47. Kwak, B. M., Parametric Optimal Design, Ph.D. Dissertation, Mechanics and Hydraulics Program, University of Iowa, Iowa City, IA. 52242, December, 1974.

48. Pickett, R. M., Jr., Rubinstein, M. F., and Nelson, R. B., "Automated Structural Synthesis Using a Reduced Number of Design Coordinates," AIAA Journal, Vol. 11, No. 4, April, 1973, pp. 489-494.

49. Schmit, L. A., and Farshi, B., "Some Approximation Concepts for Structural Synthesis," AIAA Journal, Vol. 12, No. 5, May 1974, pp. 692-699.

50. Polak, E., Computational Methods in Optimization, A Unified Approach, Academic Press, Inc., 1971.

51. Venkayya, V. B., Khot, N. S., and Reddy, V. S., Energy Distribution in an Optimum Structural Design, Technical Report No. AFFDL-TR-68-156, Air Force Flight Dynamics Laboratory, Wright-Patterson Air Force Base, Ohio 45433, March 1969.

52. Venkayya, V. B., Khot, N. S., and Reddy, V. S., "Optimization of Structures Based on the Study of Energy Distribution," Proc. of the Second Conference on Matrix Methods in Structural Mechanics, AFFDL-TR-68-150, NTIS No. AD-703-685, pp. 111-153, December 1965.

53. Ná-dai, Arpád, Theory of Flow and Fracture of Solids, Vol. II, Second Edition, McGraw-Hill, New York, 1963.

54. McGuire, W., Steel Structures, Prentice-Hall Inc., Englewood Cliffs, N.J., 1968.

55. Bresler, Boris, Lin, T. Y., and Scalzi, John B., Design of Steel Structures, Second Edition, John Wiley & Sons, Inc., New York, 1968.

56. Johnston, Bruce G. (Editor), Guide to Stability Design Criteria for Metal Structures, Structural Stability Research Council, Third Edition, John Wiley & Sons, Inc., New York, 1976.

57. Winter, G., "Compression Members in Trusses and Frames," The Philosophy of Column Design, Proc. of the Fourth Tech. Session, CRC, May 1954, pp. 53-59.

58. Gerard, G., and Becker, H., Handbook of Structural Stability, Part III - Buckling of Curved Plates and Shells, Nat. Advis. Comm. Aeron., Techn. Note, 3783, August 1957.

59. Schilling, C. G., "Buckling Strength of Circular Tubes," Journal of the Structural Division, Proc. ASCE, Vol. 91, No. ST5, October 1965, pp. 325-348.

60. Timoshenko, S. P., and Gere, J. M., Theory of Elastic Stability, Second Edition, McGraw-Hill, New York, 1961.

61. Selby, S. M., Standard Mathematical Tables. Twenty-Second Edition, CRC Press, Inc., Cleveland, Ohio 44128, 1974.

62. Yu, Wei-Wen, Cold-formed Steel Structures, McGraw-Hill Book Company, New York, 1973.

63. Arora, J. S., Haug, E. J., Jr., and Govil, A. K., Fail-Safe Design of An Open Truss Helicopter Tail Boom, Technical Report No. 32, Division of Materials Engineering, University of Iowa, Iowa City, IA. 52242, April 1977.

64. American Institute of Steel Construction, Manual of Steel Construction, Seventh Edition, 1971.

65. Wind Bracing in Steel Buildings: Final Report of Subcommittee No. 31, Trans. ASCE, Vol. 105, 1940, pp. 1730-1738.

66. Gaylord, E. H., Jr., and Gaylord, Charles N., Design of Steel Structures Including Applications in Aluminum, McGraw-Hill Book Co., Inc., New York, 1957.

67. Donnell, L. H., "A New Theory for Buckling of Thin Cylinders Under Axial Compression and Bending," Trans. ASME, Vol. 56, 1934.

68. Flügge , W., "Die Stabilität Der Kreiszylinderschale," Ingen. Arch., Vol. 3, 1932.

69. Weingarten, V. I., and Seide, P., "On the Buckling of Circular Cylindrical Shells Under Pure Bending," Journal of Appl. Mech., Proc. ASME, Vol. 28, No. 1, March 1961.

70. Yao, J. C., "Large Deflection Analyses of Buckling of a Cylinder Under Bending," Journal of Appl. Mech., Proc. ASME, Vol. 29, No. 4, September 1962.

71. Wilson, W. M., and Olson, F. D., Tests on Cylindrical Shells, Eng. Exp. Sta. Bull., Univ. Ill., No. 331, September 1941.

72. ALCOA Structural Handbook, Aluminum Company of America, Revised Edition, 1960.